UNSW SYDNEY | Australia's Global University

Australian Centre for Advanced Photovoltaics
Australia-US Institute for Advanced Photovoltaics

Annual Report 2017 – Appendix

ACAP Collaboration Grants – 2017

ACAP's competitively selected Collaboration Grants, shown below, are reported online at http://www.acap.net.au/annual-reports. This document forms part of the 2017 Annual Report of the Australian Centre for Advanced Photovoltaics and the Australia-US Institute for Advanced Photovoltaics.

6.6 Metal Plating for Next Generation Silicon Solar Cells

Lead Partner

UNSW

UNSW Team

A/Prof Alison Lennon, Dr Udo Römer, Dr Pei-Chieh Hsiao

Academic Partner

National Renewable Laboratories (NREL), Dr Paul Stradins, Dr Mathew Page, Dr Manuel Schnabel

Funding Support

ACAP

Aim

The objective of this project is to develop reliable plated metallisation processes for the metal grids of polysilicon (poly-Si) selective carrier contact cells. The project planned to develop both the plating processes (guided by optical modelling) and the measures of process reliability that would be required (e.g. adhesion of the plated metal).

Progress

In order to replace Ag screen printing as metallisation technology for high efficiency Si solar cells with transparent conductive oxide (TCO) layers, Cu plating to ITO layers has been investigated. In this project solar cells featuring a carrier selective poly-Si back surface field capped with an indium tin oxide (ITO) were fabricated. These solar cells were used as test structures for the development of a Cu plating process. Additionally, optical simulations were performed to optimise the ITO layer thickness.

The cell fabrication was a joint undertaking of UNSW and NREL. The front side processing, including the B-diffusion was performed at UNSW, the rear side fabrication, including the deposition of the carrier selective poly-Si contact and the evaporation of the ITO layer was performed at NREL. Front surface contact openings and characterisation (cell performance and finger adhesion) were then performed at UNSW. The visit of a UNSW researcher (Udo Römer) to NREL greatly assisted with the continuous processing of the solar cells and to ensure all individual process steps were adapted to match the requirements of the overall process flow.

Figure 6.6.1 shows the light I-V curve of the best solar cell and of a typical solar cell fabricated in this project. The insets show the solar cell parameters and EL/PL measurements of the typical solar cell. Both solar cells exhibit very low fill factors, due mainly to high series resistance. The PL (with current extraction) and EL measurements shown in the inset in Figure 6.6.1 show that the typical solar cell exhibits a very non-uniform series resistance distribution which contributes to the apparent shunt in the I-V curve (Sugianto et al., 2012). After excluding all other possible sources, the interface between the poly-Si and ITO layers seems to be the most likely source for the high non-uniform series resistance. NREL's best process for poly-Si fabrication includes a hydrogenation step which requires AlO_x layers to be present on all surfaces. Before ITO deposition the AlO_x was removed on the poly-Si layer in a one-side etching step. Most likely, the etching time was not always long enough to ensure complete removal of the AlO_x layer, resulting in the observed locally high series resistances.

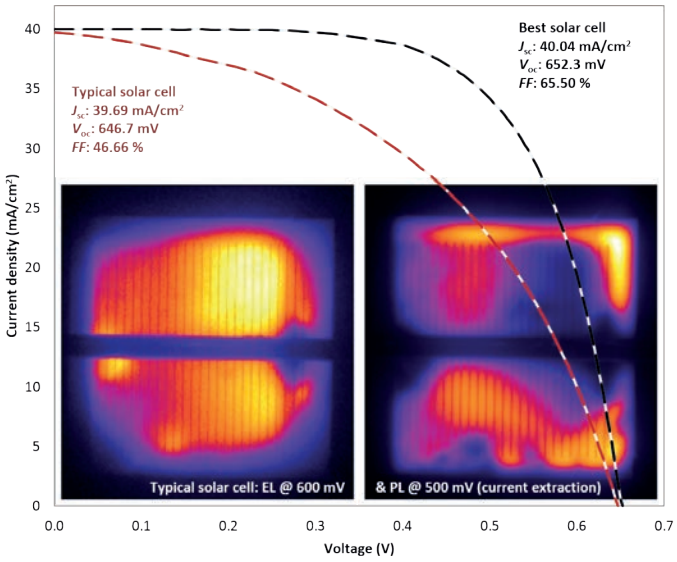

Figure. 6.6.1: Light I-V curve of the best solar cell and of a typical solar cell fabricated in this project.

Additionally, the implied V_{OC} values of the cells were lower than expected. While the implied V_{OC} values were typically in the range of 695 mV for the passivated cell precursors, they dropped to ~680 mV after wet chemical front contact opening and further to ~650 mV after Ti/Ag evaporation and lift-off. While implied V_{OC} values of 680 mV were expected from EDNA2 calculations (McIntosh and Altermatt, 2010) for a contact area fraction of 5% and a B-doping profile with a surface concentration of 1.1×10^{19} atoms/cm^3, the reason for the very low implied V_{OC} values after metallisation has not been understood so far. Despite the non-optimal IV results, the fabricated solar cells were used as test structures for the development of a Cu plating process to ITO.

Typically, Cu metal fingers plated to ITO layers show very poor adhesion. In our experiments we usually observed peeling or partial peeling of the Cu fingers after removal of a photomask (used for masking the non-plated area) with acetone. In order to improve the adhesion properties, we investigated an ITO sensitisation process that can be used for Cu plating to (I)TO during the fabrication of transparent electrodes for flat panel displays (Liu et al., 1994). The concept of this sensitisation process is to reduce the surface of SnO_x layers by electrolytic reduction in order create a thin layer of low valence of SnO_x. In contrast to fully oxidised Sn atoms, where Cu, due to its lower oxygen activity, can only adsorb, reduced Sn(II) atoms provide a much stronger bond for plated Cu atoms. While pre-experiments on ITO layers from a different source yielded very promising adhesion results with this process (see Figure 6.6.2a) (see also Li, 2016), only minor impact of different sensitisation treatments could be observed in experiments using the solar cells with evaporated ITO layers from NREL (see Figure 6.6.2b). The adhesion forces in these experiments have been obtained by using a stylus-based adhesion tester, featuring a metal stylus, scanning the sample surface and thereby peeling off the metal fingers, while measuring the lateral force (Wang et al., 2016). X-ray photoelectron spectroscopy (XPS) analysis of the evaporated ITO layers revealed that, despite the use of an InSn source with 10% Sn content, less than 1% Sn was identified in the evaporated layers. As In has a much stronger bond to O than Sn, it cannot be reduced as easily as Sn, thus explaining this result.

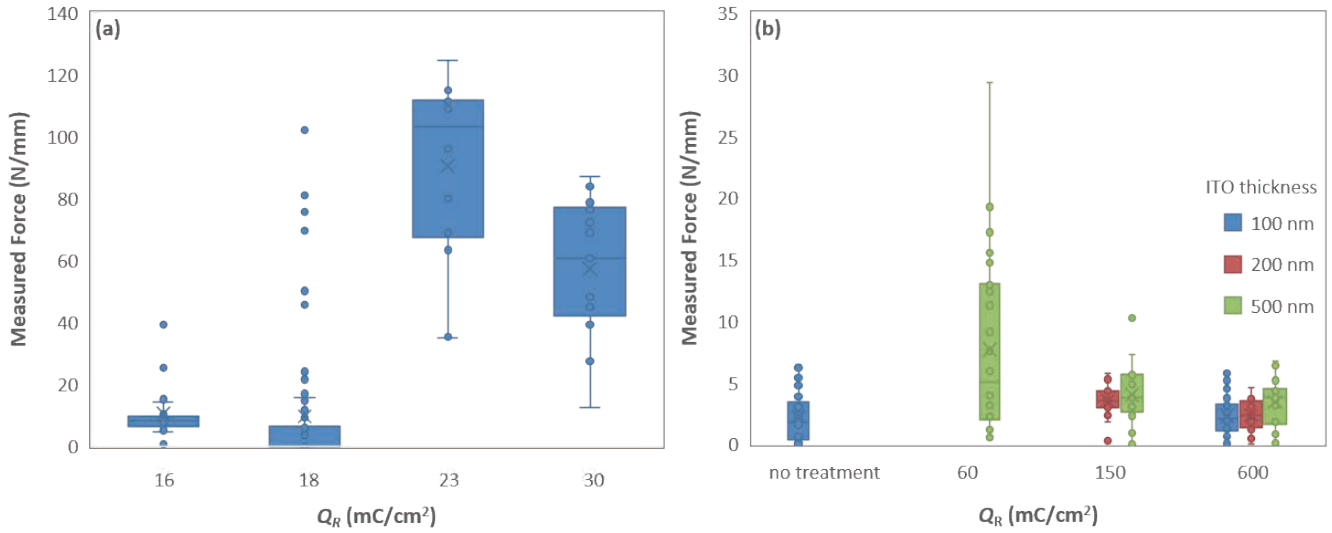

Fig. 6.6.2: (a) Results of pre-experiments on ITO layers from a different source yielded very promising adhesion results with this process and (b), only minor impact of different sensitisation treatments could be observed in experiments using the solar cells with evaporated ITO layers from NREL.

While in future experiments an InSn source with higher Sn content could be used to enable the use of a sensitisation process, an additional process for improving the adhesion of Cu plating to the low Sn I(T)O layers was investigated. After sensitising, a thin Cu seed-layer was grown with a very low current density (0.5 mAcm^{-2}), resulting in slow growth of small crystals, before plating up with a conventional process (20 mAcm^{-2}). While this process yielded only minor improvement of Cu plated to I(T)O layers a with thickness up to 200 nm, a strong increase of the measured adhesion force could be observed for 500 nm thick I(T)O layers (see Figure 6.6.3). This might be explained by the special surface morphology of the thick I(T)O layers. While all evaporated I(T)O layers showed a rough surface, the 500 nm thick layers showed partially overhanging terraces which are likely very beneficial for achieving good adhesion to this surface. Why this strongly increased adhesion has only been observed for processes involving a slow seed-layer plating process has not been understood to date.

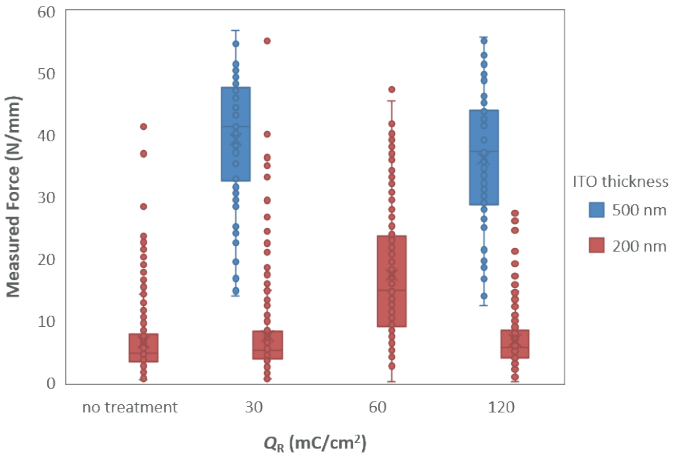

Fig. 6.6.3: A strong increase of the measured adhesion force was observed for 500 nm thick I(T)O layers.

Finally, 3D ray-tracing simulations were conducted in order to investigate the influence of different rear metallisation schemes on the optical properties of solar cells and to optimise the ITO thickness. It was found that NREL's optimised ITO layers show lower IR absorption than typical ITO layers found in literature. This has been achieved by employing lower doping densities and thus reducing free carrier absorption in the ITO layers. The simulations also showed that Cu plated directly on ITO should result in similar short-circuit current densities to Ag on ITO, while using seed-layers like Ni or W for Cu plating will for most ITO thicknesses result in a current loss of more than 0.2 mAcm^{-2} or 0.3 mAcm^{-2}, respectively (see Figure 6.6.4).

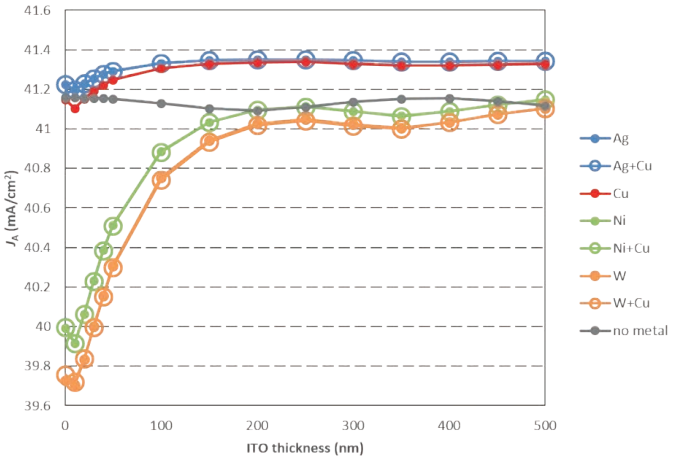

Fig. 6.6.4: A strong increase of the measured adhesion force was observed for 500 nm thick I(T)O layers.

Highlights

- Fabrication of solar cells featuring a B-diffusion on the front and a poly-Si back surface field (BSF) and ITO layer on the rear surface and understanding of the major loss mechanisms.
- Finding a suitable process for Cu plating to the ITO layer of this kind of solar cell and identifying limitations of the used ITO layers.
- Demonstration of high adhesion forces for very rough ITO layers after utilising a special Cu seed-layer plating step.

Future Work

- Optimise solar cell conversion efficiencies by omitting mistakes identified in the first cell run.
- Deposit ITO layers with much higher Sn content in order to enable sensitisation.
- Investigate suitability of ITO as a Cu diffusion barrier.

References

Liu, J.S., Laverty, S.J., Maguire, P., McLaughlin, J. and Molloy, J., 1994, "The Role of an Electrolysis Reduction in Copper-Electroplating on Transparent Semiconductor Tin Oxide," Journal of the Electrochemical Society, 141, 4, L38–L40.

Li, Z., 2016, "Chemical lithography and its applications for commercial high efficiency silicon solar cells," PhD, UNSW.

McIntosh, K.R. and Altermatt, P.P., 2010, "A freeware 1D emitter model for silicon solar cells", in 2010 35th IEEE Photovoltaic Specialists Conference, pp. 002188–002193.

Sugianto, A., Breitenstein, O., Tjahjono, B.S., Lennon, A., Mai, L. and Wenham, S.R., 2012, "Impact of localized regions with very high series resistances on cell performance", Progress in Photovoltaics: Research and Applications, 20, 4, 452–462.

Wang X. et al., 2016, "Monitoring of Adhesion for Plated Metallisation: Why Busbar Pull Tests are not Sufficient", Energy Procedia, 92, 978–983.

6.8 GaAs/Si Elongate Tandem Cells for Moderate Concentration

Lead Partner
ANU

ANU Team
Dr Matthew Stocks, Prof Andrew Blakers

Academic Partner
NREL

Funding Support
ARENA, ANU, NREL

Aim

Demonstrate the potential of mechanically stacked tandems to increase silicon module efficiency.

Progress

GaAs cell development has been undertaken in collaboration with NREL. NREL grew the active layers for the GaAs device. The precursor was 25 x 25 mm. Cell processing was then undertaken at ANU.

The major activity during 2017 was modification of the cell process sequence to enable better contacting and improvements in the removal of the sacrificial layers. The cell process relies on chromium as an adhesion layer for gold to the GaAs as can be seen in the left of Figure 6.8.1. This is necessary to ensure that the gold is not detached during the lift-off process to define the contacts. This resulted in chromium as the upward facing surface of the lower contacts.

The cell process was modified so that gold was evaporated through a shadow mask onto the GaAs cell surface prior to evaporation of the chromium and gold contacts for the rear cell contacts. The gold was aligned to the centre of the contacts and adhesion was maintained through the lift-off process. After final cell isolation, the gold contacts were then on the accessible surface for contacting.

The etching of the sacrificial layers has also been improved during 2017. A batch of cells demonstrated low voltage and non-ideal fill factors. Measurements of the step heights on the cells were made with a confocal microscope as shown in Figure 6.8.2. This indicated that some of the layers were not completely removed during processing. The etch rates for the layer removal process were re-characterised and adjusted to ensure that the entire thickness of the layers was removed. This improved both the voltage and the fill factor of the next batch

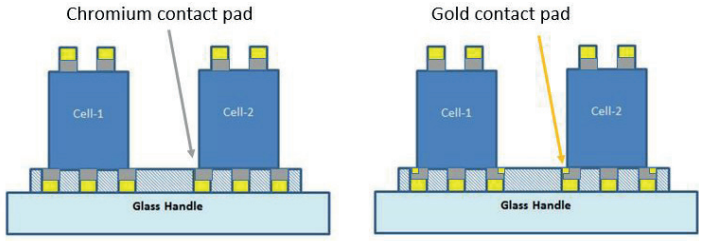

Figure 6.8.1: Schematic showing chromium adhesion layer and modified gold contacts.

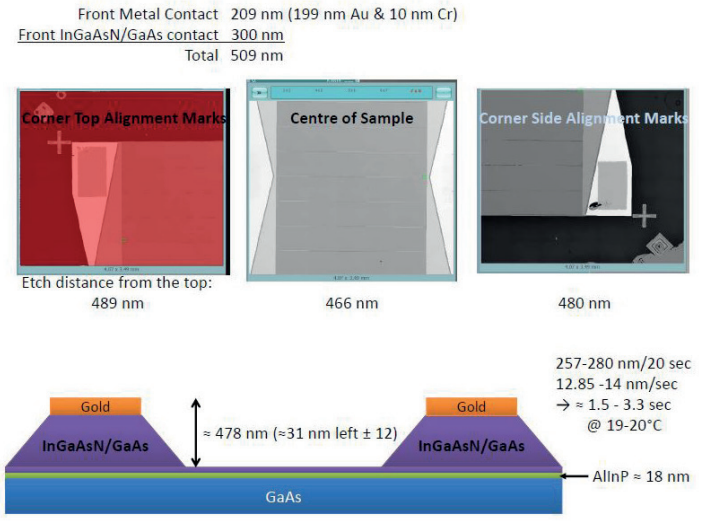

Figure 6.8.2: Confocal microscope measurements of layer heights in GaAs cells.

of cells. Subsequent processed cell batches have shown good improvement in both fill factor and voltage due to the improved interfaces.

Cells are now demonstrating very good voltage and fill factor, and consistency between cells, as can be seen in Figure 6.8.3. Voltage is now in excess of 1.06 V and fill factors greater than 84%. The addition of a double layer AR coating is expected to boost the efficiency over 25% as discussed in section PP1.3b.

The cell design and process has progressed to the point where the cells can now be used for the development of the stacked tandems described in section PP1.3.

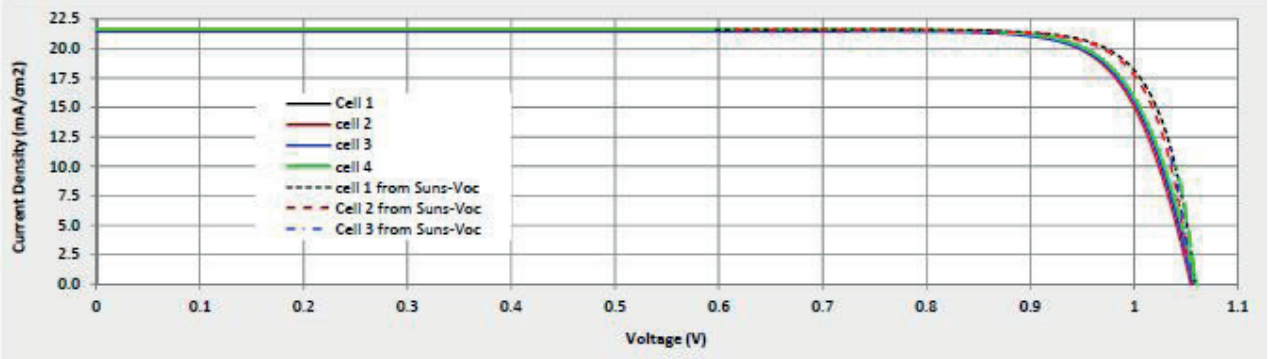

Figure 6.8.3: I-V curves showing consistency between the cells.

Highlights

- Modification of the cell contacts.
- Improvement in the V_{OC} and FF of the GaAs cell.

Future Work

- This collaborative project is now closed.

6.9 Advanced Hole-Selective Contacts to Replace Boron Diffusion

Lead Partner
ANU

ANU Team
Dr Yimao Wan, Prof Andres Cuevas, Mr Chris Samundsett, Dr Jie Cui, Ms Josephine McKeon

ANU Students
Thomas Allen, Peiting Zheng, Di Yan, Xinyu Zhang

ACAP Team
Dr James Bullock, Dr Mark Hettick, Professor Ali Javey (UCB, LBNL)

Academic Partners
University of California, Berkeley (UCB), Lawrence Berkeley National Laboratory (LBNL, including the Molecular Foundry)

Funding Support
ARENA, ACAP

Aim

One of the major factors limiting the further advancement of n-type low-cost silicon solar cells is the high temperature boron diffusion step, which causes a severe degradation in silicon material quality, with a reduction in bulk carrier lifetime by a factor of three. The advent of hole-selective heterocontacts offers a solution to the problem, plus additional advantages, including lower processing temperatures, a reduced requirement in cleanliness and a simpler fabrication procedure. This project aims to: (i) survey and trial a number of simple hole-selective contact (HSC) schemes; and (ii) transfer the most successful of these to low-cost silicon solar cells.

Progress

The screening trial of several possible candidates for HSC has been completed at ANU showing the following materials have promisingly low contact resistivity for holes: MoO_x, WO_x and NiO_x. The first proof-of-concept cells, based on both p-type and n-type substrates were also fabricated using the abovementioned three candidates demonstrating MoO_x and WO_x have great potential to replace boron diffusion to provide ohmic contact to p-type Si and junction contact to n-type Si substrates. Screening trials are also ongoing at UCB, focusing on MoO_x, WO_x, VO_x and CuZnS, complementing the absence of capability in evaporating VO_x and coating CuZnS at ANU. Proof-of-concept cells have been fabricated, showing reasonable ohmic contact to p-type silicon surfaces with a fill factor (FF) of ~50% using VO_x, but rectifying contact for CuZnS with an S-shape I-V curve. The overall trials demonstrated the best candidate for HSCs is MoO_x with FF ~60%.

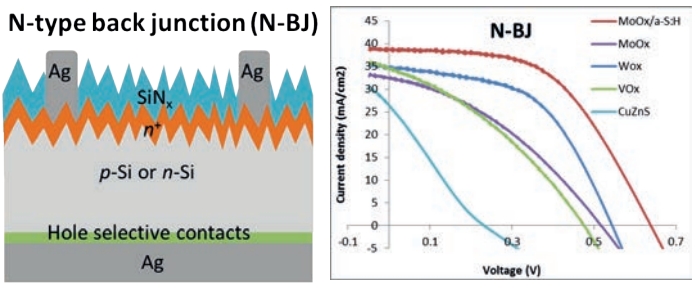

Figure 6.9.1: Screening trial results of several possible candidates for hole selective contacts.

Although the specific goal of this project is to develop HSCs for solar cells, its generic objective is to contribute to the new field of dopant-free silicon solar cells, complementing work done in a companion collaboration project. In that broader context, there has been a window of opportunity during 2016 and 2017 to develop new electron-selective contacts, including (i) magnesium fluoride, (ii) magnesium oxide, (iii) tantalum oxide, and (iv) titanium oxide. In addition, the new type of silicon solar cell (DASH) is improved to well above 20% with enhanced stabilities.

Passivated electron-selective contacts based on magnesium fluoride

Magnesium fluoride is well known for its optical, rather than electronic, properties. In this study we present a novel application to form the electron contact of silicon solar cells. The passivated electron contact is composed of deposited layers of amorphous silicon (~6.5 nm), magnesium fluoride (~1 nm) and aluminium (~300 nm). X-ray photoelectron spectroscopy revealed a work function of 3.5 eV for the MgF_2/Al stack, significantly lower than that of aluminium itself (~4.2 eV), thus enabling an ohmic contact to n-type crystalline silicon (c-Si). The optimised contact structure exhibits a sufficiently low contact resistivity of ~76 $m\Omega cm^2$, together with a very low contact recombination current density of ~10 $fAcm^{-2}$. Its implementation as a full-rear contact of n-type Si solar cells led to a 20.1% proof-of-concept device with a high open-circuit voltage of 687 mV.

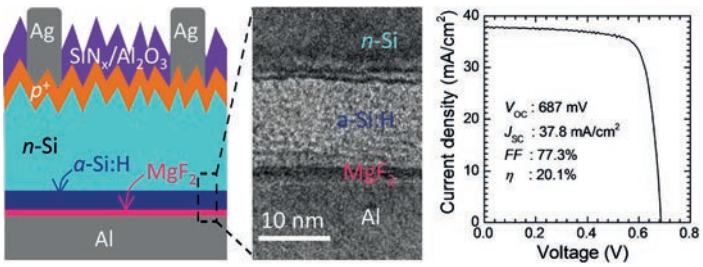

Figure 6.9.2: Passivated electron-selective contacts based on magnesium fluoride.

Magnesium oxide electron-selective contacts

A high Schottky barrier (> 0.65 eV) for electrons is typically found on lightly doped n-type c-Si wafers for a variety of contact metals. This behaviour is commonly attributed to the Fermi-level pinning effect and has hindered the development of n-type c-Si solar cells, while its p-type counterparts have been commercialised for several decades, typically utilising aluminium alloys in full-area, and more recently, partial-area rear contact configurations. Here we demonstrate a highly conductive and thermally stable electrode composed of a magnesium oxide / aluminium (MgO_x/Al) contact, achieving moderately low resistivity ohmic contacts on lightly doped n-type c-Si. The electrode, functionalised with nanoscale MgO_x films, significantly enhances the performance of n-type c-Si solar cells to a power conversion efficiency of 20%, advancing n-type c-Si solar cells with full-area

dopant-free rear contacts to a point of competitiveness with the standard p-type architecture. The low thermal budget of the cathode formation, its dopant-free nature, and the simplicity of the device structure enabled by the MgO_x/Al contact open up new possibilities in designing and fabricating low-cost solar cells.

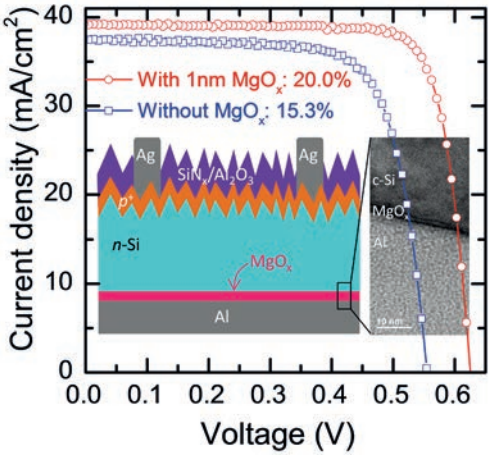

Figure 6.9.3: Passivated electron-selective contacts based on magnesium oxide.

Tantalum oxide electron-selective heterocontacts for silicon photovoltaics and photoelectrochemical water reduction

Crystalline silicon (c-Si) solar cells have been dominating the photovoltaic (PV) market for decades, and c-Si-based photoelectrochemical (PEC) cells are regarded as one of the most promising routes for water splitting and renewable production of hydrogen. In this work, we demonstrate a nanoscale tantalum oxide (TaO_x, ~6 nm) as an electron-selective heterocontact, simultaneously providing high quality passivation to the silicon surface and effective transport of electrons to either an external circuit or a water splitting catalyst. The PV application of TaO_x is demonstrated by a proof-of-concept device having a conversion efficiency of 19.1%. In addition, the PEC application is demonstrated by a photon-to-current efficiency (with additional applied bias) of 7.7%. These results represent a 2% and 3.8% absolute enhancement over control devices without a TaO_x interlayer, respectively. The methods presented in this paper are not limited to c-Si-based devices, and can be viewed as a more general approach to the interface engineering of optoelectronic and photoelectrochemical applications.

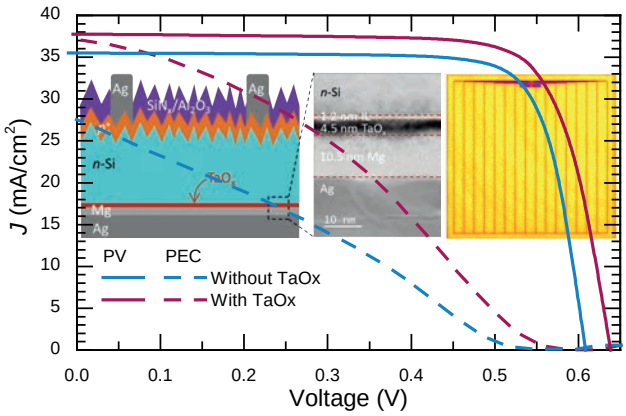

Figure 6.9.4: Passivated electron-selective contacts based on tantalum oxide.

Stable dopant-free asymmetric heterocontact silicon solar cells with efficiencies above 20%

Crystalline silicon (c-Si) absorbers have enjoyed a long-standing photovoltaics (PV) market majority share. Despite the maturity of c-Si PV technology, there remain a number of avenues to improve its cost-to-performance ratio. An especially promising idea is to switch to a heterojunction architecture that utilises metal oxides, fluorides, sulphides or organic materials to form the required selective contacts for electrons and holes. As with the maturation of any technology, a number of milestones must be met before this concept can be considered viable. This paper demonstrates two important milestones. Firstly, we show that by engineering the carrier-selective contacts an efficiency of 20.7% can be achieved – the highest value for this cell class to date. In addition, we show that this structure passes a standard stability test, maintaining > 95% of its original performance after 1000 hours in a damp heat environment – indicating its potential for longevity.

Finally, during the visit to UCB, a novel passivating thin-film zirconium oxide (ZrO_2) has been developed, providing high quality surface passivation of c-Si. A manuscript on this topic is anticipated to be submitted soon.

This project is now closed.

Highlights

- 20.1% n-type silicon solar cell with an a-Si:H/MgF2/Al full-area rear passivated contact.
- 20% n-type silicon solar cell with an MgOx/Al full-area contact.
- 19.1% n-type silicon solar cell and 7.8% photoelectrochemical water splitting reduction with a TaO_x full-area rear passivated contact.
- 20.7% n-type DASH silicon solar cell.

Future Work

- Publish a journal paper.

References

Wan, Y., Samundsett, C., Bullock, J., Allen, T., Hettick, M., Yan, D., Zheng, P., Zhang, X., Cui, J., McKeon, J., Javey, A. and Cuevas, A., 2016, "Nanoscale magnesium fluoride electron–selective contacts for crystalline silicon solar cells", ACS Appl. Mater. Interfaces, 8 (23), 14671–14677.

Wan, Y., Samundsett, C., Bullock, J., Allen, T., Hettick, M., Yan, D., Peng, J., Wu, Y., Cui, J., Javey, A. and Cuevas, A., 2016, "Conductive and Stable Magnesium Oxide Electron-Selective Contacts for Efficient Silicon Solar Cells", Adv. Energy Mater., 1601863.

Wan, Y., Samundsett, C., Bullock, J., Yan, D., Allen, T., Zheng, P., Zhang, X., Cui, J., McKeon, J. and Cuevas, A., 2016, "Magnesium fluoride based electron-selective contact", IEEE 43rd Photovoltaic Specialists Conference (PVSC), 2540–2542.

Wan, Y., Karuturi, S.K., Samundsett, C., Bullock, J., Hettick, M., Yan, D., Peng, J., Narangari, P.R., Mokkapati, S., Tan, H.H., Jagadish, C., Javey, A. and Cuevas, A., 2017, "Tantalum Oxide Electron-Selective Heterocontacts for Silicon Photovoltaics and Photoelectrochemical Water Reduction", ACS Energy Letters.

Bullock, J., Wan, Y., Xu, Z., Essig, S., Hettick, M., Wang, H., Ji, W., Boccard, M., Cuevas, A., Ballif, C. and Javey, A., "Stable dopant-free asymmetric heterocontact silicon solar cells with efficiencies above 20%", Submitted.

6.10 Advanced Light Trapping for High Efficiency Si Cells

Lead Partner
ANU

ANU Team
Prof Andrew Blakers, Dr Ngwe Zin,

AUSIAPV Partner: Georgia Institute of Technology (GIT), USA
University Center of Excellence for Photovoltaics (UCEP) – Ajay D Upadhyaya, Prof Ajeet Rohatgi

Academic Partners

University of Central Florida (UCF) (added following Dr Zin's move to UCF)

Florida Solar Energy Center (FSEC)

Funding Support
ARENA, ANU, GIT

Aim

Light trapping in most high efficiency silicon solar cell designs entails a textured front surface and a planar rear surface. Silicon solar cells incorporating double-sided pyramidal texture (DST) are capable of superior light trapping. However, the DST structure increases surface recombination. Modifying the rear texture in DST cells has the potential not only to improve light trapping significantly by more effective scattering, but also reduces surfaces, leading to increased cell conversion efficiency. Improved, highly effective and low-cost methods of light trapping will be developed that are compatible with very low surface recombination rates (5 $fAcm^{-2}$). This work will build upon and optimise existing work in modifying DST devices that has yielded very good light-trapping and low surface recombination rates.

Progress

This project has now been completed. This collaboration with the Georgia Institute of Technology and the University of Central Florida (which joined the project informally when Dr Ngwe Zin moved there in the second half of 2016) has demonstrated interdigitated back contact (IBC) solar cells incorporating rounded textured pyramids at the rear surface. The project demonstrated for the first time that rounded rear textured pyramids improve the optic and reduce the surface recombination concurrently. As compared to the structure with planar rear, rounded rear textured pyramids provide Lambertian reflection that improves light trapping significantly, while reducing surface recombination comparable to that on the planar substrate. The benefits of rounded textured pyramids were demonstrated in the development of IBC silicon solar cells reaching a conversion efficiency of 24% from this research.

Light trapping in most high efficiency silicon solar cell designs involves a textured front surface and a planar rear surface. The light trapping in these cells is less than ideal because a significant fraction of light rays incident to the rear surface are reflected into the escape cone of a front pyramid and are coupled out. Modifying the rear surface, such as by a Lambertian reflector, redirects the first-pass light to avoid this optical path and therefore increases the photogeneration current (see Figure 6.10.1).

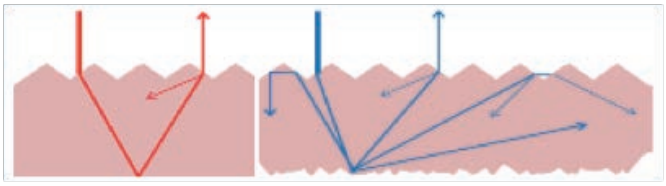

Figure 6.10.1: Comparison of rays when the rear surface is specular (red) and Lambertian (blue).

The team investigated double-sided texture incorporating rounded rear pyramids to increase light trapping while maintaining comparatively low surface recombination. For recombination study, samples were prepared with symmetrically planar, textured and rounded pyramids on both front and rear surfaces; while light-trapping samples have identical front side pyramidal texture, but with planar, texture or rounded texture at the rear. They first formed random pyramidal structures on all samples, followed by using an acid solution of 1:10 HF:HNO3 to create rounded texture pyramids. The acid etch was varied from 0 s, 30 s, 60 s and 90 s to create rounded pyramid structures resulting in pyramid heights of 3.6 µm, 2 µm, 1.5 µm and 1 µm, respectively, for all samples, except that front textured pyramids of light-trapping samples were masked during the acid etch. All samples were then passivated with the high quality hydrogenated amorphous PECVD SiN_x, developed at ANU. Figure 6.10.2 illustrates the 2D profile and 3D optical measurements of textured and rounded textured samples.

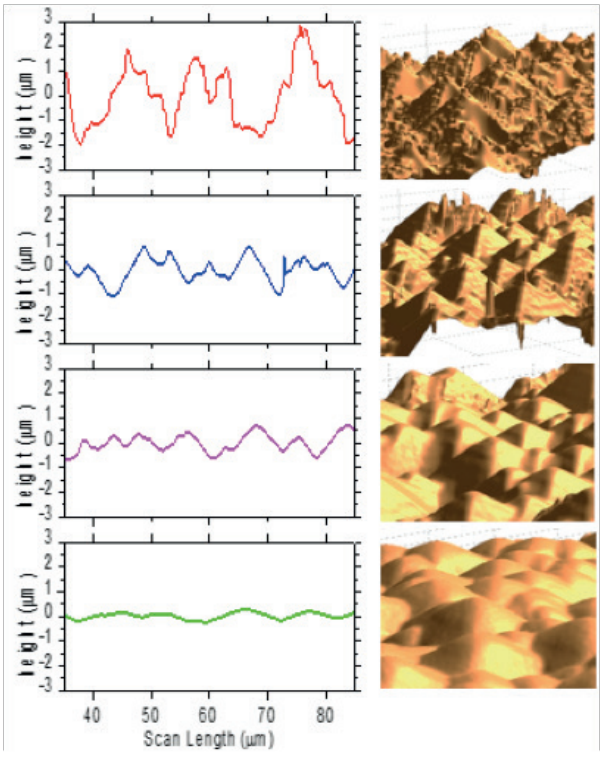

Figure 6.10.2: 2D surface profile and 3D images of textured pyramids scanned by the confocal microscope.

The recombination current prefactor J_o and effective carrier lifetime (T_{eff}) were measured by photoconductance decay (see Figure 6.10.3). Of all samples, the No R_{Etch} (i.e. 0 s rounding etch) sample has the largest J_o (per side) of 15 fAcm^{-2}; this is expected since it has the largest surface area and the sharpest peaks and valleys as compared to other samples. The J_o is significantly reduced by etching 1.6 µm of silicon (i.e. down to ~5 fAcm^{-2}, which is only 2 fAcm^{-2} higher than the planar sample). Thereafter, the J_o reduces only slightly at a ~0.5 fAcm^{-2} for each half-micron of Si etched. Further etching of the sample in HF:HNO_3 removes the pyramids and planarises the surface.

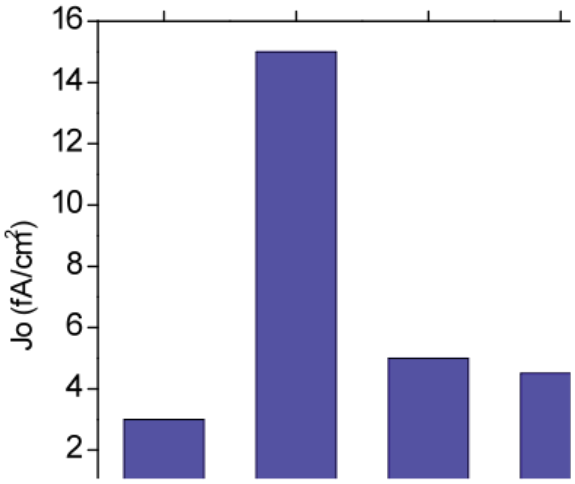

Figure 6.10.3: J_o of samples whose front and rear surfaces are (i) planar, (ii) textured with No R_Etch, Short R_Etch, Medium R_Etch and Long R_Etch.

Additional sets of samples having symmetrical planar, textured and rounded pyramid structures were prepared and passivated with a stack of thin oxide (SiO_2) and LPCVD SiN_x– a passivation and insulation dielectric stack used in the development of IBC silicon solar cells. One set of samples was measured for J_o and T_{eff} at ANU, and then sent to UCF to assess the degradation, while the other set was sent to GIT. The GIT team passivated the samples with a stack of SiO_2 and PECVD SiN. Table 1 shows J_o and effective carrier lifetime (T) of samples measured at ANU, GIT and UCF. There is a slight degradation observed with samples measured at ANU and UCF, even after six months. In general, passivation samples undertaken at GIT are also comparable to that at ANU.

The optical behaviour then was assessed by spectrophotometry and a wafer ray tracer (see pvlighthouse.com) at ANU. Figure 6.10.4(a) plots the measured total absorption against wavelength for each sample. It was difficult to conclude much from these results because we cannot distinguish between absorption in the silicon and absorption in the rear Al (i.e. parasitic absorption). It is evident, however, that there is a substantial difference in behaviour between the samples, emphasising that the variations in rear rounding have a significant impact on optical behaviour. We then employ ray tracing to determine (i) the current density generated in the silicon J_{gen} over the range 950–1200 nm, and (ii) optical pathlength enhancement Z(λ) (see Figure 6.10.4(b)). The ray tracing suggests that there should be an optimal rear pyramid angle. With 54.7° on the front and rear surface, many rays are coupled out of the cell in the first pass, and with a planar rear surface, many rays are coupled out of the cell after the second pass. An angle between 0 and 54.7° leads to superior light trapping. Thus, we experimentally observe that recombination at the rear surface is dramatically reduced, from 15 fAcm^{-2} to ~ 3 fAcm^{-2} by a short rounding etch. From ray tracing, we expect there to be an optimal rounding time that maximises light trapping, but this has neither been confirmed nor contradicted by optical experiments.

Lastly, back-contact silicon solar cells featuring rear rounded textured pyramids were developed to assess the feasibility of integrating rounded texture in the cell fabrication process. Samples with rear planar (treated as a control) and rounded pyramidal textured conditions were used. A single rounding condition with the etch duration of 60 s was adopted in this evaluation. Table 3 shows the current-voltage (J-V) of the cells measured under one-sun illuminated condition using an in-house solar simulator. Efficiencies in the range of 23.6–24.4% were attained. Relative to the cell with rear planar, the cell with rounded rear pyramids have achieved an increased J_{SC} of 0.25 mAcm^{-2} (from an average of three rear-rounded textured cells compared to that of rear planar cells), despite the cell substrate being thinner by at least 60 µm. However, a small reduction in V_{OC} is observed, as expected. Besides, the champion cell with rounded rear pyramids also suffers some fill factor (FF) loss of 0.5%, relative to the cell with planar rear, possibly due to unknown non-ideal recombination since the pseudo FF in the DST cells with rounded pyramids is lower than that in the cell with planar rear. Further investigations will uncover unexpected FF losses.

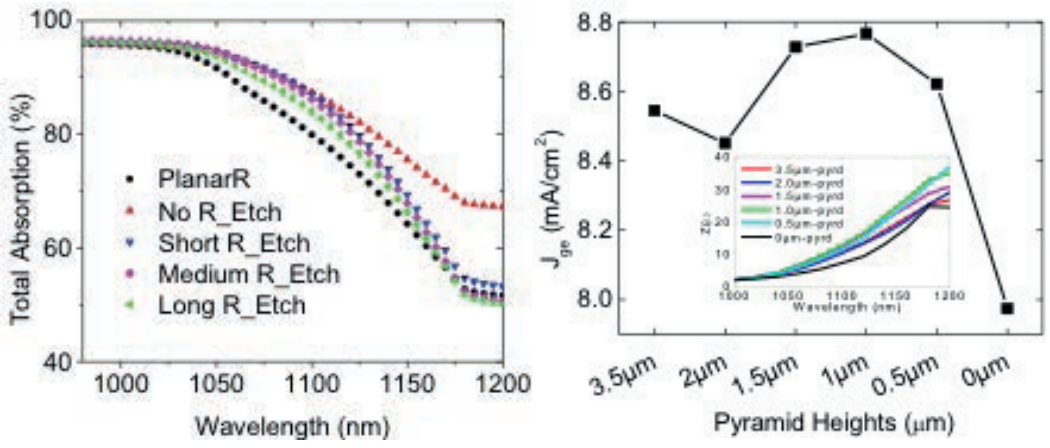

Figure 6.10.4: (a) Total absorption 1-R-T of samples with different front and rear surface conditions measured by the spectrometry technique. Measured T is effectively zero on samples with Al (1 µm) at the rear. Apart from the control that has planar morphology on both front and rear, the samples have identical front texture but differing rear texture; and (b) J_{gen} simulated for the wavelength of 950–1200 nm by the wafer ray tracer. The pathlength enhancement Z is shown in the inset figure.

		thickness (μm)	T_{eff} (μs)	T_{bulk} (μs)	Jo (fA/cm^2)	iVoc (mV)
ANU-P	planar	390	1780	29896	22	697
ANU-0R	tex	300	222	1550	155	651
ANU-30R	tex-30R	287	313	1063	75	659
ANU-60R	tex-60R	270	671	12436	45	684
ANU-90R	tex-90R	262	892	21923	33	692
GIT-P	planar	390	2205	8229	9	719
GIT-0R	tex	300	249	2219	109	659
GIT-30R	tex-30R	287	293	723	62	659
GIT-60R	tex-60R	270	635	4010	40	684
GIT-90R	tex-90R	262	791	9669	35	690
UCF-P	planar	390	1554	11665	23	690
UCF-0R	tex	300	210	2869	155	642
UCF-30R	tex-30R	287	275	722	75	645
UCF-60R	tex-60R	270	612	5265	45	675
UCF-90R	tex-90R	262	1554	7422	33	683

Table 6.10.1: Results of recombination study samples measured at ANU, GIT and UCF. Measurements were undertaken at the carrier injection of 5×10^{15} cm^{-3}.

Techniques of fabricating rounded textured pyramids, together with recombination and optical analysis results have also been disseminated to the collaborating GIT partner. GIT partners are also in progress to take full advantage of rounded textured pyramid structures in their high efficiency solar cell developments.

Further collaborations between ANU and UCF, which arose during the project, also continue in areas of investigating passivated contact solar cells, industrial high efficiency silicon solar cells, high quality junction formation and passivation.

Highlights

- Sample exchanges between ANU, GIT and UCF.

Future Work

- Further characterisation and analysis of samples.
- Write up project report.

6.11 Advanced Luminescence Studies of Si Wafers and Cells

Lead Partner
ANU

ANU Team
Prof Daniel Macdonald, Dr Hieu Nguyen

Academic Partner
Dr Mowafak Al-Jassim, Dr Steve Johnston, National Renewable Energy Laboratory (NREL), USA

Funding Support
ARENA, ANU, NREL

Aim

This project aims to combine complementary expertise at ANU and NREL in the field of luminescence characterisation of materials for solar cells. In particular, the advanced high resolution luminescence methods developed at NREL for thin-film photovoltaic materials will be applied to some outstanding challenges in silicon photovoltaics, especially in relation to understanding key defects in silicon solar cells and deposited layers.

Progress

This two-year project was commenced in July 2016. Dr Nguyen from ANU made a one-week visit to NREL in August 2016, during which time he familiarised himself with the numerous high resolution tools available at NREL and defined collaborative research topics in detail. Dr Nguyen then made a 7-month visit to NREL from March to November 2017 to carry out these activities.

Highlights

- Seven-month visit to NREL by Dr Nguyen (March to November 2017).
- Invention of a camera-based photoluminescence (PL) technique to image nanometer-thin coating layers with micron-scale spatial resolution.
- Invention of a spectral PL-based technique to quantify and map sheet resistances of heavily doped regions in Si solar cells with spatial resolution approaching the fundamental limit.
- Capability expansion for the PL-imaging system at NREL by Dr Nguyen: a UV-excitation source for imaging high bandgap materials and a polariser for imaging defects in c-Si wafers.
- Two co-authored papers published in the journal *Solar RRL*. The first of these featured as the journal's cover story for that issue (see Figure 6.11.1).
- One invited talk by Dr Nguyen at the 27th Workshop on c-Si Solar Cells and Modules, Breckenridge, CO.
- NREL's support (AU$120K in-kind plus equipment access) for Dr Nguyen's ACAP fellowship, which will be commenced in January 2018.

Future Collaboration

The project has been very successful in building a collaboration between ANU and NREL. The NREL team hosted and provided Dr Nguyen with the technical support and access to their state-of-the-art characterisation facilities during his seven-month visit. In return, Dr Nguyen helped the NREL team establish new capabilities for their luminescence spectroscopy and imaging tools, expanding applications into many high bandgap materials and defects in photovoltaic materials and devices. Dr Nguyen has also transferred the developed characterisation techniques to the scientists at NREL.

The project has established a solid foundation for a strategic, long-term collaboration between the two characterisation teams of Prof Daniel Macdonald at ANU and the principal scientist Dr Mowafak Al-Jassim at NREL. In particular, Dr Nguyen has secured a committed support of AU$120K in-kind and equipment access from the NREL team for research activities related to photovoltaic device/material characterisation for the next three years, as part of an ACAP fellowship. Also, a prospective visit to ANU by Dr Mowafak Al-Jassim in early 2018 will further define strategic directions for future collaborations between the two groups.

References

Nguyen, H.T., Johnston, S., Basnet, R., Guthrey, H., Phang, S.P., Dippo, P., Al-Jassim M., and Macdonald, D., 2017, "Imaging thickness and refractive index of dielectric films with unprecedented spatial resolution using photoluminescence", Solar RRL 1, 1700157.

Nguyen, H.T., Johnston, S., Paduthol, A., Harvey, S.P., Phang, S.P., Samundsett, C., Sun, C., Yan, D., Trupke, T., Al Jassim M. and Macdonald, D., 2017, "Quantification of sheet resistance in boron-diffused silicon using micro-photoluminescence spectroscopy at room temperature", Solar RRL 1, 1700088.

6.12 De-cohesion Analysis of Printed Solar Modules

Lead Partner
CSIRO

CSIRO Team
Dr Fiona Scholes, Dr Hasitha C Weerasinghe, Dr Doojin Vak

CSIRO Student
Xiaojin Peng (PhD Student)

Academic Partners
Stanford University (USA), Prof Reinhold H. Dauskardt / Nick Rolston (PhD Student)

Georgia Institute of Technology (USA), Prof Samuel Graham

Funding Support
ACAP / AUSIAPV

Aims

The aim of this project is to quantitatively analyse the adhesion between layers and the cohesion of each layer of large-area printed perovskite-based and organic solar cell modules employing newly developed quantitative mechanical analysis systems in collaboration with Prof Reinhold Dauskardt's research group at the Stanford University. Printed modules consisting of different device structures and printed systems exposed to different environmental conditions are being evaluated during this project. The mechanical integrity of existing and new encapsulation architectures exposed to different environmental stress conditions for prolonged periods are also being evaluated.

Progress

Primarily over the first year of the project, the CSIRO team has focused on producing efficient perovskite-based solar cell (PSC) devices on flexible polymer substrates using roll-to-roll (R2R) printing methods. Several printing trials were conducted under ambient conditions to optimise the printed layers of the devices. Flexible PSC devices with PCE > 10% have been demonstrated. The R2R processed printed structures (PET | ITO | ZnO | perovskite, PET | ITO | ZnO | perovskite | PEDOT:PSS, PET | ITO| ZnO | perovskite | PEDOT:PSS | MoO_3 | Ag) were prepared in the same manner as the high efficiency complete devices and were sent to Stanford University for mechanical fracture analysis using the double cantilever beam (DCB) test (see Figure 6.12.1). Perovskite photoactive thin films are a highly tuneable system, with numerous inorganic and organic cations readily incorporated to modify optoelectronic properties, and the effect of various cations on the mechanical properties of perovskites have been largely overlooked. Therefore, during the first part of this project, the cohesion energy of flexible perovskite systems containing various cation combinations of methylammonium (MA) and formamidinium (FA) were analysed. The calculated cohesion energy (G_c) of these systems is shown in Figure 6.12.2(a). Furthermore, Figure 6.12.2(b) illustrates a comparison of cohesion energy of different systems prepared using other additives such as caesium (C_S), butylammonium (BA), and 5-aminovaleric acid (AVA). A trade-off was observed between Gc and PCE, likely due to the fact that design for efficiency has dominated the development of perovskite solar cells while mechanical integrity has to date been an afterthought.

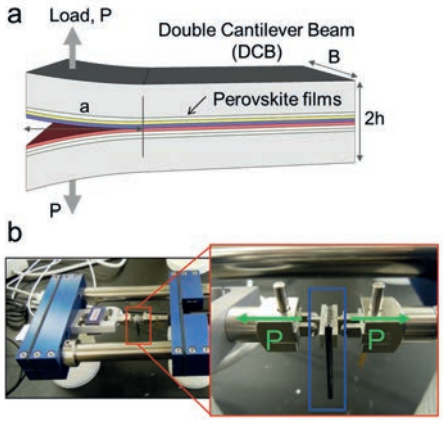

Figure 6.12.1: (a) Schematic of the double cantilever beam geometry used for mechanical testing to quantify Gc; and (b) photographs of the mechanical testing set-up, comprising a sample loaded.

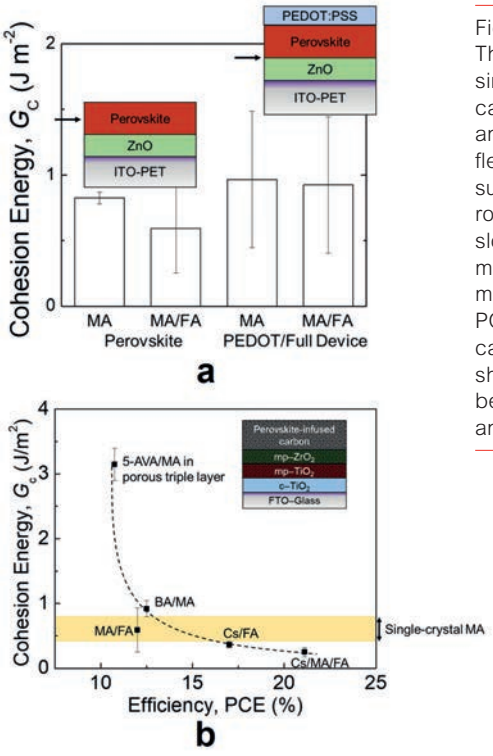

Figure 6.12.2: (a) The measured G_C for single- and double-cation perovskites and devices on flexible ITO-PET substrates using roll-to-roll (R2R) slot-die coating method; and (b) the measured G_C and PCE as a function of cation composition, showing a trade-off between reliability and efficiency.

Phenyl-C61-butyric acid methyl ester (PCBM) is a widely used electron transport layer in low-cost p-i-n perovskite solar cells. Seldom reported, PCBM brings tremendous challenges with respect to scaleable manufacturing methods due to its aggregation tendencies which also impact mechanical integrity and stability of devices. We have been able to successfully substitute PCBM with a non-fullerene indacenodithienol-based molecule, 3,9-bis(2-methylene-(3-(1,1-dicyanomethylene)-indanone))-5,5,11,11-tetrakis(4-hexylphenyl)-dithieno[2,3-d:2',3'-d']-s-indaceno[1,2-b:5,6-b'] dithiophene, (ITIC) as an electron transport layer (ETL) under ambient conditions without active humidity or temperature control and with the use of non-halogenated solvents. A double cantilever beam (DCB) test was used to evaluate the mechanical integrity of ITIC-based systems compared with the PCBM-based systems through measuring the fracture energy (G_c) of thin films. DCB results are outlined in Figure 6.12.3 and ITIC systems exhibited a 16-fold increase compared with PCBM systems. Furthermore, DCB results indicate that PCBM is one of the most fragile materials used in perovskite solar cells, with a G_c below 0.2 Jm^{-2} and ITIC is a more mechanically robust alternative to PCBM and other fullerene derivatives.

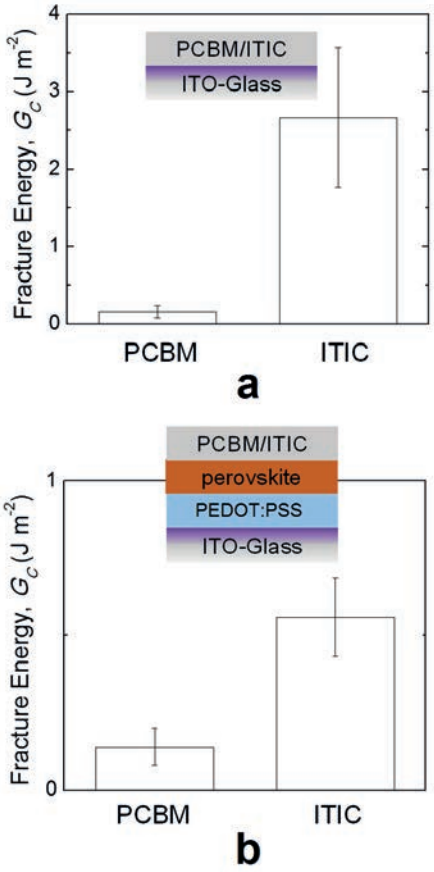

Figure 6.12.3: The measured Gc values of PCBM or ITIC systems deposited on (a) ITO-glass and (b) perovskite, showing a significant increase in mechanical integrity for ITIC-based systems.

Highlights

- The effect of cation composition of the perovskite layer has been studied for the first time and it was found that the multiple -cation perovskite has lower fracture energy than the single-cation perovskite.
- Mechanical stability issues with PCBM-based perovskite systems have been identified.
- In comparison with PCBM, ITIC has been demonstrated as a more suitable candidate for an electron transport layer, offering superior mechanical properties and upscaling compatibility.
- Preliminary results gathered during this project on the de-cohesion analysis of perovskite-based structures has been published in an international journal and were presented at several conferences held in Australia and USA.
  - "Effect of Cation Composition on the Mechanical Stability of Perovskite Solar Cells", Advanced Energy Materials.
  - "Organic and Perovskite-based Photovoltaics on Flexible substrates: Fabrication and Encapsulation", EMN Americas Meetings, Orlando, FL, USA.
  - "Effect of Composition and Microstructure on the Mechanical Stability of Perovskite Solar Cells", 5th ACAP Conference, Melbourne, Australia.
  - "Effect of heat, UV radiation, and moisture on the de-cohesion kinetics of inverted organic solar cells", AUCAOS Symposium, Kingscliff, New South Wales, Australia.

Future Work

We will continue to further improve the efficiency of flexible, R2R printed PSC devices by introducing alternative electrode materials and fabrication processes such as gravure and reverse gravure coating methods. Evaluation of these printed PSC systems using mechanical fracture analysis facilities available at the Stanford University will also be continued. It is also expected that comparative aging experiments will be performed by storing the printed films under different environmental conditions to evaluate if double-cation cells (FAI-based PSC devices) are more resistant to moisture. Furthermore, lifetime studies on the encapsulated PSC devices/ modules followed by DCB tests will also be carried out.

6.13 Determining Charge Lifetime and Mobility Dynamics in Organic Semiconductors for Photovoltaic Applications

UoM Team
A/Prof Trevor Smith, Dr Wallace Wong, Dr David Jones

UoM Students
Ms Kyra Schwarz, Mr Ahmed Alqatari

NREL / University of Colorado Boulder, USA Team
Prof Garry Rumbles, Dr Obadiah Reid

Funding Support
AUSIAPV, ARC, UoM, NREL

Aims

- Acquire expertise in the use of time-resolved microwave conductivity (TRMC) with a view to future implementation of this method in Australia to assist the broader photovoltaic community.
- Conduct time-resolved microwave conductivity measurements on new high performance OPV materials.
- Construct a novel long timescale transient absorption spectroscopy system and conduct measurements of these materials under the lowest possible light fluence conditions to determine excited state kinetics in the absence of multi-excitonic effects.

Progress

Prof Garry Rumbles visited Melbourne for two weeks during 2017. His visit facilitated discussions with colleagues at UoM, Monash, RMIT, UNSW and others on a number of topics relating to ACAP-supported work. In particular, discussions concerning the intricacies of TRMC measurements proved highly valuable in selecting the most appropriate specifications for the system to be installed in Melbourne as a result of a successful collaborative grant application between the UoM and Monash University nodes, and RMIT University. Further discussions on the provision of such an instrument have also been held with a commercial company, but its installation has been delayed until 2018. During his visit, Prof Rumbles also attended the 2017 Asia-Pacific Solar Research Conference in Melbourne.

Attempts to have a student visit NREL for a period of time to perform TRMC measurements on their system have been hampered by visa and other access issues, so alternatives to this are being pursued. The TRMC instrument to be purchased has been delayed and is due for installation in 2018.

The construction of transient absorption apparatus that is capable of recording transient absorption data on femtosecond to microsecond timescales is nearing completion in the UoM node, and is in the final stages of implementation and optimisation. This instrument is being constructed by MSc. student, Mr Ahmed Alqatari, assisted by a research assistant employed part-time through this project. This apparatus will permit excitation of samples, ranging from solutions through to thin films, using our existing tuneable, low pulse energy, high pulse repetition rate femtosecond laser system, but rather than using the usual optical delay between the pump and probe pulses, an electronic delay will trigger the output of a white-light probe pulse from a commercial super-continuum laser. The laser exhibits significant timing jitter between it being triggered and when a white light pulse is emitted. A timer unit records the actual time of emission relative to the trigger time and this time is tagged to the spectrum recorded for each particular event. These measurements are recorded at ~2,000 spectra/second. This approach may also be adapted to a transient absorption microscope currently being developed, which will enable the transient absorption dynamics to be mapped over micrometre spatial scales in thin films. Intermediate timescales (to ~4 ns) will be accessed by a longer translation stage currently being installed. Simultaneously, we have developed a system capable of recording time-resolved emission images of long-lived samples that will be of use for studying luminescent materials with long-lived excited states, such as perovskites, and will provide complementary information to the long timescale transient absorption data.

Highlight

- The long timescale transient absorption apparatus based on a high repetition rate, low pulse energy laser system is producing its first preliminary data.

Future Work

- Professor Garry Rumbles and/or Dr Obadiah Reid will visit Melbourne again during 2018 to help with the optimisation and benchmarking of the TRMC system to be based in Melbourne.
- New materials are being synthesised that show great promise for applicability in photovoltaic applications. A/Prof Trevor Smith and/or postdoctoral fellow, Chris Hall, will visit NREL to perform TRMC measurements on existing materials and these new compounds to benchmark results ahead of the installation of the system in Melbourne during 2018. Parameters such as sensitivity and time resolution that the new instrument must reach will be set.
- The long timescale transient absorption apparatus will be used to investigate the excited state dynamics of new materials being synthesised in the Jones and Wong groups. Minor optimisation of this instrument should provide higher signal to noise data covering spectral data spanning several orders of magnitude in time, which will help us identify the photophysical processes occurring in these materials and thereby facilitate methods to optimise their performance.
- The TRMC and transient absorption instruments will be used to study time-resolved processes in a wide range of polymeric and small molecule organic materials as well as perovskite-based materials being developed through other initiatives.

6.14 Screening Singlet Fission in Organic Semiconductors for Photovoltaic Applications

UoM Team

Dr David Jones, Prof Ken Ghiggino, A/Prof Trevor Smith, Dr Lars Goerigk

UoM Students

Ms Kyra Schwarz, Ms Saghar Masoomigadarzi

Princeton University (USA)

Prof Gregory Scholes

Georgia Tech, USA

Prof Seth Marder

RMIT University

A/Prof Tachibana

Funding Support

AUSIAPV, ARC, UoM, Princeton University, Georgia Tech

Aims

- Develop a reliable spectroscopic screening method for detecting singlet fission in organic semiconducting materials.
- Investigate the application of time-resolved 2D spectroscopy for characterising singlet fission.
- Screen existing organic semiconductor materials library and new organic materials from AUSIAPV partners for singlet fission.

Progress

Singlet fission (SF) is a process in which one singlet excited state shares its energy with a neighbouring chromophore and makes a triplet pair. As a result, it has the potential to increase the efficiency of solar cells. However, there are only a few known compounds that undergo singlet fission with high yield, such as tetracene, diphenyltetracene, rubrene, pentacene, diphenylisobenzofuran and zeaxanthin, so it is important to design new chromophores for singlet fission. On the other hand, this process is highly dependent on the crystallinity of the film and the coupling between neighbours, as for these systems SF is an intermolecular process. The possible solution would be SF based on an intramolecular process in which molecular coupling and orientation are less critical in determining the SF efficiency. We have designed new chromophores based on an acceptor-donor-acceptor strategy with two acceptors having low energy triplet states. One of the main requirements of SF is energy level matching, i.e. the energy of the singlet state should be greater than or equal to twice the energy of the triplet state, and time-dependent density function theory (TD-DFT) was used to evaluate the excited state energy level of the proposed compounds. As a result of these calculations, a series of small molecules and polymers, based on building blocks comprising benzodithiophene (BDT), as an electron-rich unit, and bisthiophene-2,5-dihydropyrrolo[3,4- c]pyrrole-1,4-dione (DPP), as the electron acceptor unit, were synthesised and characterised. Measurements required to identify the presence of triplet states are complicated since the triplet state should lie at an energy that would exhibit (weak) emission in the near infrared region (NIR) of the spectrum. NIR emission spectroscopy has been performed at low temperatures in order to find evidence for phosphorescence indicative of the energy of the triplet state between the ground and first excited singlet state. A weak emission has been detected at ~1200 nm, very close to the energy predicted by computational methods, and suggestive of an energy level landscape amenable to SF. Triplet energies were also studied by sensitisation processes using palladium octaethylporphyrin (PdOEP) as a triplet sensitiser to populate the triplet.

Time-resolved transient absorption measurements over a wide range of wavelengths and timescales have been performed using a series of instruments to record the formation of singlet and triplet excited states and indicate the presence of SF. These measurements have been performed in collaboration with A/Prof Tachibana at RMIT University.

Attempts to perform 2D ultrafast spectroscopic measurements have been thwarted to date by the denial for a visa that would have enabled PhD candidate Ms Saghar Masoomigadarzi to screen the new compounds using this approach. Another of our recent PhD graduates, Dr Kyra Schwarz, began a postdoctoral position in the Scholes group at Princeton during 2017, which should enable these screening measurements to be performed in the near future.

We have initiated a screening program using the spectroscopic techniques developed in-house on materials within the ACAP network that may support SF. These materials have a structure analogous to those synthesised using the design criteria for $BDT(DPP)_2$ above. We have identified an excellent candidate that appears to support SF in a solution-processed film, and in the solid state.

Prof Scholes visited UoM during 2017, which facilitated further discussions on the potential of using 2D spectroscopy methods for screening potential SF materials. Prof Seth Marder visited UoM in January 2018.

Figure 6.14.1: Prof Greg Scholes (Princeton), far left, and Prof Garry Rumbles (NREL/University of Colorado Boulder), second left, with Prof Ken Ghiggino and A/Prof Trevor Smith during their collaborative visits to UoM in December 2017.

Highlights

- New materials exhibiting hallmark indicators of SF have been synthesised and tested using steady-state and ultrafast laser spectroscopic techniques. A manuscript reporting this work is in preparation for submission.
- A materials screen of known compounds, with similar structural features to the $BDT(DPP)_2$ discussed above, has identified a candidate material which appears to be a better SF material in the solid state than $BDT(DPP)_2$. A more detailed characterisation of this material is currently underway.

Future Work

- We have undertaken a program to synthesise derivatives of the materials discovered to date exploiting approaches to enhance the efficiency of triplet state formation in an attempt to further increase the efficiency of the SF process.
- UoM team member, David Jones will visit both USA partners in 2018 to finalise elements of this work and pursue other forms of funding to continue this area of research.

References

Masoomi-Godarzi, S., Tachibana, Y., Smith, T.A. and Jones, D.J., “Intra vs. intermolecular singlet fission in new donor-acceptor organic compounds for potential application in organic photovoltaic solar cells”, in preparation.

Masoomi-Godarzi, S., Smith, T.A. and Jones, D.J., “New Donor-Acceptor based compounds for singlet fission”, SPIE Photonics West (accepted).

6.16 Design Optimisation of Silicon Sub-Cells in GaAsP/Si Tandem Cells

Lead Partner
UNSW

UNSW Team
A/Prof S. Bremner, A/Prof A. Ho-Baillie, Dr H. Mehrvarz, Prof M. Green

UNSW Student
Chuqi Yi

Academic Partner
Ohio State University (OSU): Dr T. Grassman, Prof S. Ringel

Funding Support
ARENA, ACAP

Aim

The aim of this project is to determine the optimum design for an active silicon substrate operating as the bottom sub-cell in a III-V/Si multi-junction solar cell. This must be done with a process flow compatible with III-V growth.

Progress

Working with our partners at OSU, the growth of GaP buffer–based III-V material on silicon has continued, using OSU's groundbreaking growth approach (Grassman, 2009). Experimental results for two typical GaP on Si solar cells, p-type front junction and n-type rear junction, have been compared with simulation results from simulation models that were previously built in Sentaurus technology computer-aided design (TCAD). The IRV of GaP/Si for the measured samples were identified by fitting the measured and simulated EQE data. Key silicon cell design aspects such as doping profiles were then examined to gain insights into the effect of GaP layer on the design and performance of silicon bottom cells.

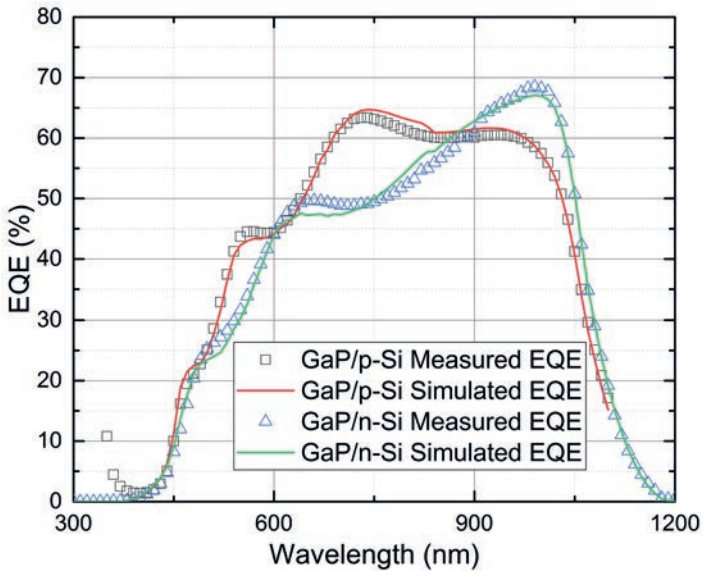

Figure 6.16.1: Simulated and measured EQE for GaP/p-Si front junction and GaP/n-Si rear junction cells. With no anti-reflection layers these results indicate lifetime preservation for the silicon wafer after III-V material growth.

Figure 6.16.1 shows the results for the measured and simulated EQE data of the GaP on p- and n-type silicon cells plotted together, where the solid lines represent the best fit using our TCAD model. The first thing to note is that these results are for structures with no anti-reflection coating (ARC) layers, with the results presented and photoluminescence imaging indicating the minority carrier lifetime has been preserved. This lifetime preservation is responsible for the p-type silicon solar cell design with a GaP layer delivering an open circuit voltage of 595 mV, in excess of the 580 mV level required for one of the project's milestones.

As can be seen in Figure 6.16.1, the TCAD model provides a reasonable fit between measured and simulated EQE data, especially at short and long wavelengths. This is achieved by varying the interface recombination velocity (IRV) at the front and rear (i.e. the level of recombination at the Si interfaces). A GaP/Si IRV of 5×10^4 cms^{-1} is extracted for both polarity cells, indicating a fairly good interface with low dislocation density was achieved for GaP nucleation on both p-type and n-type silicon substrates (simulations of previous samples have indicated IRVs of 5×10^4 cm^{-1} and higher). Previous results as part of this project have shown that the GaP/Si IRV is a critical design parameter for any multi-junction device (Almansouri, I., et al., 2015).

The same models that were used to achieve such good fitting of the EQE data from the fabricated two-cell topologies were then used to further explore how the front surface field– (FSF) junction design affects the silicon solar cell performance. For GaP/p-Si cell, front emitter doping profiles with peak doping density and junction depth ranging from 1×10^{17} to 1×10^{20} cm^{-3} and 0.25 to 10 µm were examined. The simulation results as shown in Figure 6.16.2 indicate, while heavily diffused emitter is preferred for better contact with GaP layer (Almansouri, I., et al., 2015), the intentional long drive-in step is responsible for the low spectral response of the fabricated cell, especially in the short wavelength range. When the emitter peak doping is low ($\leq 1 \times 10^{18}$ cm^{-3}), varying of the junction depth has only a minimal impact on the cell's predicted spectral response. However, when the peak doping is high, a shallow junction is preferred.

These results have been incorporated into the next round of samples to check experimental results against the model predictions. The incorporation of rear texturing has been achieved, but experimental results are pending to validate the model and allow predictions as to the optimum design. In addition, a model incorporating amorphous silicon passivation has been developed with the first experimental results due soon.

Highlights

- Delivery of silicon solar cell with an open circuit voltage of 595 mV satisfying one key milestone of the project.
- Preservation of minority carrier lifetime, proven by EQE and photoluminescence imaging methods as well as photoconductance decay.
- Good matching of Sentaurus TCAD–based model to experimental results from both p- and n-type wafer silicon solar cell designs. The modelling suggests the front surface field doping profile requires fine-tuning to optimise carrier collection for rear junction (n-type wafer) designs.

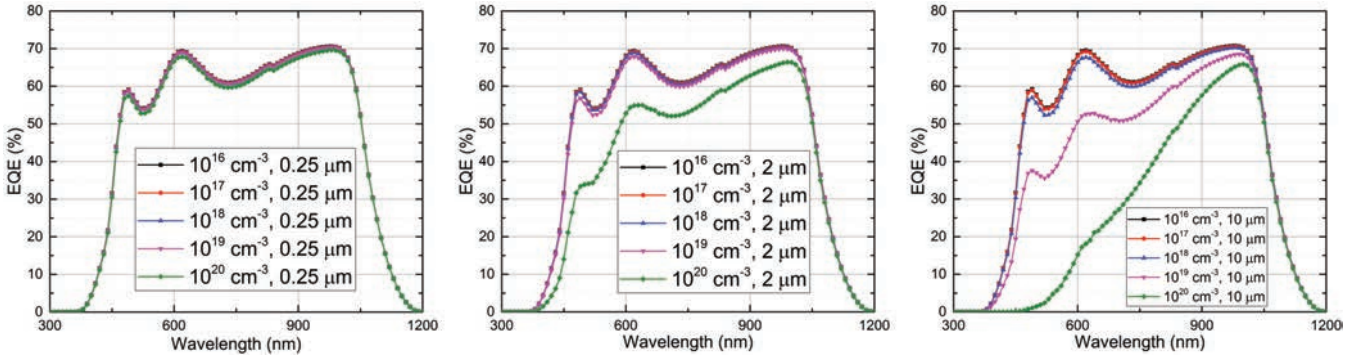

Figure 6.16.2: Simulated EQE for GaP/n-Si cell with various peak doping (PD) level and junction depth (JD) for the front surface field (FSF) diffusion. Junction depths of 0.25, 2.0 and 10.0 µm are shown for various peak doping levels. These results suggest the design of the FSF Is a critical part of any final device.

Future Work

- Deposition of GaP buffers on silicon wafers with optimised diffusion profiles is proceeding and the first wafers with rear texturing are being processed, with deposition on these structures to follow soon after. The characterisation results for these structures will be compared to predictions made by our Sentaurus TCAD models and further optimisations implemented.
- Investigations of the mechanism for preserving the minority carrier lifetime during III-V growth will continue. Initial results have proven confusing with further studies planned to resolve the mechanism.
- The passivation of the rear surface by amorphous silicon will also be undertaken and the results compared with a model for this passivation These results and insights will be used to support OSU's ongoing work on III-V/Si multi-junction solar cells and UNSW's own development of the next generation of silicon sub-cells.

References

Grassman, T., et al., 2009, "Control and elimination of nucleation-related defects in GaP/Si(001) heteroepitaxy", Applied Physics Letters, 94, 232106.

Almansouri, I., et al., 2015, "Designing bottom silicon solar cells for multijunction devices," IEEE Journal of Photovoltaics, 5(2), 683–690.

6.17 Cost Evaluation of Emerging PV Technologies

Lead Partner
UNSW

UNSW Team
Dr Anita Ho-Baillie, A/Prof Renate Egan, Prof Martin Green

UNSW Student
Nathan Chang

ACAP Team
CSIRO, Monash

Academic Partners
NREL

Overview

Energy from photovoltaics is increasingly competitive in many markets, yet studies point to the need for continuous improvements in efficiency and cost to provide increased market share and to create new markets. Incremental changes in efficiency and cost are expected to continue to drive down the prices of the incumbent technologies: silicon and, to a smaller extent, CdTe. Further, opportunities exist for step-change through new materials, such as the organohalide perovskites, and new structures, such as tandem solar cell devices.

A key criterion in progressing these new technologies from research to commercialisation is an accurate projection of the manufacturing cost. For emerging technologies many things change with scale, with location and over time so the performance and cost in high volume production can only be estimated. Nevertheless, well-informed analysis is required and provides the basis for making useful decisions while recognising and estimating this uncertainty.

This collaborative project combined the world-leading technical expertise and close links to manufacturing at UNSW in Australia with the established credibility in techno-economic analysis at NREL. The formal collaboration reinforced the established relationships and knowledge sharing in the areas of manufacturing costing and techno-economic analysis.

Aims

The project targeted enhanced collaboration with world-leading techno-economic analysts at NREL and delivered well-informed analysis of manufacturing costs for key ACAP technologies to assist in guiding research directions and decision making.

This project outcomes were aligned with program PP4 and are aligned with NREL's objectives in techno-economic analysis.

Progress

For developing technologies, many of the input values needed for costing are unknown. Working with colleagues at NREL, principally with Michael Woodhouse, the team at ACAP has developed novel approaches that permit the consideration of a range of allowed values for each cost parameter in order to carry out uncertainty analysis. This approach delivers outputs that can be used to focus research and development resources on the key cost drivers.

To develop the uncertainty analysis, a nominal value is recorded as the best estimate of the input parameter, while low and high values represent the uncertainty range. The impact of the uncertainty in each parameter is assessed using Monte Carlo analysis. Typically, 5,000 scenarios are generated, and each input parameter is independently assigned a random value according to a "two half normal distribution", where the median of the distribution is the nominal estimate, and the 10th and 90th percentile marks provide the low and high estimates respectively.

The distribution of the cost results from each scenario is evaluated to indicate the uncertainty of the calculated results and delivers a probability distribution for the total module manufacturing cost. This probability distribution can be used to compare different proposed sequences to assess the impact of a proposed change. It can then be used to provide a figure of merit of the cost impact of assumptions and uncertainties in the model.

This costing methodology can be carried out iteratively, as processes and knowledge develop, producing cost estimates relatively quickly. The approach offers the advantage of an early identification of key cost drivers and areas of cost uncertainty. It can be used to indicate that a different process sequence needs to be considered, or that further work is required to refine some cost uncertainties.

To permit a market readiness assessment and to allow comparison with more mature module technologies, a $/$W_p$ value can be derived from reported and forecast module efficiency for the developing technology. Further, for the end customer, the $/W data for the module alone is insufficient to calculate the market value of the technology. Other factors such as the lifetime of the module and the additional costs of mounting, connecting and maintaining a system need to be combined to give the levelised cost of electricity (LCOE) in $/kWh. To assess the efficiency and lifetime requirements, an LCOE calculator is then used to compare the proposed technology with LCOE values for different markets.

The combination of manufacturing costing in $/m^2 and the uncertainties in that costing, along with market comparisons of $/W and LCOE can be used to inform research directions for an emerging technology.

Figure 6.17.1: Nathan Chang, presenting on manufacturing cost analysis of photovoltaic cell and module technologies, 26 July 2017.

The Cost Evaluation of Emerging PV Technologies met all its targets, objectives and deliverables.

- Developd skills and methods in informed analysis of manufacturing cost for key ACAP technologies to assist in guiding research directions and decision making.
- Developd a strong collaboration with leading techno-economic analyst at NREL, Michael Woodhouse.
- Costing of two key technologies (perovskite on glass and rear-contact silicon).
- Created a solid foundation to extend the costing to other ACAP technologies such as roll-to-roll printing and advanced rear contact technologies including passivation, plating and hydrogenation.
- Produced two publications on cost analysis of advanced technologies, Chang, et al., 2017 and Chang, et al., 2018a.
- Met the requirements of PP4 milestone for March 2017; analysis on two technologies being investigated within ACAP.

Highlight

- The manufacturing costing task has developed novel methods for assessing the manufacturing costing of new technologies.

Future Work

- This project closed in late 2017, having met all its deliverables. A strong working relationship has developed with Michael Woodhouse at NREL that is expected to be further progressed with Nathan Chang as an ACAP postdoctoral fellow.

References

Chang, N.L., Ho-Baillie, A.W.Y., Basore, P.A., Young, T.L., Evans, R. and Egan, R.J., 2017, “A manufacturing cost estimation method with uncertainty analysis and its application to perovskite on glass photovoltaic modules”, Progress in Photovoltaics, 25(5), 390–405, DOI: 10.1002/pip.2871.

Chang, N.L., Ho-Baillie, A.W.Y., Vak, D., Gao, M., Green, M.A. and Egan, R.J., “Manufacturing cost and market potential analysis of demonstrated roll-to-roll perovskite photovoltaic cell processes”, Solar Energy Materials and Solar Cells, 174, 314–324, DOI: 10.1016/j.solmat.2017.08.038.

Chang, N.L., Ho-Baillie, A.W.Y., Wenham, S., Woodhouse, M., Evans, R., Tjahjono, B., Qi, F., Chong, C.M. and Egan, R.J., “Guiding Research Directions for c-Si Photovoltaics – Manufacturing Cost Analysis for Standard and New Silicon Solar Cell Technologies”, submitted.

ANU Solar Seminar: “Manufacturing cost analysis of photovoltaic cell and module technologies”, 1 November 2017.

Chang, N., UNSW, Public Research Seminar, “Manufacturing cost analysis of photovoltaic cell and module technologies”, 26 July 2017.

6.18 Studying Thermal Effects of Boron-Oxygen (B-O) Related Light-Induced-Degradation (LID)

Lead Partner
UNSW

UNSW Team
Dr Brett Hallam

UNSW Student
Moonyong Kim

Academic Partner
University of North Carolina, Charlotte (UNCC)

Ohio State University Team
Prof Abasifreke Ebong

Funding Support
ARENA

Aim

The aim of this project is to determine the effect of thermal processing on modulating B-O defect concentrations and the ability to mitigate light-induced degradation. This study will reduce the effects of light-induced degradation by > 50% by optimising thermal firing profiles for silicon solar cells. In the process, it will develop in situ characterisation tools for investigating light-induced defects in silicon solar cells and other recombination active defects in low-quality silicon.

Progress

A light-tight enclosure for QSS-PC measurements with bias light capabilities was built in 2016. Additional modifications to the tool in 2017 included the purchase of a new low-intensity light source and a photodiode to accurately measure the illumination intensity. The in situ lifetime monitoring technique was modified in 2017 to include an automatic extraction of recombination properties. Results generated using this approach are shown in Figure 6.18.1 from Kim (2017). The in situ lifetime monitoring technique was used in Hallam (2017) and Kim (2017) to investigate the fundamental properties of B-O defects.

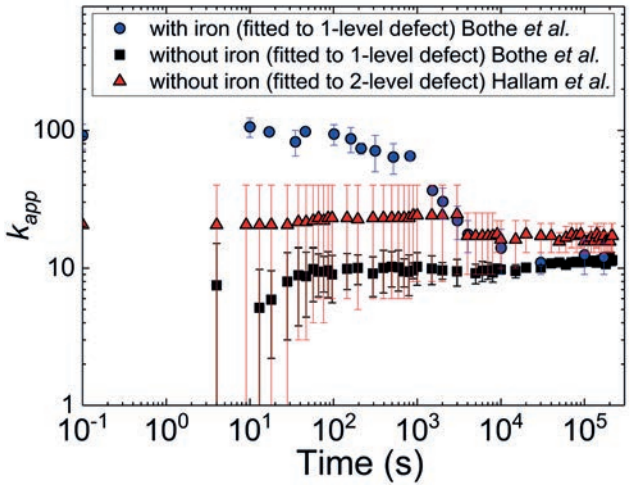

Figure 6.18.1: Apparent capture cross-section ratio (k_{app}) that was fitted to either a single-level defect of the slow-forming recombination centre (SRC) (Bothe, 2016) or a two-level defect (Hallam, 2017) during light soaking with 0.02 suns at room temperature using in situ QSS-PC lifetime measurement, with iron ($[Fe_i] = 2.6 \pm 0.5 \times 10^{11}$ cm^{-3}) and with an undetectable iron concentration ($[Fe_i] < 1 \times 10^{9}$ cm^{-3}). Image adapted from Kim (2017).

Examples of in situ lifetime data are shown in Figure 6.18.2(a) and (b) from (Kim, 2017). This work has shown strong evidence for the role of interstitial iron in B-O defect studies, providing further evidence of a single defect being responsible for B-O related degradation.

Work towards the thermal reduction of B-O related light-induced degradation in this project has begun. A research visit to UNCC was conducted in November 2017 to perform experiments on the thermal reduction of B-O defects during fast firing. Preliminary tests indicate a reduction of the B-O defect concentration by 30% from a normalised defect density of 6.75×10^{3} µs^{-1} down to 4.75×10^{3} µs^{-1} (see Figure 6.18.3). Simultaneously, the firing has been shown to introduce a separate metastable defect, typically causing light-induced

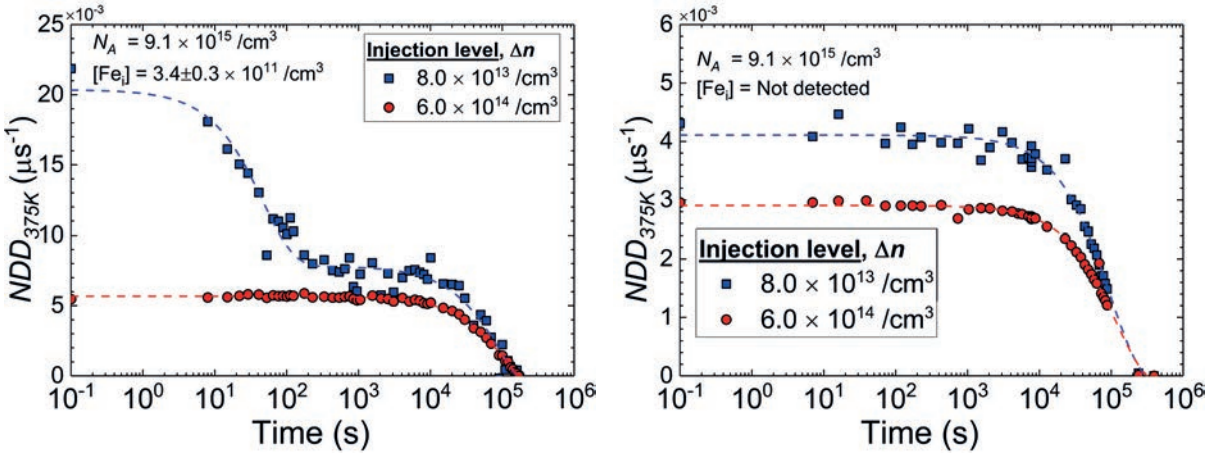

Figure 6.18.2: Normalised defect density at 375 K (NDD_{375K}) of (a) a sample with $[Fe_i] = 3.4 \pm 0.3 \times 10^{11}$ cm^{-3} ; and (b) a sample without iron versus dark annealing time at 375 K. NDD_{375K} was based on the lifetimes at two different injection levels ($\Delta n_1 = 8.0 \times 10^{13}$ cm^{-3} and $\Delta n_2 = 6.0 \times 10^{14}$ cm^{-3} where Δn_2 is the cross-over point) and was measured at an elevated temperature of 375 K. Solid lines are the single exponential fits and the dash lines are the two exponential fits. Images from Kim (2017).

degradation in p-type multicrystalline solar cells, called light- and elevated temperature-induced degradation (LeTID). An abstract has been submitted jointly with UNCC to the Seventh World Conference on Photovoltaic Energy Conversion (WCPEC-7).

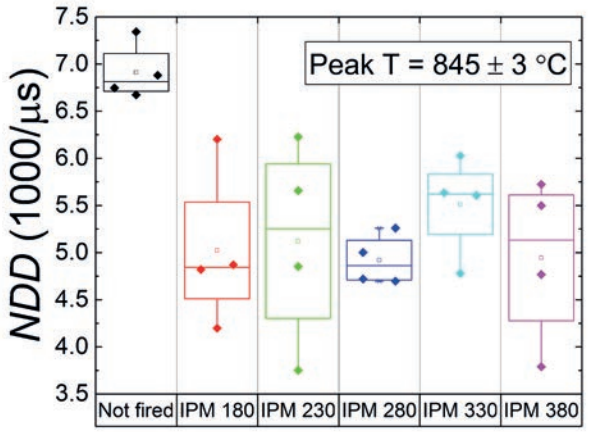

Figure 6.18.3: The normalised defect density (NDD) with different belt speeds at a peak wafer temperature of 845 ± 3°C, showing a significant reduction in the NDD with thermal processing.

Highlights

- The research in 2017 determined the impact of interstitial iron on apparent B-O defect properties. This study identified the potential influence of interstitial iron in early B-O defect studies that have been used to drive the formulation of B-O defect theories in the last 10 years. The work has shown strong evidence for the existence of a single B-O defect.
- To eliminate B-O degradation, we have shown a strong reduction in the normalised defect concentration through fast firing with rapid cooling rates over 100°Cs-1. Although this technique does not completely eliminate B-O LID, this approach could be used in conjunction with illuminated annealing, to offer a more complete solution for eliminating B-O related LID.

Future Work

- Future work will optimise the high temperature process to reduce the extent of B-O related LID. This will be investigated using a high-powered laser and fast-firing furnaces.
- For remaining defects, we will use a rapid advanced hydrogenation process.
- We will also further investigate the correlation between firing conditions and the extent of LeTID.

References

Bothe, K. et al., 2006, “Electronically activated boron-oxygen-related recombination centers in crystalline silicon”, J. Applied Physics. 99(1), 13701.

Hallam, B. et al., 2017, “Recent Insights into Boron-Oxygen Related Degradation: Evidence of a Single Defect”, Solar Energy Materials and Solar Cells, 173, 25–32.

Kim, M. et al., 2017, “Impact of Interstitial Iron on the Study of Meta-stable B-O Defects in Czochralski Silicon”, in press, J. Applied Physics.

6.19 Origin of Interface Defect Levels for High Efficiency Silicon Solar Cells

Lead Partner
UNSW

UNSW Team
Dr Ziv Hameiri

UNSW Students
Yan Zhu, Shuai Nie

Academic Partners
Arizona State University (ASU), Dr Mariana Bertoni

Funding Support
ACAP Collaboration Grant, UNSW MREII, ARC DECRA

Aims

The main goals of this project are:

- To investigate the temperature dependence of various passivation layers, considering that solar cells in the field only rarely operate at the standard measurement condition of 25°C (usually much higher).
- To develop new characterisation methods for contact passivation and to obtain the electrical properties of the passivated interfaces.
- To accurately model the electrical properties of various passivation films by means of advanced characterisation methods; special care will be given to the most common ones (silicon nitride, aluminium oxide and amorphous silicon).
- To assist with the development of advanced passivation layers for high efficiency solar cells, using the obtained information.

Progress

Surface passivation is a critical consideration when designing high efficiency solar cells. All advanced solar cell structures are based on high quality surface passivation. A key requirement for improving surface passivation quality is to investigate the electrical properties of the dielectric. However, almost all the previous studies were conducted at room temperature (25°C), which differs from the actual operating condition of solar cells in the field. In this project, we investigate the performance of the most commonly used surface passivation layer in the photovoltaic industry, silicon nitride (SiN_x), in the temperature range of 0°C–100°C. Additional measurements, at even higher temperatures (up to 250°C), are used to reveal the temperature dependence of the fundamental properties of this layer.

Six n-type float zone (FZ) silicon wafers were etched to different thicknesses (from 150 µm to 270 µm), RCA cleaned and then passivated with identical plasma-enhanced chemical vapour deposited (PECVD) SiN_x (both sides).

The lifetime measurements of these samples were done using a customised lifetime tester that was developed as part of this project at UNSW. The system allows measurements in the wide temperature range from -190°C to 400°C. It uses two light sources (a Xenon flash and a controllable LED) in order to achieve a wide range of carrier injection. The wafers were measured under quasi-steady-state (QSS) and transient conditions using the generalised analysis mode. The generation rate was calibrated by comparing QSS and transient measurements at each temperature. Evaluation of the passivation quality was based on the extraction of surface recombination velocity (SRV) from the effective lifetime (τ_{eff}) measurements. This was done by a linear fit of $1/\tau_{eff}$ as a function of 1/W (where W is the wafer thickness), where the SRV is extracted from the slope of the fit. The quality of the linear fit was evaluated using the R-square value and we set the lower limit of R-square value as 0.85.

Figure 6.19.1 presents τ_{eff} as a function of the excess carrier density (Δn) of the 200 µm thick wafer, at different temperatures. As can be seen, τ_{eff} increases with increasing temperature for the entire Δn range. Similar results were obtained for all other wafers (independent of their thickness). The extracted SRV from the linear fit is shown in Figure 6.19.2 as a function of Δn for the entire temperature range. The tested SiN_x passivation demonstrates a continuous decrease of SRV with increasing Δn. Meanwhile, a significant improvement of the surface passivation (as indicated by a lower SRV) is observed with increasing temperature. It is interesting to notice that at a higher temperature the SRV is almost independent of the injection level. This is the first time that SRV of an SiN_x surface passivation layer is extracted at this range of temperatures. This study indicates that no degradation of SiN_x surface passivation is expected at high operation temperatures (on n-type substrate).

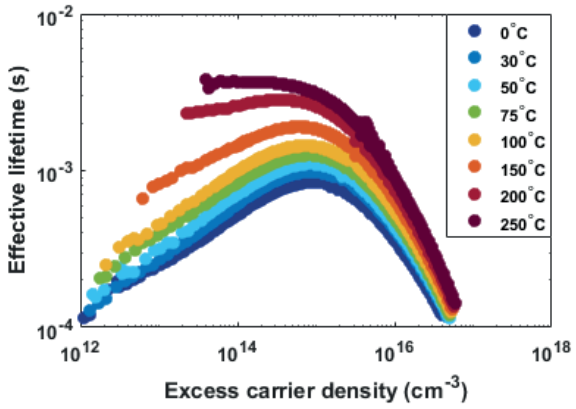

Figure 6.19.1: τ_{eff} as a function of Δn of an n-type silicon wafer passivated by SiN_x at different temperatures.

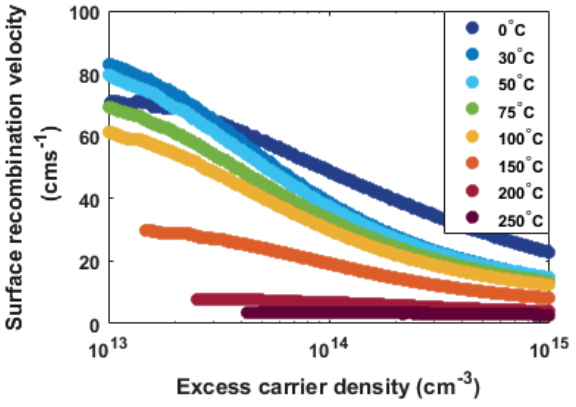

Figure 6.19.2: SRV as a function of Δn of an n-type silicon wafer passivated by SiN_x at different temperatures.

Highlights

- An ASU PhD student visited UNSW at the beginning of 2017 (January–April).
- The UNSW Taste of Research project was extended to a Fourth-Year Thesis project. The student received a High Distinction on the thesis and was awarded a full international scholarship (EIPRS) for a PhD. She will start her PhD in Semester 1, 2018.
- A conference paper based on this project was presented in the 27th PVSEC (November 2017, Japan).
- Two abstracts based on the project will be submitted to the World Conference on Photovoltaic Energy Conversion (June 2018, USA).
- A journal paper is under preparation.

Future Work

- Measurement of SiN_x passivated samples after two weeks in environmental chamber.
- Measurement of SiN_x passivated samples using surface photo voltage at ANU.
- Measurement of AlO_x passivated samples.

6.20 Developing Laser Processed Large-Area Front Deep Junctions and Heterojunction Passivated Back Contacts

Lead Partner
UNSW

UNSW Team
Dr Ivan Perez-Wurfl

UNSW Students
Tian Zhang, Zibo Zhou

Academic Partners
NIST (USA), Dr Brian Simonds

Funding Support
ACAP, NIST (in-kind)

Aims

The main goal of this project is to develop a laser annealing system to fabricate deep junctions on silicon wafers with reduced thermal stress. The system uses line and large-area CW lasers to achieve this. Reduction in thermal stress is achieved by increasing the substrate temperature, with either another laser or a hot plate, prior to melting. Also, controlling the heating and cooling rates by varying the scanning speed and power helps to reduce stress. With this system we have demonstrated low doped emitters 10 microns in thickness with a diffusion length at least twice as long as the emitter.

The second part of this project aimed at demonstrating the application of lasers on silicon solar cell fabrication using a nanosecond pulsed laser to fabricate poly-Si/tunnelling SiO_2/Si heterojunction passivated contacts. However, the low doping of both emitter and base made it necessary to investigate other contacts that would result in ohmic behaviour to low doped regions. To this end we have investigated antimony and some of its alloys to achieve ohmic contacts to low doped n-type layers.

Progress

During the first year of the project we completed three of the four project aims put forward for this proposal, namely: establishing a robust high power dual-beam laser annealing/melting system at NIST, demonstrating 3–10 μm deep junctions, and fabricating laser processed poly-Si/tunnelling SiO_2/Si heterojunction passivated back contacts.

After the first year we identified the need to implement COMSOL simulation to model the laser process to improve our understanding of CW laser thermodynamics. This need led to the main focus of this year's work, the creation of a reliable numerical model capable of reproducing experimental results. The model is also able to explain the high amount of stress that results from the laser process.

Highlights

Numerical modelling of the transient and steady state thermodynamic effects of CW laser processing on silicon

- Modelling of the laser process was achieved using COMSOL multi physics along with the Heat Transfer module. The model is able to predict the molten depth and temperature profile for a given laser power. A simulated result can be seen in Figure 6.20.1. As we are interested in modelling line or full-area lasers, a 2D model is sufficient to accurately reproduce the actual experimental process. The laser beam is represented by a CW heat source with varying width and translational speed across the wafer surface. The power of the laser and its speed can be adjusted to study the molten pool depth as well as the temperature profile within the silicon substrate.
- The numerical model incorporates temperature-dependent thermal properties of silicon up to its melting point. The model also calculates phase changes in solid silicon to determine the depth of the molten pool due to laser exposure. A 2D temperature profile is also calculated to estimate the amount of thermally induced stress as can be seen in Figure 6.20.2.

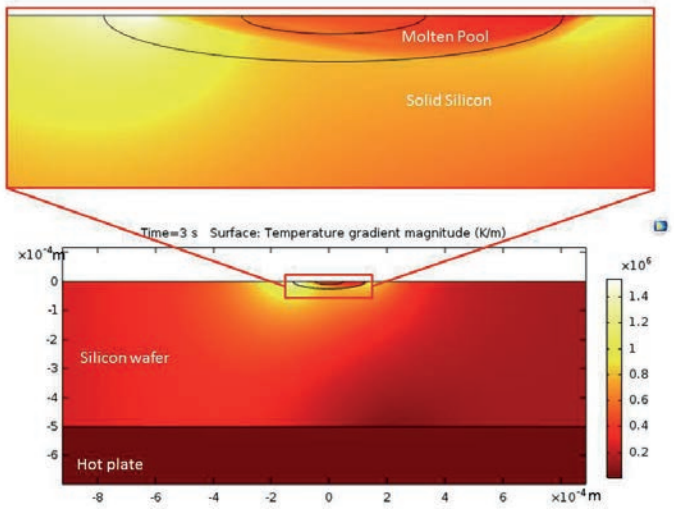

Figure 6.20.1: Molten pool size and shape along with the temperature gradient (TG) for a 245 W line laser process.

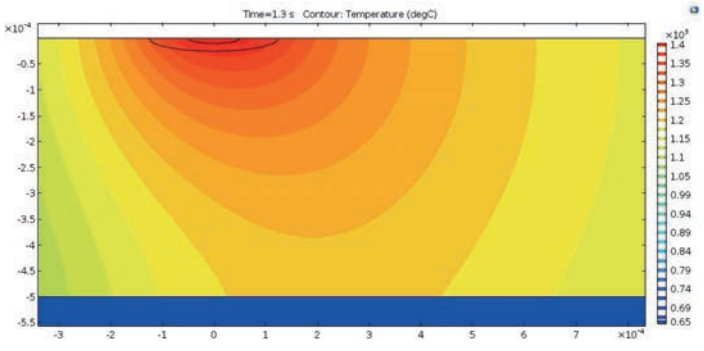

Figure 6.20.2: COMSOL steady state simulation with the isothermal contours obtained with a 0.4 m/min 140 W line laser heating the silicon wafer on a 650°C hotplate.

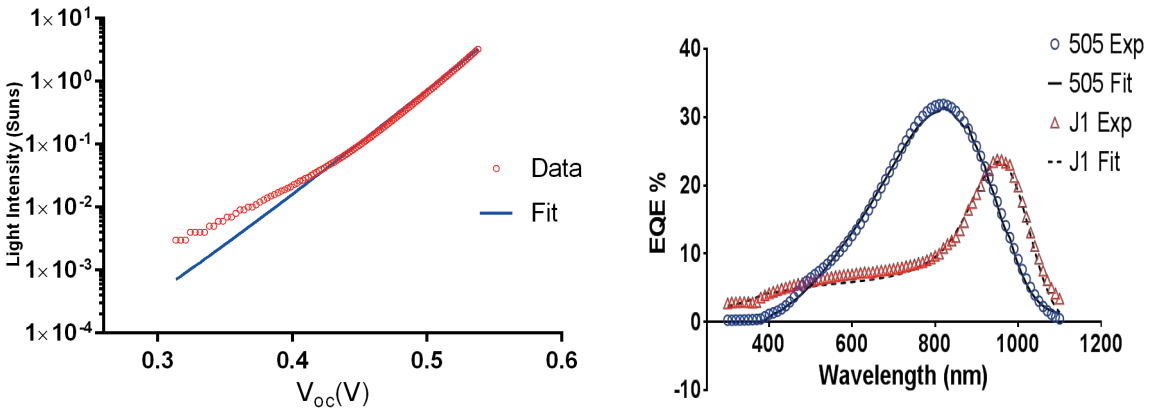

Figure 6.20.3: Suns-V_{OC} and EQE of solar cells with 10 μm deep, 5 x 10^{17} cm^{-3} P doped emitters.

Solar cell with deep junctions formed with a CW line laser process

- A 1 cm^2 solar cell with a 10 μm deep, 5 x 10^{17} cm^{-3} P doped emitter, was fabricated allowing the extraction of the lifetime of the emitter and base after laser processing.
- Suns-V_{OC} measurements indicate a solar cell limited by recombination in the bulk of the structure (n=1). Further modelling of the measured EQE fitted using PC-1D, demonstrates that this recombination mainly occurs in the base of the cell, that is, the material that was not melted during the laser process. The measured suns-V_{OC} and EQE can be seen in Figure 6.20.3.
- Numerical fitting confirms a minority carrier lifetime of 1.2 μs for the emitter and only 50–100 ns for the remainder of the wafer. These results are consistent with the dislocation density reported previously which showed a severe density of defects in the bulk and a comparably low defect density in the emitter region. A proper dark and illuminated I-V of this cell is still unattainable due to severely limiting rectifying contacts on the low doped emitter.

Future Work

So far we have been unable to demonstrate a proper dark and illuminated I-V of solar cells produced through large-area laser processing. The main limitation has been the lack of linear contacts to the low doped emitter. In order to avoid a second diffusion or a localised laser doped region, we believe it would be beneficial to attain an ohmic contact to low doped n-type emitters. We have demonstrated that neither Ti nor Ni results in linear contacts to these low doped regions, even after a high temperature anneal. We have therefore started work on Sb based contacts.

Publication of the work done for this project is underway. A comprehensive paper summarising the physics of the laser processing along with the resulting defects and methods to mitigate them has been submitted for consideration at a reputable scientific journal. The results that can be potentially obtained with Sb-based contacts could result in valuable experimental results that would lead to a second publication.

6.21 Novel Light-Trapping Technique in Solar Cells

Lead Partner
UNSW

UNSW Team
Dr Supriya Pillai, Dr Michael E. Pollard, Prof Darren Bagnall

UNSW Students
Claire E.R. Disney, Atom Chang

Academic Partners
Arizona State University, Prof Christiana Honsberg, Prof Stuart Bowden, Dr Som Dahal, Mr Sangpyeong Kim

Funding Support
ACAP, ARENA, UNSW

Aim

An investigation of whether parasitic absorption in metals can compromise light absorption in cells and to clarify the future of plasmonic structures as potential light-trapping layers in solar cells. One of the main objectives of the project was to check the feasibility of using embedded dielectric structures to potentially act as a practical and economical rear light-trapping layer for solar cells.

Progress

Simulations and experimental work was undertaken to ascertain the suitability of such embedded structures.

Nanosphere (NS) lithography was used as part of the project where deposition was using spin coating technique, which is a fast and cheap way of fabricating the structures. The spin-coating process was optimised and large-area features were fabricated on whole wafers, the diffraction patterns clearly showing the uniformity of the layers. Quantitative analysis of such fabricated structures was performed using SEM images and Fourier transform. The concentration of the different polystyrene nanospheres (PSNS) and the spin speeds were optimised.

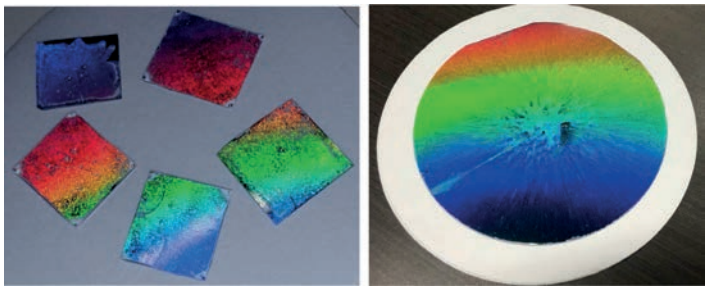

Figure 6.21.1: Large-area uniform deposition of the NS before metal overcoating clearly showing a strong diffraction pattern.

Figure 6.21.1 is a representative image of the large-area fabrication on full size wafers accomplished showing clear diffraction patterns visually identified by the strong colours at different angles. In low magnification (large-area) SEM images, we typically observe “grains” of closely packed NS with varying orientations as seen in Figure 6.21.2(a) and (b), even though the whole surface may be covered by a monolayer array. The accumulation of individual hexagonal patterns with different rotations results in the frequency profile showing ring patterns as shown in Figure 6.21.2(c) and sharp peaks in the line profile (Figure 6.21.2(d)). By integrating the line profiles taken from the centre to the edge over all in-plane angles, the quality (overall uniformity) of the NS films can be found. The appearance of a clear and sharp ring, with a spatial frequency matching the expected periodicity, indicates that the surface is covered by a uniform NS monolayer. Hence, the more intense and narrower the peak, the better the quality factor, signifying large-area uniform arrays.

The detailed fabrication process of the NS was submitted as a paper for the Asia-Pacific Solar Research Conference in Canberra in December 2016.

NSs of different sizes and pitch were deposited onto thinned wafers and overcoated with silver (embedded NS). The schematic of the structure along with an SEM image is shown in Figure 6.21.3. One of the challenges of the project was the thinning of the wafers to provide proof of concept as it is expected that the enhancement would be greater for the thinner samples. Wafers 200 µm thick were thinned using wet etching and thinned down to ~50 µm. The thinned samples were then bonded to fused silica.

Spectral PL and PL imaging was used to measure the performance of the samples fabricated. A clear enhancement in the spectral PL was observed for the embedded NSs compared to planar reflectors for the same sample configuration as shown in Figure 6.21.4(a). The results from the samples were further verified using PL imaging to account for variation in the large-area samples as shown in Figure 6.21.4 (b). The PL counts from the PL images from different areas were averaged to arrive at the total PL count for the sample. Unlike spectral PL, PL imaging provides response form a larger area. Both results are compared to a planar silver reflector.

Following concerns about parasitic absorption in the metal of such rear reflectors impeding useful absorption in Si, a detailed study was performed using simulations on different types of plasmonic rear reflectors to understand absorption in the metal versus absorption in the semiconductor. The results were interesting and revealed that at resonant wavelengths

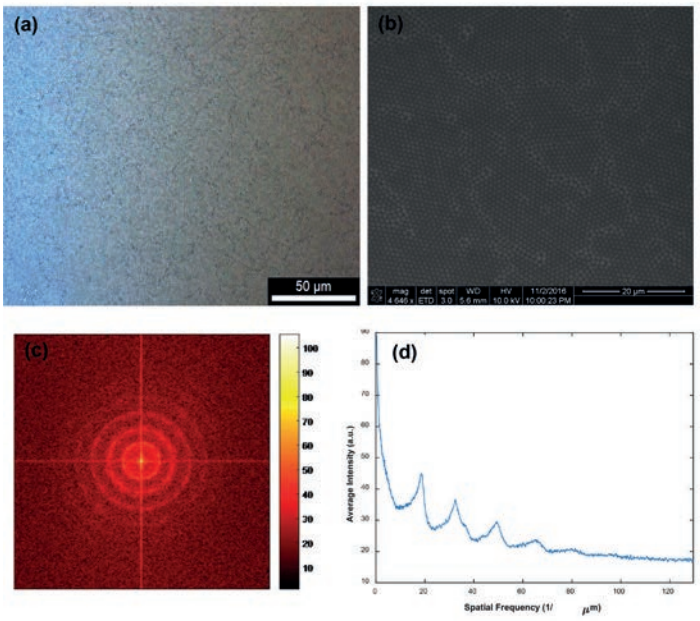

Figure 6.21.2: Large-area uniform 0.99 µm monolayers deposited by NS suspensions with optimal concentrations: (a) 100 x magnification optical microscope; (b) SEM image; (c) frequency domain profile of the SEM image in (b); and (d) intensity line profile of (c).

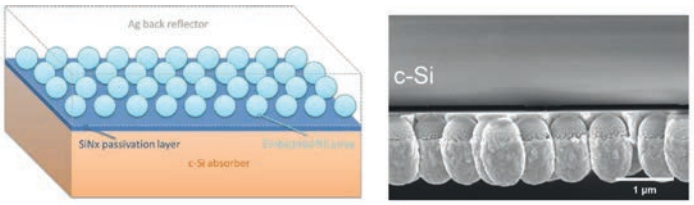

Figure 6.21.3: (L) Designed (inverted view) and (R) SEM cross-section images of experimental structure – nanospheres overcoated with silver.

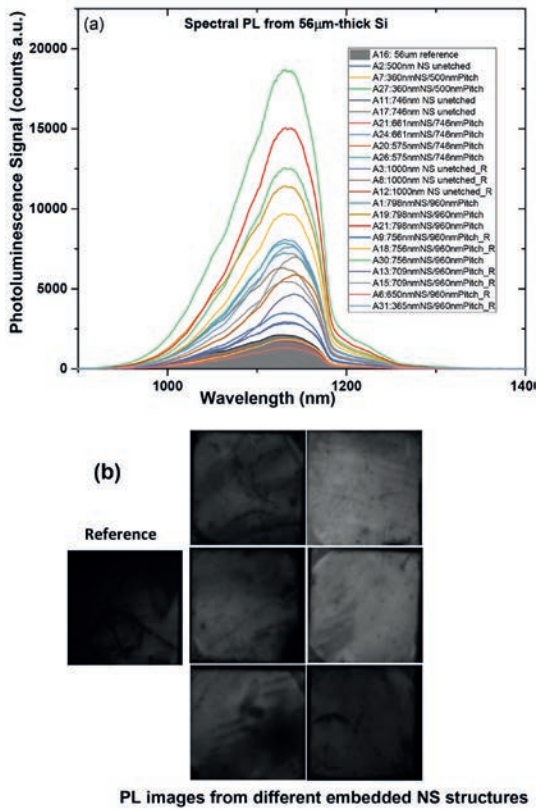

Figure 6.21.4: (a) Spectral PL measurements of samples with different size and pitch of NSs overcoated with silver. The shaded region in grey represents the reference plots (planar metal reflector); and (b) PL images of some of the samples. Also shown is a reference sample for comparison.

high parasitic losses in the metal could also be associated with high absorption enhancement in the solar cell. Resonant peaks for these types of structures were identified as shown in Figure 6.21.5(a), and their scattering behaviour was examined (Figure 6.21.5(b)). It was found that for these types of structures, large angle scattering dominates in most cases, leaving a net positive impact relative to a rear mirror. However, this balance between parasitic absorption and large angle scattering should be factored in to selecting the correct geometries for nanotextured rear reflectors. Overall, it can be concluded that higher absorption in the metal need not always be problematic for plasmonic light-trapping structures, and may not need to be avoided. Rather, it can potentially be associated with strong enhancements to absorption in the active layer of the cell. These results are now published in Scientific Reports, 2017.

Highlights

- The project successfully demonstrated large-area fabrication of plasmonic rear reflectors using dielectric nanospheres.
- Proof of concept to check the feasibility of these embedded dielectric structures to potentially act as a rear light-trapping layer for solar cells was established through optical characterisation.

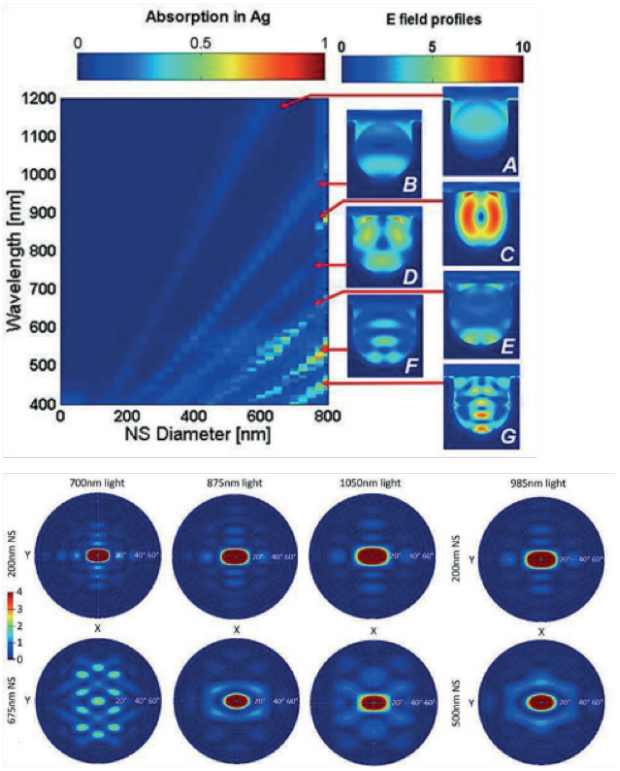

Figure 6.21.5: (a) Absorption in Ag at the rear of Si for varied NS diameters with an 800 nm period showing the different resonances. "0" diameter is a rear mirror alone; and (b) far-field scattering plots showing the angles at which light is scattered back into the Si from the rear interface of the cell for 800 nm period NSs. The wavelengths selected were at resonance for the 675 nm NS case, and off resonance for the 200 nm NS case. 700 nm resonance C, 875 nm resonance B, 1050 nm light – between resonance A and B – shows the large boost in large angle scattering between resonances.

- It was also concluded through extensive simulation work that by using correct geometries, higher absorption in the metal need not always be problematic for plasmonic light-trapping structures, and may not need to be avoided, but rather can potentially be associated with strong enhancements to absorption in the active layer of the cell. This project has now closed.

References

Chang, Y., Pollard, M.E., Payne, D.N.R., Pillai, S. and Bagnall, D. M., 2016, "Nanosphere Lithography for Fast and Controlled Fabrication of Large Area Plasmonic Nanostructures in Thin Film Photovoltaics", 3rd Asia-Pacific Solar Research Conference, 29 November – 1 December 2016, Canberra.

Disney, C.E., Pillai, S. and Green, M.A., 2016, "Do parasitic losses outweigh the performance benefits in plasmonic solar cells?", 4th ACAP and 3rd Asia-Pacific Solar Research Conference, 29 November – 1 December 2016, Canberra.

Disney, C.E., Pillai, S. and Green, M.A., 2016, "Parasitic absorption in plasmonic light trapping structures for solar cells: Do the performance benefits outweigh the losses?", International PVSEC-26, Singapore 24–28 October 2016.

Disney, C., Pillai, S. and Green, M.A., 2017, "The Impact of parasitic loss on solar cells with plasmonic nano-textured rear reflectors", Sci. Rep., 7(1) 12826.

A second journal manuscript has been drafted for submission to Appl. Phys. Letters.

6.22 Interfacial Engineering for High Performance Organic Tandem Solar Cells and Perovskite Solar Cells

Lead Partner
Monash University

Monash Team
Dr Wenchao Huang, Prof Yi-Bing Cheng

International Partner
Team
Professor Yang Yang (UCB, LBNL) University of California, Berkeley

Aim

Due to the thinness of the active layer, light absorption is a critical issue limiting further improvement in OPV and perovskite device performance. In order to use the solar radiation more efficiently, a promising approach is to use tandem solar cells combining two photoactive layers to improve the light absorption. The aim of this project is to collaborate with UCLA to develop highly efficient tandem organic solar cells.

Progress

As the interconnection layer in the fabrication of tandem cells requires a heat treatment, the use of a highly thermal stable front sub-cell plays an important role in developing a high performance tandem solar cell. The key aspects of this work are to (1) understand the relationship between morphology, photophysics, device performance and thermal stability in the single junction organic solar cell and (2) develop highly efficient organic tandem solar cells.

The polymer poly[2,6′-4,8-di(5-ethylhexylthienyl)benzo[1,2-b;3,3-b]dithiophene]3-fluoro-2[(2-ethylhexyl)carbonyl] thieno[3,4-b]thiophenediyl] (PBDTTT-EFT), also called PTB7-Th, in particular, has recently attracted intense attention due to the excellent device performance in both polymer/fullerene and polymer/polymer solar cells. Here, we demonstrate the correlation between morphology, device performance and thermal stability in polymer/fullerene solar cells based on different fullerene acceptors (PC71BM and ICBA) blended with a low bandgap polymer PBDTTT-EFT. Based on this project, a paper was published in *Advanced Energy Materials* (Huang et al., 2017). Morphology is characterised with grazing incidence wide angle X-ray scattering (GIWAXS) and resonant soft X-ray scattering (R-SoXS), which together reveal that the PBDTTT-EFT:ICBA blend exhibits a lower polymer crystallinity, lower fullerene domain purity and smaller fullerene domain size compared to PDBTTT-EFT:PC71BM blends, as shown in Figure 6.22.1. Although the highly mixed morphology has led to the geminate and non-geminate recombination (confirmed by transient absorption and transient photovoltage decay measurement), it is important to prevent unfavourable coarsening upon heat treatment.

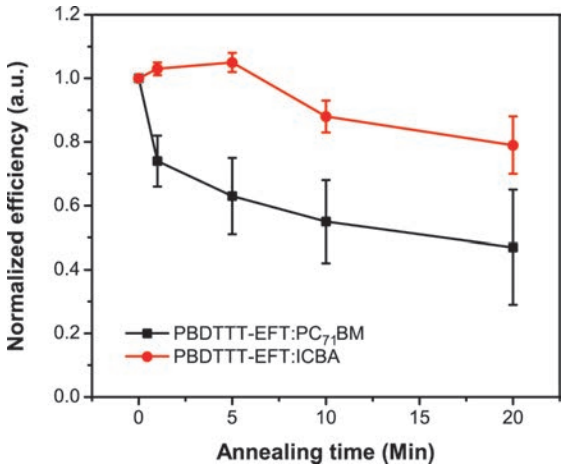

Figure 6.22.2: Normalised device efficiency as a function of annealing time. The blend films were annealed at 90˚C.

As shown in Figure 6.22.2, when the ICBA blend is annealed at 90°C, device efficiency experiences a slight increase at the initial stage (within 5 minutes). The device exhibits a slight decrease in its efficiency only after 10 minutes annealing because the coarsening of the fullerene domain results in the poor exciton separation. In contrast, the device based on PBDTTT-EFT:PC71BM has very poor thermal stability. Device efficiency continuously decreases as a function of annealing time, exhibiting only half of its initial value after 20 minutes of thermal annealing.

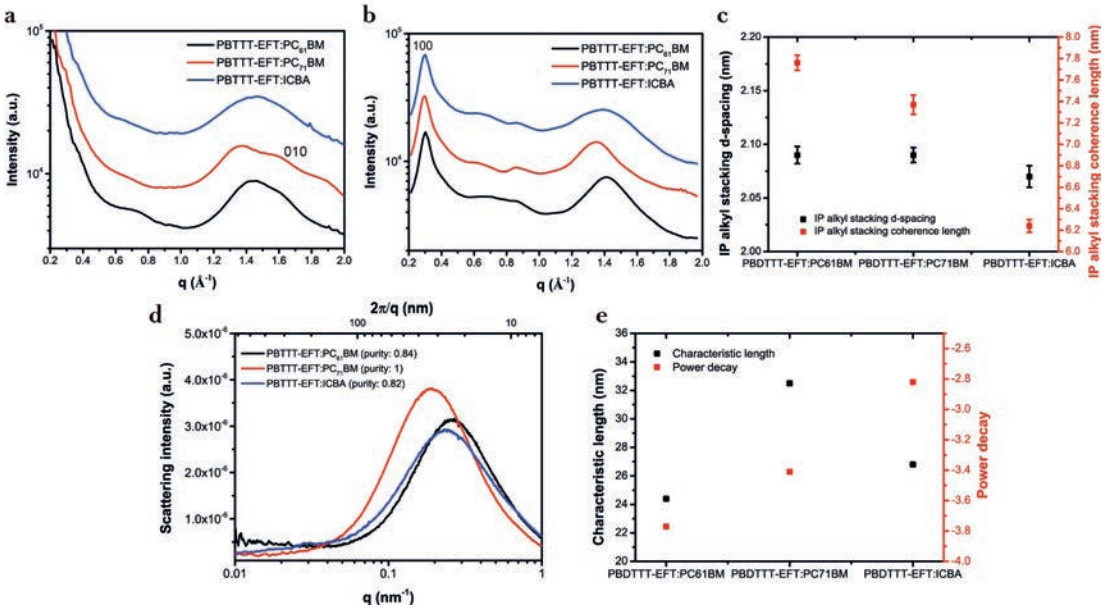

Figure 6.22.1: Line profile of various PBDTTT-EFT:fullerene blends cut from 2D GIWAXS patterns: (a) out-of-plane (OOP) direction; (b) in-plane (IP) direction; (c) lamellar d-spacing and coherence lengths; (d) Lorentz-corrected R-SoXS profiles of various PBDTTT-EFT:fullerene blends (Scattering profiles were taken at the X-ray energy of 284.0 eV); and (e) fit parameters from R-SoXS scattering profiles.

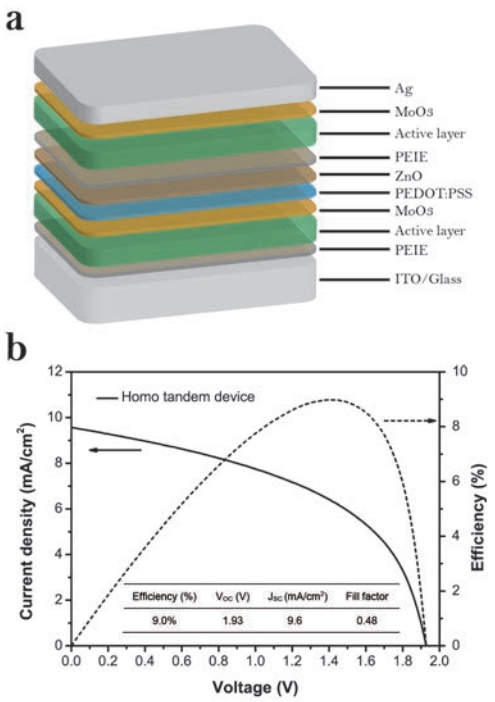

Figure 6.22.3: (a) Schematic of the double-junction device architecture. The front sub-cell is fabricated by PBDTTT-EFT:ICBA blends; and (b) device performance of homo-tandem solar cells.

Based on its good thermal stability, PBDTTT-EFT:ICBA blend is a promising candidate for use in tandem solar cells. The use of a homo-tandem architecture however is able to increase light absorption in the cell without suffering the severe recombination that would occur in a thick single-junction cell. As shown in Figure 6.22.3(a), an architecture of ITO/PEIE/active layer/MoO_3/PEDOT:PSS/ZnO/PEIE/active layer/MoO_3/Ag is used in our homo-tandem solar cell with both front and rear sub-cells made of the PBDTTT-EFT:ICBA blend. Figure 6.22.3(b) shows J-V curve characteristics of homo-tandem solar cells. A power conversion efficiency of 9% has been achieved in this device, with a short-circuit current of 9.6 $mAcm^{-2}$ and an ultra-high open circuit voltage of 1.93 V, which is the highest open circuit voltage reported for a double-junction fullerene-based tandem cell. It also should be noted that tandem solar cells are able to output an efficiency of over 8.5% at an operating voltage of 1.5 V, which shows potential for application in driving a water splitting system.

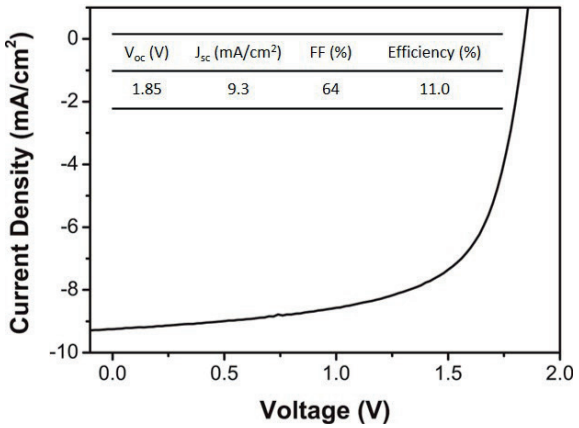

Figure 6.22.4: Device performance of non-fullerene tandem solar cells based on the front sub-cell of PDBT-T1/TPH-Se and the rear sub-cell of PBDBT/ITIC.

In addition, the partnership also developed highly efficient non-fullerene organic tandem solar cells based on another thermally stable non-fullerene blend of the polymer poly{dithieno[2,3-d:2'3'-d']benzo[1,2-c:4,5-c']dithiophene-co-1,3-bis(thiophen-2-tl)-benzo-[1,2-c:4,5-c']dithiophene-4,8-dione} (PDBT-T1) and the small molecules selenium annulated triperylene hexaimides (TPH-Se) as the front sub-cell. Due to the amorphous nature of TPH-Se, the most of TPH-Se molecules are molecularly mixed in the amorphous region of PDBT-T1. The phase separation can be effectively suppressed under heat treatment. The tandem device based on using the blend of PDBT-T1/TPH-Se as the front sub-cell and the blend of poly[(2,6-(4,8-bis(5-(2-ethylhexyl)thiophen-2-yl)benzo[1,2-b:4,5-b']dithiophene))-alt-(5,5-(1',3'-di-2-thienyl-5',7'bis(2-ethylhexyl)benzo[1',2'-c:4',5'-c'] dithiophene-4,8-dione))]) (PBDBT) and 3,9-bis(2-methylene(3-(1,1-dicyanomethylene)-indanone))-5,5,11,11-tetrakis(4hexylphenyl)-dithieno[2,3-d:2',3'-d']-s-indaceno[1,2-b:5,6-b']dithiophene) (ITIC) as the rear sub-cell can achieve an efficiency of 11% with a short-circuit current of 9.3 $mAcm^{-2}$, an open circuit voltage of 1.85 V and a fill factor of 64%, as shown in Figure 6.22.4.

Highlights

- Due to the highly mixed morphology, PBDTTT-EFT:ICBA blends exhibit enhanced thermal stability compared to the other blends.
- Development of non-fullerene tandem solar cells by using a thermally stable front sub-cell of PDBT-T1 and TPH-Se with an efficiency of 11%.

References

Huang, W.C., Gann, E., Chandrasekaran, N., Prasad, S.K.K., Chang, S.Y., Thomsen, L., Kabra, D., Hodgkiss, J.M., Cheng, Y.B., Yang, Y. and McNeill, C.R., 2017, "Influence of Fullerene Acceptor on the Performance, Microstructure, and Photophysics of Low Bandgap Polymer Solar Cells." Advanced Energy Materials, 7(11).

6.23 Rear Contact Solar Cells with Nanophotonic Light Trapping

Lead Partner
UNSW

UNSW Team
Dr Michael Pollard, A/Prof Bram Hoex, Dr David Payne, Prof Darren Bagnall

UNSW Students
Alexander To, Yuan-Chih Chang

USA Partner
Prof Harry Atwater (California Institute of Technology / CalTech)

European Partners
Professor Albert Polman, Andrea Cordaro, Verena Neder, Dimitry Lamers (AMOLF, the Netherlands)

Dr Alexander Sprafke (MLU Halle-Wittenburg, Germany)

Dr Tasmiat Rahman, Dr Stuart Boden (University of Southampton, UK)

Aim

This collaboration with CalTech, AMOLF and MLU Halle-Wittenburg, extending previous collaboration with the University of Southampton, investigates the use of dielectric nanoparticles, known as Mie resonators, as front and rear surface structures for light management in interdigitated back contact (IBC) solar cells. These Mie resonators, operating in the wave optics regime, can be engineered to enhance optical absorption in thin and flexible monocrystalline silicon solar cells. Furthermore, these structures do not require direct patterning of the silicon surface, allowing planar silicon active layers to be used and a concomitant reduction in surface recombination. The project has led to further improvement to the planar IBC baseline and wafer thinning processes at UNSW, determination of appropriate geometries for front (SiN_x) and rear (a-Si) Mie resonator arrays, and successful demonstration of a scaleable nanoimprint process for producing these structures. Work is currently underway to finish integrating the Mie resonator structures with thinned IBC solar cells, while global interest in the planar IBC baseline process has presented many opportunities for collaboration with additional international partners.

Progress

Optical losses are typically the most significant factor limiting the efficiency of commercially available IBC solar cells (Smith et al., 2016). These cells currently rely on a combination of dielectric coatings and micron-scale texturing of the active silicon layer for anti-reflection (AR) and light trapping. Unlike conventional alkaline texturing, AR and light-trapping layers based on dielectric Mie resonator arrays can be applied to almost any substrate, including multicrystalline silicon wafers and thin and flexible crystalline silicon (c-Si) membranes. In this project, we have designed and fabricated Mie resonator arrays suitable for application to planar IBC solar cells, along with making significant improvements to the n-type planar IBC process at UNSW (Rahman, 2017).

The choice of material for the Mie resonators was dictated by both their optical requirements and the material's practical relevance. Light scattering by Mie resonators, or indeed any dielectric feature, is stronger when the contrast between the refractive index of the structure and the host matrix is increased. Additionally, these resonant structures should be placed close to the high-index active silicon layer to permit strong optical coupling and maximise absorption in the silicon. While it remains possible to use a thin interfacial layer for surface passivation, it is desirable to use established and industrially relevant materials that are able to serve as both the passivating and scattering medium. We therefore investigated Mie resonators made from hydrogenated PECVD silicon nitride (SiN_x:H) for the front surface and amorphous silicon (a-Si:H) for the rear.

Geometries for front surface SiN_x Mie resonator arrays were determined using coupled mode theory simulations. Extending previous work at AMOLF (Spinelli et al., 2012; 2013), these simulations showed that a simple square lattice arrangement of SiN_x Mie resonators yields an average non-weighted surface reflectance below 4%, with further potential for optimisation. These designs were successfully fabricated on SiN_x-coated silicon test samples using soft conformal nanoimprint lithography (SCIL). Figure 6.23.1 shows an focussed Ion beam (FIB) cross-section of a single SiN_x Mie resonator fabricated with this approach. Simulated and experimental reflectance curves are shown in Figure 6.23.2, along with an inset image of the sample. The surface is clearly darker than a conventional single layer SiNx ARC, with the typically blue-violet colour replaced by near-black.

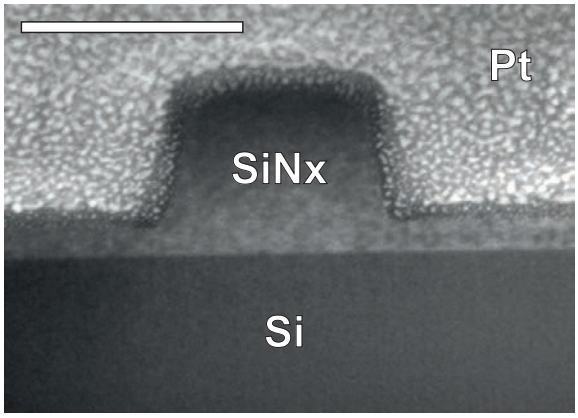

Figure 6.23.1: An FIB cross-section of a single nanoimprinted SiN_x Mie resonator (Scale bar: 200 nm).

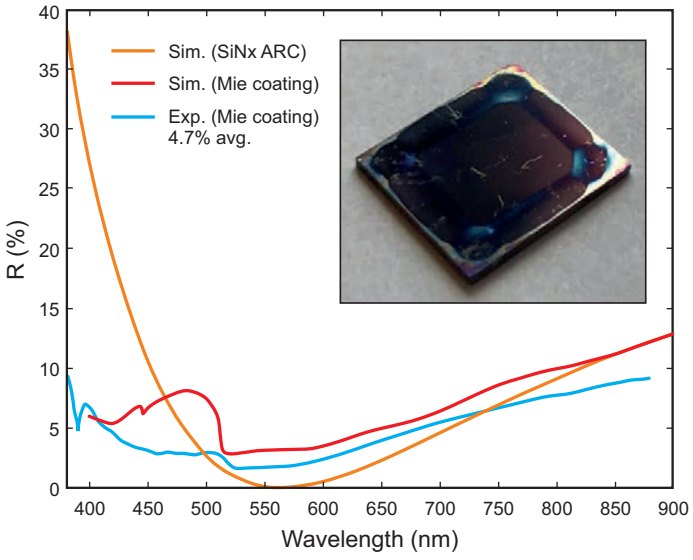

Figure 6.23.2: Experimental and simulated reflectance of a SiN_x Mie resonator array (Inset: photo of the measured sample)/

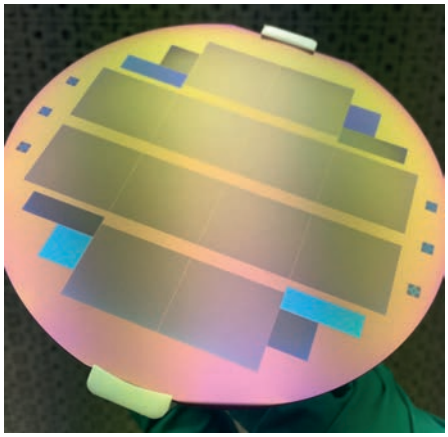

Figure 6.23.3: A part-processed wafer of IBC cells following boron and phosphorous diffusion

For backscattering from the rear surface of a solar cell, amorphous silicon Mie resonators embedded in a low index host (e.g. polymer, or even air) are practically ideal. Not only is the refractive index both high and well-matched to that of the c-Si absorber, but the absorption coefficient for the near-infrared wavelengths reaching the rear surface is an order of magnitude lower than for c-Si, resulting in negligible parasitic absorption. This contrasts with the use of a-Si:H on the front surface, where there would be significant parasitic losses from short wavelength absorption. Amorphous silicon is also one of the most effective passivating materials for c-Si solar cells therefore, like the front surface, the Mie resonators can be fabricated directly in the passivation layer.

Various geometries for rear surface a-Si Mie resonators embedded in low index polymer (n=1.5) were investigated by finite-element simulation. The effects of particle size, sidewall angle, distribution and separation from a rear surface metal mirror were systematically studied over the 600–1200 nm wavelength range. Individual resonator scattering and first-order diffraction from the particle distribution were optimised in unison to ensure maximum scattering inside the light cone of the planar silicon slab (i.e. total internal reflection). First-order diffraction efficiency greater than 90% can be achieved over a very wide wavelength range. Total absorption and peak current density for a range of substrate thicknesses were determined by using these rigorous wave optical results as inputs to a subsequent incoherent calculation (OPTOS formalism, (Eisenlohr et al., 2015). For all thicknesses, the optimised arrays yield absorption remarkably close to the Lambertian limit.

UNSW was primarily responsible for developing the planar IBC baseline process and providing completed cells to AMOLF for subsequent nanoimprinting. While it is desirable to have a high efficiency baseline, the ultimate goal for the cell process was for it to be robust, reliable and with minimal cell-to-cell variation. This has been achieved, with the latest batch of 96 cells exhibiting variation between wafers of less than +/- 0.5% in V_{OC} and +/- 5% in J_{SC}. Further improvements to the baseline process include front surface $POCl_3$ diffusion and HNA etching for impurity gettering and removal, a 6% absolute increase in fill factor by an improved metallisation which lowered series resistance, improved handling procedures to reduce contamination and increase yield, and transfer of cell processes to additional tools to provide process redundancy.

This project has enabled continuation and strengthening of pre-existing collaborations with AMOLF and the University of Southampton, along with initiation of collaboration with new partners CalTech and MLU Halle-Wittenburg. Promotion of the planar IBC baseline has led to truly global interest. Opportunities for future collaboration have been created with Warwick University, Oxford University, Cambridge University and Tokyo University of Agriculture and Technology, as well as unsolicited requests from US institutes for collaboration in the area of silicon-based tandem cells and additional projects at AMOLF and the University of Southampton.

Highlights

- Detailed theoretical study of both front and rear surface Mie resonator arrays.
- Successful demonstration of a nanoimprinted Mie resonator–based anti-reflection and light-trapping layer in a conventional PECVD silicon nitride coating.
- A stable baseline process for planar IBC cells, enabling and encouraging collaborative efforts with many additional partners.

References

Eisenlohr, J., Tucher, N., Hohn, O., Hauser, H., Peters, M., Kiefel, P., Goldschmidt, J.C. and Blasi, B., 2015, „Matrix formalism for light propagation and absorption in thick textured optical sheets“, Opt. Express 23 (11), A502–A518.

Rahman, T., To, A., Pollard, M.E., Grant, N.E., Colwell, J., Payne D.N.R., Murphy, J.D., Bagnall, D.M., Hoex, B. and Boden, S.A., 2017, “Minimising bulk lifetime degradation during the processing of interdigitated back contact solar cells”, Prog. in Photovolt.: Res. Appl., 1–10.

Smith, D., Reich, G., Baldrias, M., Reich, M., Boitnott, N. and Bunea, G., 2016, “Silicon solar cells with total area efficiency above 25%”, IEEE 43rd Photovoltaic Specialists Conference (PVSC).

Spinelli, P., Verschuuren, M.A. and Polman, A., 2012, “Broadband omnidirectional antireflection coating based on subwavelength surface Mie resonators”, Nat. Commun., 3, 692.

Spinelli, P., Macco, B., Verschuuren, M.A., Kessels, W.M.M. and Polman, A., 2013, “Al2O3/TiO2 nano-pattern antireflection coating with ultralow surface recombination”, Appl. Phys. Lett., 102, 233902.

6.24: Alignment-Free Photothermal Deflection Spectrometer: From University to Industry

Lead Partner

UNSW

UNSW Team

Dr Michael Pollard, Dr Ivan Perez-Wurfl, Dr Binesh Puthen-Veettil

Industry Partner

Open Instruments Pty Ltd: Dr Henner Kampwerth

Funding Support

ARENA, ACAP

Aim

Second-generation photovoltaic devices employ increasingly thin films of photoactive materials. Highly important examples are those based on CZTS and perovskites, which are showing huge promise for commercial deployment. These materials can have their electrical and optical properties tuned over a wide range by altering their constituent elements and growth methods. As with all optimisation procedures, accurately measuring the effect of material changes is critical.

One of the most important parameters to measure is the optical absorption spectrum. Unfortunately, this can be problematic. Currently available instruments are not typically sensitive enough to extract an accurate absorption spectrum from thin-film materials. This is particularly true for measurements in the so-called "sub-bandgap" region; a region containing vital information on defects and Urbach tails, which are key determinants of material quality. Without detailed feedback on their material characteristics, researchers have to work blindly via trial and error.

From 2013 to 2015, ARENA funded the development of a photothermal deflection spectrometer (PDS) at UNSW. With ultra-high sensitivity, this instrument was able to accurately measure absorption spectra, fulfilling all expectations and exceeding the performance of commercially available absorption spectrometers by three orders of magnitude (1000x). Since commissioning, it has become popular among researchers in several research groups, allowing them to obtain the information they need to develop next generation devices.

This ACAP-funded project, building on the previous ARENA results, has made huge strides towards instrument commercialisation. The system will be – by a wide margin – the world's most sensitive optical absorption spectrometer.

For successful commercialisation, the most important hurdle to be overcome was the incredibly time-consuming mechanical alignment of the sample. Novice users, or even experienced ones measuring unusual samples, could easily take more than an hour for sample alignment. Funding from this ACAP project enabled a highly effective collaboration between UNSW and Open Instruments Pty Ltd, allowing this important hurdle to be surmounted.

Outcome

We are pleased to report that the alignment issues plaguing the laboratory prototype instrument have been successfully overcome. After evaluating the performance of all components affecting the sample alignment, we extended our evaluation to the entire system layout. This deeper analysis of the overall instrument has allowed us to not only solve the alignment issue, but also decrease the system footprint by 25–30%, eliminate all motorised stages, and use a lower cost probe beam detector. All of these factors are welcome side effects for the subsequent commercialisation phase. Furthermore, it is necessary to ensure that researchers are able to make good use of this near-commercial prototype. We will therefore be installing the fully functional system, closely matching the eventual commercial unit, in the laboratories at UNSW.

The current state of the project is detailed in the following project deliverables.

Development of an alignment-free sample stage

Solving the alignment issue became significantly more challenging than envisaged. It was quickly noted that simply altering the sample mount would not entirely eliminate the alignment issue. Following the evaluation phase, it was decided that redesigning the entire system layout would be the most efficient solution to ensure long-term reliability and guaranteed reproducibility. The new system design required extensive use of the manufacturing facilities available at Open Instruments. A range of custom components were machined, all of which required testing and evaluation.

Fig. 6.24.1: Current photothermal deflection spectrometer

The differences between the original lab prototype and the current system, shown in Figure 6.24.1, are:

- The cantilever beam path has become both folded and encapsulated. Folding the beam permits the use of longer throw distances within a smaller footprint, while encapsulation ensures that there is no disturbance from air flow in the system. For a long time, air flow was an unrecognised source of signal degradation. These changes have increased both the signal-to-noise ratio and reproducibility.
- The sample stage was relocated and the system orientation changed such that the user has easy access to the stage for sample changes. Along with the encapsulation, this dramatically reduces the possibility of the user bumping into the instrument and disrupting the optical alignment.

- The detector sampling the excitation beam and providing the lock-in reference was changed to a broadband pyroelectric device connected to a custom made electronic amplifier. This solved the weak signal and sporadic behaviour of the previous detector, which would often prevent lock-in amplification of the extremely low level PDS signal.
- The tunable light source (monochromator) was upgraded to include a different grating. This has increased excitation beam throughput and therefore signal-to-noise ratio.
- The sample stage now operates with the surface to be measured fixed at a known reference plane, therefore samples of different thicknesses can be measured without any change to the system alignment.

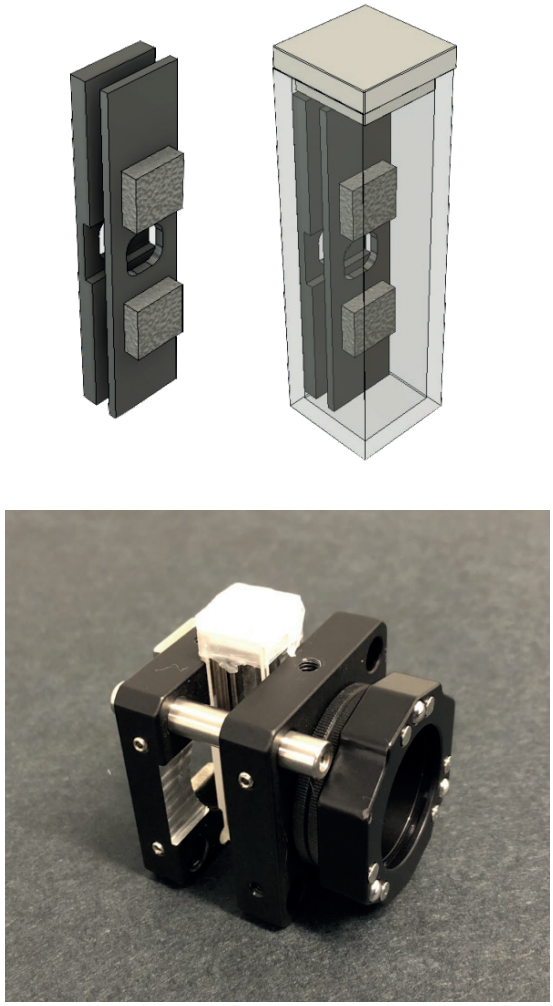

Fig. 6.24.2: CAD and optical images of the design now used for the alignment-free lab prototype at UNSW.

Several variations of the sample stage have been developed. Figure 6.24.2 shows CAD and optical images of the design now used for the alignment-free lab prototype at UNSW. This particular design allows continued use of pre-existing cuvettes and sample sizes. A more recent variation of the sample stage, intended for incorporation into the final commercial prototype, allows for much larger sample sizes and positional flexibility.

Control software and release via CD

Scientific measurement instruments usually gain widespread use only if they are user friendly. However, it is recognised that there are always some applications where advanced researchers may wish to adapt a system to new research objectives. It is therefore desirable to have this flexibility built into the system, while maintaining ease of operation for standard use cases, a philosophy that is shared by Open Instruments. In addition to the system layout being accessible and built from largely off-the-shelf components, the control software can be readily modified if required. During the course of this project, the software was completely redesigned from the ground up to be modular and flexible. It has been coded in LabVIEW, one of the most commonly available and easily understood programming languages at universities.

As CDs are now rarely used, the final control software will be released online and made available to users on a USB mass storage device upon request.

PDS prototype commissioned and users trained within two hours

While the lab system is operational, the control software for the final commercial prototype is currently undergoing functional verification. This will be completed within the next two months, allowing the final milestone to be achieved and the system to be released to users by Q2 2018.

Highlights

- A large step towards commercialisation of the world's most sensitive photo-absorption spectrometer.
- Design and verification of an alignment-free sample stage, now in daily use on the lab prototype.
- An expedited route to market by redesigning the system layout and careful component selection.

6.25 Development of GaAsBi-Based 1.0–1.2 eV Sub-Cells for Multi-Junction Solar Cells on Silicon Substrates

Lead Partner
UNSW

UNSW Team
A/Prof S. Bremner, A/Prof Anita Ho-Baillie

UNSW Students
Hongfeng Wang, Hayden Lobry

Academic Partner
Arizona State University

Arizona State University Team
Prof Christiana Honsberg, Prof Richard King

Funding Support
ACAP Collaborator Grant

Aim

The major goal of this project is to develop a gallium arsenide bismide–based sub-cell with a band gap in the 1.0–1.2 eV range suitable for inclusion in fully monolithic four-stack multi-junction solar cells. A multiple quantum well design will be developed with growth on germanium an end goal, with potential photovoltaic performance being assessed by a suite of characterisation techniques.

Progress

The first task undertaken was establishing GaAs growth on Ge. This consisted of developing a migration enhanced epitaxy (MEE) initiated growth procedure. After thermal treatment to clean the Ge surface the temperature was lowered to 250˚C. The Ga flux was set to 0.1 monolayer per second and an As overpressure in the 10^{-7} Torr range was used. An alternate deposition of Ga and As was then used for 25 cycles to create a seed GaAs layer. The GaAs epitaxy after the MEE process can be divided into two steps. The first one is low temperature slow growth conducted at 500°C with a growth rate of 0.1, the second step is high temperature fast growth conducted at 600˚C with a growth rate of 0.3. It has been shown that the 600˚C growth temperature would lead to a smooth surface, the root-mean-square (RMS) values from atomic force microscope (AFM) scans exhibited a decrease trend with an increment of growth temperature from 520˚C to 600˚C. Each step lasts for one hour respectively, therefore the entire structure consists of 400 nm GaAs and 7 nm (25 monolayers) MEE GaAs. Subsequent GaAs growth can then proceed at higher growth rates.

A number of factors were checked to see the best possible approach to the GaAs growth, looking at final surface roughness through atomic force microscopy, and X-ray diffraction and transmission electron microscopy results for crystal quality. Some of the results are shown in Figure 6.25.1. A 650˚C anneal prior to GaAs MEE was found to provide an improved surface smoothness and the use of As4 in preference to As2 was confirmed in this way. Also shown are TEM images for GaAs grown on Ge substrates with no evidence of dislocation formation seen for direct GaAs on Ge. By contrast, when the GaAs MEE step was replaced by AlAs MEE (same fluxes) there appears to be dislocation formation, suggesting no advantage to this approach. These results indicate fine-tuning of the growth is required and that more stringent substrate cleaning is needed, as the dislocation are most likely originating from the Ge surface. The suspicion of Ge contamination is reinforced by the pinholes seen in the AFM images.

The first batch of GaAsBi multiple quantum well samples on GaAs substrates were also grown and characterised. These consisted of five 8 nm layers of GaAsBi grown at various temperatures (380˚C, 410˚C, 440˚C) with 32 nm GaAs grown at 580˚C (Richards et al., 2015). Samples were capped with 100 nm GaAs at 600˚C. Time integrated photoluminescence spectra were obtained for the 380˚C samples for fluxes of Bi corresponding to Bi source temperatures of 660˚C, 700˚C and 730˚C. The results are shown for PL emission at 7 K and room temperature in Figure 6.25.2 where it is noted that the emission energy for the quantum wells increased with Bi flux, this is in contrast to the intuitive trend of more Bi being in the GaAsBi with higher Bi flux. The conclusion of lower Bi content with increased Bi flux was confirmed using Rutherford Backscattering Spectroscopy.

The trend of decreasing Bi content is believed to be due to the extreme surface segregation of Bi during growth, but no definitive explanation is yet available. Temperature-dependent PL measurements for the 380°C series of samples revealed an S shape to the emission energy as the temperature increased. This S shape became more pronounced for higher Bi flux, suggesting a greater density of trap states for the higher Bi flux

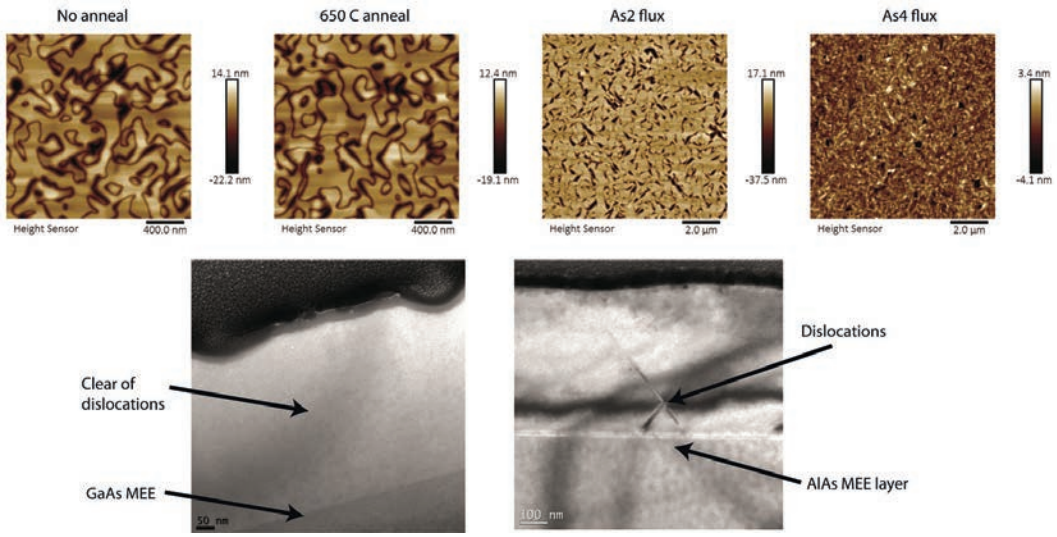

Figure 6.25.1: Top: Atomic force microscopy images of GaAs surface of GaAs on Ge samples showing impact of 650˚C anneal (left two images) and the impact of As4 versus As2 (right two images). Bottom: Transmission electron microscopy images showing GaAs on Ge with (left) presence of dislocations in direct GaAs on Ge, (right) seeming absence of dislocations in sample with AlAs MEE included instead of GaAs MEE.

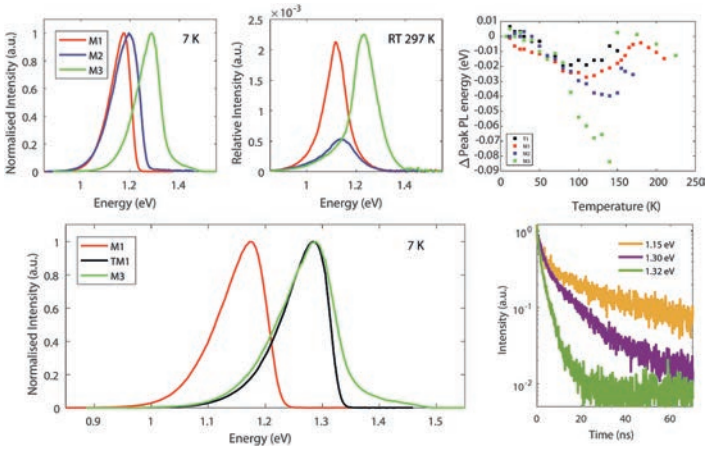

Figure 6.25.2: Photoluminescence results for series of GaAsBi multiple quantum well samples. Top: A series grown at 380˚C with Bi source temperatures at 660˚C (M1), 700˚C (M2), and 730˚C (M3) show a counter-intuitive trend in emission energy. Emission energy versus temperature for these samples shows an S shape that is enhanced with increased Bi flux. Bottom: Results for sample grown at 410˚C with 660˚C Bi source temperature (TM1) showing similar emission energy to M3. Time resolved decay curves taken at different emission energies show very different decay time constants, indicative of trap states.

samples. Time resolved photoluminescence was also used to examine samples, with further growths at temperatures of 410˚C and 440˚C to increase Bi desorption from the growing surface and decrease trap density. As shown in Figure 6.25.2 the emission energy for the 410˚C sample corresponded to that for the highest Bi flux 380°C sample. A broad spectrum was seen and when TRPL measurements were performed using a photon counting technique at different emission energies it was noted that there were very different decay time constants associated with the different energies. This again suggests the presence of traps that elongate carrier lifetime before recombination. These results suggest optimising the GaAsBi growth will require a higher temperature plus tuning the Bi flux in order to not have an oversupply, which seems to lead directly to a large density of traps despite the Bi incorporation being lower.

Highlights

- Growth of GaAs on Ge and vicinal Ge substrates achieved by a low temperature MEE method.
- Growth of GaAsBi quantum wells showing photoluminescence emission in the 1.0–1.2 eV range.
- Decrease in Bi content observed with increased Bi flux, a result not explainable by any current models for Bi incorporation. This result has been confirmed by other laboratories growing GaAsBi.
- Improved emission with increased growth temperature indicating material quality improvement.

Future Work

- Further tuning of the growth of GaAsBi will continue.
- Time resolved photoluminescence spectroscopy of grown material will also continue, assessing the trap state density
- Development of a model for the incorporation rate of Bi in GaAsBi will be undertaken.
- Difficulties in obtaining a pristine Ge surface prior to MEE has led to the development of a new surface preparation technique based on buffered HF. This will deliver a clean surface for loading Into the MBE system. Final growth of GaAsBi multiple quantum well device on a Ge substrate will follow soon after this.

References

Richards, R.D. et al., 2015, “Growth and structural characterization of GaAsBi/GaAs multiple quantum wells”, Semiconductor Science and Technology, 30, 094013.

6.26 Advanced Hydrogenation and Mitigation of LeTID on PERC Cells Made From 1366 Technologies Direct Wafer® Multi-Crystalline Silicon Material

Lead Partner
UNSW

UNSW Team
Dr Catherine Chan, Dr Alison Ciesla, Prof Stuart Wenham

USA Partners
Team
Dr Adam Lorenz, Dr Rob Steeman

Aim

This project aims to implement UNSW's advanced hydrogenation technology into high efficiency PERC cells made from 1366 Technologies' Direct Wafer® material. This material is made using a kerfless, low-cost, low-CAPEX, proprietary wafering process with promise to halve the cost of silicon wafers. Due to the unique wafering method, Direct Wafer® has many advantages over conventionally cast high performance multicrystalline silicon (HP mc-Si) and has the potential to be superior in electronic quality to such wafers. This is primarily due to the lack of dislocation clusters that form during traditional casting processes, as well as tighter control over impurity and doping concentration. Recently, over 20% conversion efficiency was achieved on full-area PERC devices manufactured by Hanwha Q-Cells using Direct Wafer®. The goal of this project is to help close the efficiency gap between PERCs fabricated on Direct Wafer® and the champion R&D PERCs currently achieved on conventional HP mc-Si (> 22%). In addition, the project aims to find solutions to suppress LeTID (light- and elevated temperature induced degradation) in Direct Wafer®, which has been found to be a major hurdle for PERCs – affecting not only HP mc-Si material as originally thought, but virtually all materials to some degree including Cz and even the highest quality FZ wafers.

Progress

In the first half of this two-year project, Direct Wafer® samples were sent to UNSW for testing including lifetime test structures and both full area Al-BSF and PERCs . Firstly, the response of the Direct Wafer® material to conventional hydrogenation processes (i.e. firing in an infrared fast firing furnace with PECVD passivating films) was assessed. It was found that Direct Wafer® material responded quite differently to these processes than conventional HP mc-Si. Importantly, these wafers responded much more strongly to hydrogenation, with larger improvements in bulk lifetime after firing than for HP mc-Si. In addition, slightly higher peak firing temperatures were required to achieve good hydrogen passivation of the bulk material than what is typically required for HP mc-Si. Due to the unique proprietary method for producing Direct Wafer®, the material has virtually no dislocations which are one of the major defects causing a reduction in lifetime in conventional casted HP mc-Si material (see Figure 6.26.1). However, Direct Wafer® has much smaller grains (of the order of hundreds of microns) and hence a very large density of grain boundaries (see Figure 6.26.2). Since most grain boundaries can be reasonably passivated with hydrogen, this is not considered to be detrimental but could explain why a higher firing temperature is required to achieve good passivation of the bulk material.

Several UNSW advanced hydrogenation processes were then applied to the material, designed to control the charge-state of hydrogen atoms within silicon to enhance their diffusivity and reactivity with defects. Without any refinement or optimisation for Direct Wafer®, the potential for improvements in material quality were demonstrated. An improvement in the bulk lifetime of 20% was achieved, and a 0.2% absolute efficiency increase was

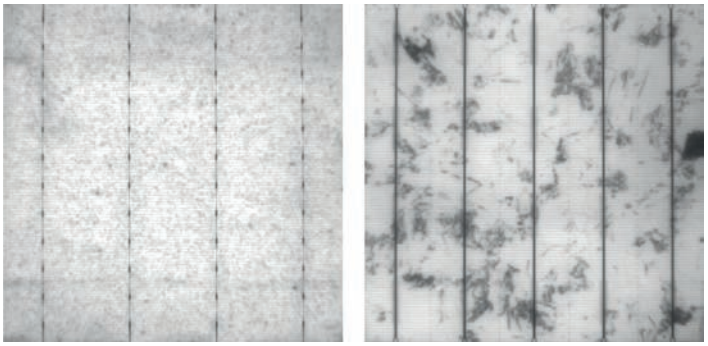

Figure 6.26.1: Photoluminescence images of PERCs made from Direct Wafer® material (left) and standard high-performance multicrystalline silicon (right). Performance-limiting dislocations appearing as dark regions in the HP mc-Si are not present in the Direct Wafer® material.

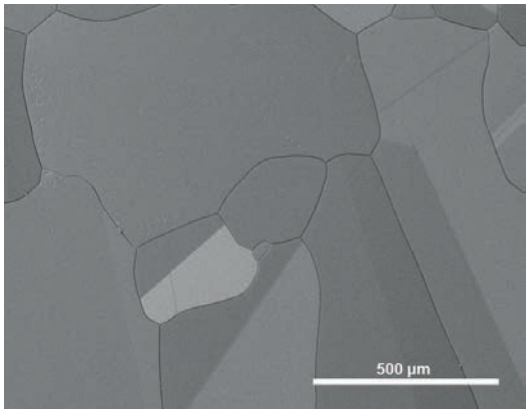

Figure 6.26.2: Scanning electron microscope image of Direct Wafer® surface, showing the small size of the grains in this novel material.

achieved on small 3 x 3 cm cells with full aluminium back surface field (Al-BSF) rear. With further optimisations and adaptations of the advanced hydrogenation processes it is likely that significantly larger improvements can be achieved. Optimisations to achieve the maximum possible bulk lifetimes, and studies to understand the lifetime limiting defects of the material and how they respond to hydrogen will be a large focus of the ongoing project.

Ultimately, for cheaper wafer sources to be able to compete with conventional higher lifetime wafer sources, they need to be incorporated into high efficiency solar cell architectures such as the Passivated Emitter and Rear Cell (PERC). However, a problem has been plaguing the PV industry as it has transitioned from the Al-BSF structure to the higher efficiency PERC architecture. A degradation in minority carrier lifetime of silicon wafers occurs when exposed to illumination at elevated temperatures, similar to those that would be experienced in

the field. This was reported in 2012 and is known as light- and elevated temperature-induced degradation (LeTID). This has also been referred to in the literature as mc-Si CID (carrier-induced degradation), since the degradation is caused by excess carrier injection and was once thought to be exclusive to mc-Si. However, despite degradation being most severe in mc-Si solar cells, with up to 16% relative power loss being reported, LeTID seems to be a ubiquitous problem appearing also in Cz (monocrystalline) PERCs . Not surprisingly, Direct Wafer® also shows some susceptibility to the same defect. Wafers and cells were subject to degradation tests using both industry standard degradation conditions of 75°C and 1000 Wm^{-2} illumination as well as accelerated degradation tests using UNSW's laser system which can assess LeTID extent within only a few seconds, as opposed to several days. Through applying a range of lab-scale LeTID mitigation processes on small PERCs made from Direct Wafer® material, we were able to suppress the LeTID extent by up to 90% (stable after several hundred hours of degradation testing), giving good indication that the LeTID in Direct Wafer® material can be significantly reduced or even eliminated through specialised optimisation (Figure 6.26.3).

Much progress has been made on understanding the LeTID defect in mc-Si, although its exact nature is still largely unknown. Due to the nature of the wafering process, 1366 Technologies can grow their wafers with highly tuneable parameters such as grain size, impurity concentration and resistivity. Understanding the effect that these parameters have on LeTID is likely to provide clues towards identifying the defect responsible for LeTID. Thus, detailed studies of the kinetics of degradation and regeneration on this wafer type are currently underway.

Highlights

- Improved minority carrier lifetime of Direct Wafer® material using advanced hydrogenation treatments.
- 0.2% absolute improved initial efficiency and 90% reduction in LeTID achieved on small-area cells made from 1366 Direct Wafer® material.
- UNSW team visit to 1366 Technologies in Bedford, Massachusetts in June 2017.

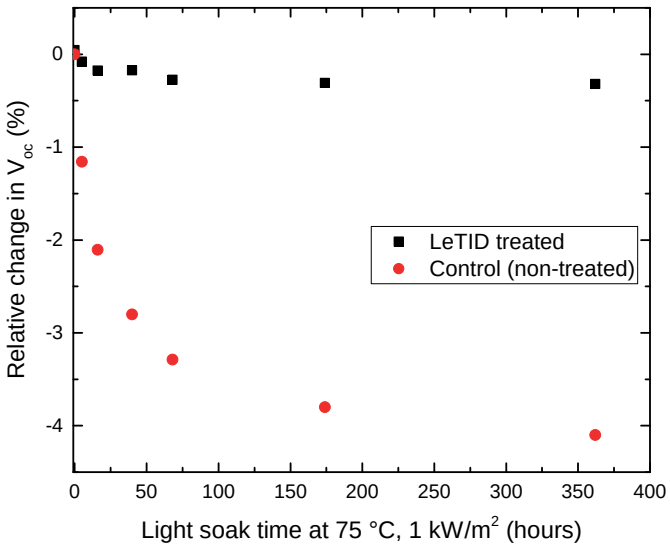

Figure 6.26.3: Relative change in V_{OC} during light soaking at 75°C and 1 kWm^{-2} illumination under halogen lights for high efficiency PERCs made using a type of Direct Wafer® material that shows some susceptibility to LeTID. One sample received LeTID treatment (black squares) while the control sample (red circles) did not receive LeTID treatment.

Future work

In the second half of the project to be carried out in 2018 we will aim to:

- Modify the advanced hydrogenation process to better suit the Direct Wafer® material and achieve higher minority carrier lifetimes and increased cell efficiency.
- Demonstrate the advanced hydrogenation and LeTID mitigation techniques on full size 156 x 156 mm wafers and cells using new tools available to process large wafers at the Solar Industrial Research Facility (SIRF).
- Further study the kinetics of the LeTID defect in Direct Wafer® material compared to HP mc-Si to gain a better understanding of the degradation and regeneration mechanisms.

6.27 Silicon Nanocrystal Carrier Selective Contacts for Silicon Solar Cells

Lead Partner
UNSW

UNSW Team
Prof Gavin Conibeer, Dr Ivan Perez-Wurfl, Dr Robert Patterson

USA Partners
Team
Natcore Technology Inc, Rochester NY: Dr Dennis Flood, Dr David Levy

Aim

This project aims to combine expertise on silicon quantum dots (QDs) and high efficiency solar cells with the market-tested industrial technology of passivated black silicon and liquid phase deposited (LPD) nanocrystal films from our partner, Natcore, to design high quality carrier selective contacts that are cost-effective and compatible with silicon solar cell fabrication technology.

An ARC Linkage proposal has been written and submitted with partner Natcore Technology Inc. as the major output of this project in its first year.

Progress

The project aims to develop a proposal for black silicon onto the front side and silicon QDs onto the back side to replace the PECVD deposited a-Si:H that is currently used on both sides of an IBC-SHJ solar cell. This deposition technique is highly novel and challenging, requiring significant innovations in surface chemistry and low temperature heterojunction fabrication. These innovations and cost reductions for this cell type have the potential to reduce its fabrication cost per Watt below all other cell types, while retaining its position as the most efficient silicon photovoltaic device.

An ARC Linkage proposal has been written and submitted, which proposes two key innovations.

The first innovation is to simultaneously improve the passivation and anti-reflection properties of "black" silicon fabricated from a wet chemical etch technique using silver nanoparticles onto the front surface of silicon solar cells, see Figure 6.27.1. Black silicon is known to have excellent anti-reflection across the visible spectrum due to nanostructures with sub-wavelength dimensions (Oh et al., 2012). However, black silicon still has many challenges in its implementation, including relatively high surface defect concentrations requiring passivation and leading to short charge carrier lifetimes overall from devices. Natcore has demonstrated surface defect passivation that preserves desirable long charge carrier lifetimes in the bulk, on the order of 100 microseconds. This work proposes to provide the low temperature passivation required to push this lifetime into the millisecond range.

The second innovation is to use silicon QDs to form a passivating layer on the back surface of a silicon solar cell that mimics the excellent passivation obtained from amorphous silicon deposited by PECVD, see Figure 6.27.2. This passivation arises from the widened bandgap and favourable band offsets that a-Si has relative to bulk silicon. These are properties that

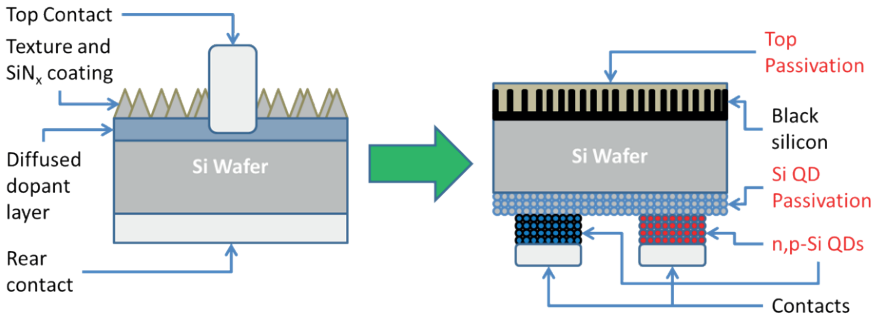

Figure 6.27.1: Innovations on the typical device architecture addressed in this project. (a) Typical homojunction solar cell with front-side texturing with an SiNx deposition and a diffused back surface field (BSF) or Passivated Emitter and Rear Cell (PERC) structure; and (b) all back contacted silicon heterojunction solar cell using silicon QDs and black silicon. Silicon QDs will be on the order of ~5 nm and the feature size of Natcore's black silicon is approximately 50 x 500 nm pillars.

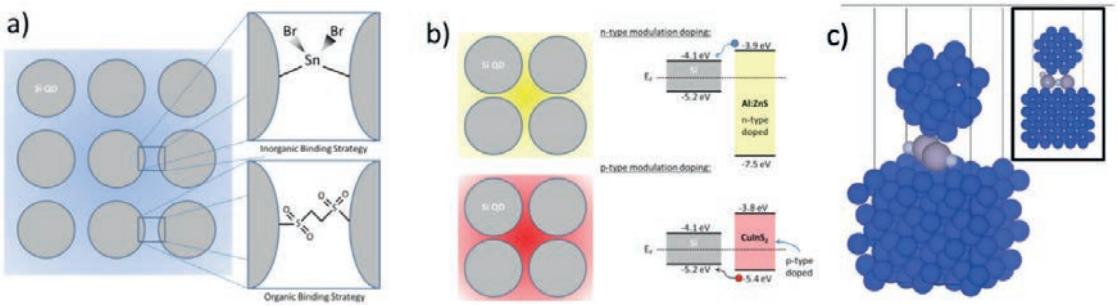

Figure 6.27.2: (a) Silicon QD binding strategies showing inorganic $SnBr_2$ and organic ethanedisulphonic acid binding two silicon surfaces together, where Sn transitioning to the more stable 4+ state and deprotonation of the sulphonic acids lead to bonding respectively. In both cases, the initial concentration of the binding agent in solution is critical to achieving good binding and also good conductivity through the nanostructured film. A mild thermal process between 80°C and 175°C to remove solvent and drive binding reactions will be performed; (b) modulation doping strategies using wide bandgap n-type aluminium doped zinc sulphide and narrower bandgap intrinsically p-type copper indium disulphide as modulation doping materials that donate the desired charge carrier type due to band offset and Fermi level matching; and (c) example of an atomistic model of a silicon surface with a silicon QD on top bound by two SnF_2 molecules.

silicon QDs share, due to advanced quantum confinement effects. Deposition of the QDs onto silicon wafer surfaces by low-cost spin-coating or dipping processes, the patterning of dopants and mild thermal processes to dry the QD films will be required. These techniques are used routinely at UNSW in the colloidal QD program (Zhang et al., 2017).

Progress on deliverables after one year

Deliverable 1 is for submission of a journal paper on the passivation of interfaces. It is too early for this deliverable to have been met, but the work on the project will be used to extend sections of the conference paper (see Deliverable 3) into a journal paper in the second and third year of the project.

Deliverable 2 is for submission of a journal paper on carrier selective contacts. It is too early for this deliverable to have been met, but the work on the project when funded will be used to extend other sections of the conference paper into a journal paper in the second and third year of the project.

Deliverable 3 is for submission of a conference paper on the fabrication of QD materials to the Euro PVSEC conference. At this stage of the project (1 year in) an abstract has been submitted to the World PVSEC in Hawaii in June 2018, which incorporates the Euro PVSEC, on QD solar cells.

Highlights

- Linkage proposal completed and submitted to ARC with partner Natcore. An outcome is expected in March or April 2018.
- Design of the two key innovative steps of the project, for design of a silicon QD heterojunction passivation layer and passivation schemes for the silicon QDs in the heterojunction layer.

References

Oh, J., Yuan, H.C. and Branz, H. M., 2012, “An 18.2%-efficient black-silicon solar cell achieved through control of carrier recombination in nanostructures”, Nat. Nanotechnol. 7, 743–748.

Zhang, Z., Chen, Z., Yuan, L., Yang, J., Zhang, J., Wen, X., Chen, W., Stride, J., Conibeer, G., Patterson, R.J. and Huang, S., 2017, “Significant Improvement in the Performance of PbSe Quantum Dot Solar Cell by Introducing a CsPbBr3 Perovskite Colloidal Nanocrystal Back Layer”, Adv. Energy Mater., 7 (5), 1601773 DOI: 10.1002/aenm.201601773.

6.28 P-type Hybrid Heterojunction Solar Cells

Lead Partner
UNSW

UNSW Team
Dr Brett Hallam

UNSW Students
Daniel Chen, Moonyong Kim

Academic Partner
Arizona State University

Arizona State University Team
Prof Zachary Holman

Funding Support
ARENA

Aim

The aim of this project is to develop methods to assess and improve the effectiveness of bulk hydrogenation in heterojunction solar cells. The passivation of boron-oxygen (B-O) defects and grain boundaries will be demonstrated on samples with amorphous silicon passivated p-type silicon. From this, we will fabricate p-type heterojunction solar cells with gettering and bulk hydrogenation and assess the impact of illuminated annealing processes on a-Si heterojunction surface passivation layers. We will also develop a p-type hybrid heterojunction solar cell structure with bulk hydrogenation and gettering.

Progress

A method for assessing and improving the effectiveness of bulk hydrogenation in heterojunction solar cells was developed. This method is using prefabrication gettering and bulk hydrogenation, with subsequent removal of the surface layers and the reapplication of a low-temperature silicon nitride layer, consistent with the expectations with amorphous silicon passivation. For multicrystalline wafers, PL imaging can then show the effectiveness of grain boundary passivation. For Cz wafers, subsequent light soaking and a comparison before and after light-soaking can show the effectiveness of B-O defect passivation wafers (see Figure 6.28.1). This can be enhanced by using injection level–dependent lifetime curves to study recombination properties. Examples of the technique are shown in Figure 6.28.2 (Hallam, 2017).

High-intensity illuminated advanced hydrogenation processes have been applied on a-Si-based heterojunction structures. We have shown improvements in the bulk and effective lifetime through this process. However, initial testing has indicated that the advanced hydrogenation process has led to a deterioration of the a-Si passivation properties with a slight increase in the dark saturation current density from 5.2 fAcm^{-2} to 8.1 fAcm^{-2}. Figure 6.28.3 shows the changes in the extracted recombination properties before and after an illuminated hydrogen passivation process. Further analysis is required to understand the mechanisms.

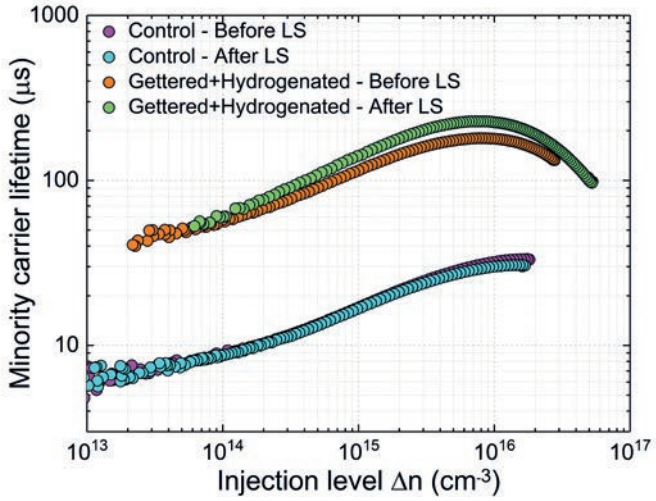

Figure 6.28.1: Injection level–dependent lifetime curves of a control sample before and after light soaking (LS), and on a sample with prefabrication gettering and bulk hydrogenation. No degradation of lifetime occurs during LS, suggesting that the samples are free from B-O related light-induced degradation.

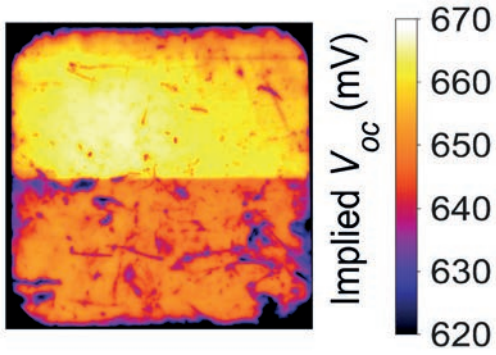

Figure 6.28.2: PL image of a test structure fabricated with prefabrication hydrogenation (top half) and without prefabrication hydrogenation (bottom half) highlighting the importance of bulk hydrogenation for heterojunction structures fabricated on p-type silicon. Image adapted from (Hallam, 2017).

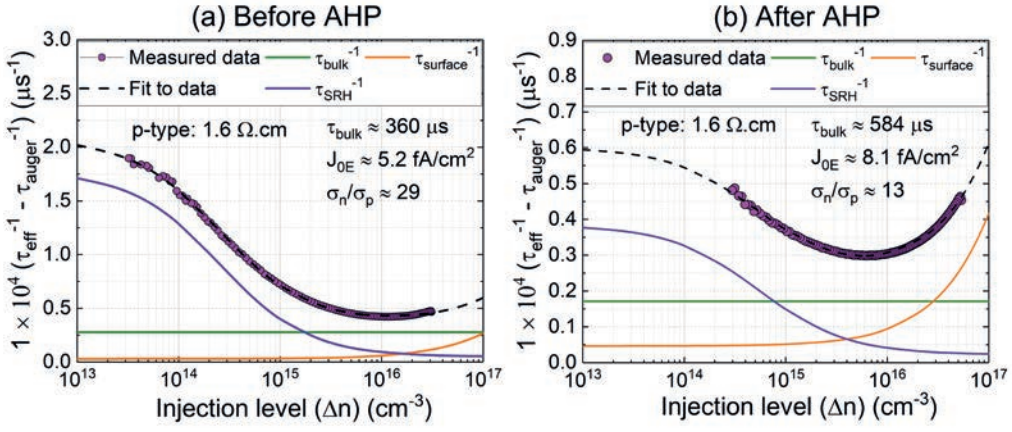

Figure 6.28.3: Injection level–dependent lifetime analysis for a heterojunction lifetime test structure with prefabrication gettering and bulk hydrogenation on p-type silicon (a) before and (b) after an advanced hydrogenation process. The advanced hydrogenation process enhances bulk lifetime but leads to a slight deterioration of the surface passivation.

Group	J_{SC} (mA cm^{-2})	V_{OC} (mV)	FF (%)	pFF (%)	η (%)
Al-BSF screen print	37.0	643	79.5	–	18.9
Control	38.0	621	68.9	80.2	16.3
Hydrogenated	39.2	628	66.4	74.6	16.4
Gettered	38.8	643	68.9	79.6	17.2
Gettered + Hydrogenated	39.3	692	69.6	78.3	18.9

Table 6.28.1: Summary of I-V results from cells fabricated with and without prefabrication gettering and hydrogenation. Data from Hallam, 2018.

We have successfully demonstrated the importance of gettering and bulk hydrogenation for p-type heterojunction solar cells, with an improvement in the open circuit voltage of 70 mV for p-type Cz silicon to reach open circuit voltages of 692 mV. Figure 6.28.4 shows I-V data highlighting the impact of prefabrication gettering and hydrogenation(Hallam, 2018). The application of an advanced hydrogenation process increased the open circuit voltage substantially, to reach a world record independently confirmed value of 703 mV for p-type Cz silicon. This result has been submitted to the IEEE-PVSC (Chen, 2018). Initial test structures on p-type multicrystalline silicon have shown open circuit voltages of 692 mV.

Test hybrid heterojunction structures with conventional front surface processing and a heterojunction rear structure have been fabricated. Initial results show implied open circuit voltages of 675 mV, and will be processed into hybrid heterojunction solar cells in 2018. An abstract has been submitted to IEEE-PVSC (Kim, 2018).

Highlights

- This year, we have demonstrated the importance of gettering and bulk hydrogenation for p-type heterojunction solar cells.
- We have achieved a world record independently confirmed open circuit voltage of 703 mV for p-type Cz silicon.
- We have also reached an open circuit voltage of 695 mV for a metallised test structure fabricated on p–type multicrystalline silicon.

Future Work

- Future work will continue assessing the impact of illumination on silicon heterojunction structures.
- We will continue the development of the technology and fabricate hybrid heterojunction solar cells in 2018.
- This will also lead into our new ARENA-funded project, to see efficiencies of 24% on p-type Cz wafers by 2021.

References

Hallam, B. et al., 2017, “The role of hydrogenation and gettering in enhancing the efficiency of next-generation Si solar cells: An industrial perspective”, Physica status solidi (a) 214, 1700305 (Feature article).

Hallam, B. et al., 2018, “Pre-Fabrication Gettering and Hydrogenation Treatments for Silicon Heterojunction Solar Cells: A Possible Path to >700 mV Open-Circuit Voltages Using Low-Lifetime Commercial-Grade p-Type Czochralski Silicon”, Solar RRL, 1700221. https://doi.org/10.1002/solr.201700221.

Chen, D. et al. Submitted abstract to IEEE-PVSC, 2018.

Kim, M. et al. Submitted abstract to IEEE-PVSC, 2018.

6.29 Development of Online Educational Resources for PV Manufacturing Education

Lead Partner
UNSW

UNSW Team
A/Prof Bram Hoex

UNSW Students
Jing Zhao, Daniel Chen, Moonyong Kim, Alex To, Jack Colwell, Utkarshaa Varshney

QESST Team
Prof Stuart Bowden, Dr Andre Augusto

Funding Support
ACAP, UNSW

Aims

The photovoltaic technology and manufacturing course is a core component of the under- and postgraduate degree in Photovoltaic Engineering at UNSW. The course aims to:

- introduce the students to the technologies used to manufacture solar cells
- expose the students to a solar cell manufacturing environment and critical manufacturing concepts such as device design, yield, process optimisation
- develop students' ability to optimise a production line with various interrelated processes and process equipment.

As solar cell production lines are very costly and, unfortunately, not available in Australia, it was decided to create a virtual production line to ensure that students could be exposed to a solar cell manufacturing environment. The first iteration of the "virtual production line" was developed by Stuart Wenham and Anna Bruce (2005) and was shown to be very popular with the students and very effective in achieving the intended learning outcome. Very recently the "virtual production line" was further developed, rebranded as the 'PV Factory', and moved to the cloud to ensure that it can be used by students worldwide (PV Factory, 2016). The PV factory was developed in a project by UNSW, Arizona State University (ASU), PV Lighthouse and was partly funded by ACAP. The PV Factory has also shown to be very popular with students and successful in achieving the intended learning outcomes, and it is currently used at more than five academic institutions worldwide (including ASU) and by various solar cell manufacturing companies.

The PV factory is only one, albeit a paramount, part of the PV manufacturing course and is particularly useful in tutorials. It cannot effectively be used to explain the underlying physics and chemistry that underpin the various processes used in solar cell manufacturing and is not flexible enough to discuss recent developments in the field. Consequently, this is done via traditional lectures which are prepared by the individual teacher(s) at the various institutions.

The aim of this project was to develop an online educational resource similar to PV Education (Honsberg and Bowden,) focused on PV manufacturing. The goal is to make this the global "de facto" standard resource for PV manufacturing. The text Is complemented by tailor-made videos and/or animations which will assist the students in improving their understanding of the various concepts in the field.

Progress

The main objective of 2017 was to release the first version of the PV Manufacturing website by the beginning of 2018. A project team was formed consisting of an animator (Jing Zhao), video producers (Daniel Chen, Moonyong Kim, Andre Augusto), writers (Daniel Chen, Moonyong Kim, Alex Tom, Andre Augusto), and a graphical designer (Alex To). All the content was trailed In the SOLA3020 course and some of the videos were published on UNSW's E-Learning channel on YouTube (https://www.youtube.com/user/UNSWelearning). In December 2017 we registered the PV-Manufacturing.org domain and the population of the first iteration of the website was completed in January 2018. We decided to use the WordPress platform as it has a low barrier to entry and ensures that the maintenance of the website is relatively straightforward.

Highlights

- The first iteration of the PV-Manufacturing.org website was completed and published in January 2018. It currently covers the photovoltaic value chain from sand to silicon solar cells and includes text, tailored videos and animations.
- The goal was to establish it as the de facto standard reference for solar cell manufacturing.

Future Work

- The objective is to add further text, videos and animations to the website and to keep the information up to date.

References

Honsberg, C.B. and Bowden, S., PVCDROM, available: http://pveducation.org/.

PV Factory, 2016, available: https://factory.pvlighthouse.com.au/.

Wenham, S. and Bruce, A., 2005, "Analysis and simulation of manufactured screen-printed solar cells," in 31st IEEE Photovoltaic Specialist Conference, 1659.

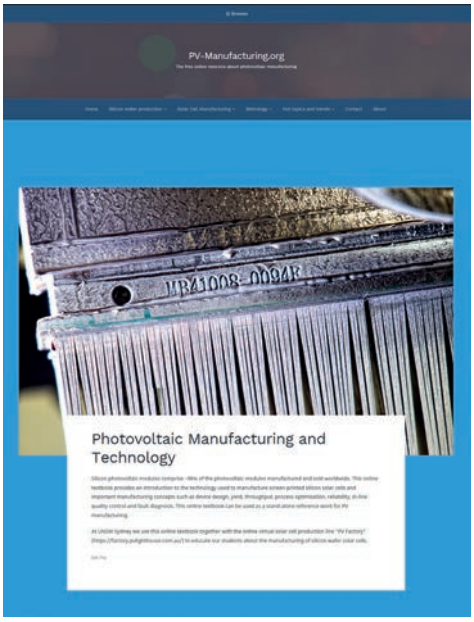

Figure 6.29.1: Screenshot of the homepage of PV-Manufacturing.org (photo of a multicrystalline silicon ingot after wafer slicing: Picture courtesy of Trina Solar).

6.30 Rapid Optical Modelling of Black Silicon

Lead Partner
UNSW

UNSW Team
Dr David Payne, Dr Malcolm Abbott, Tsun Fung

Australian Partner
PV Lighthouse Pty Ltd, Dr Keith McIntosh

Academic Partner
Technical University of Denmark, Dr Rasmus Davidson, Dr Maksym Plakhotnyuk

Funding Support
ACAP

Aim

Black silicon texturing has long been advocated for its unique optical properties, but recent advances in fabrication techniques and surface passivation have led to a dramatic increase in interest, particularly for multicrystalline wafers where the ability to create black silicon could enable diamond wire sawing and consequently reduce wafer costs. There is therefore a growing demand for efficient and well-tested optical modelling of black silicon and yet relatively little research has been carried out in this area. This project aims to address this need by developing an experimentally validated, cloud-based black silicon modelling tool.

Progress

In order to successfully develop and validate a modelling tool, a large dataset of measured characteristics from representative samples is required for comparison. This project therefore began with the fabrication of a variety of black silicon textured samples created using the reactive ion etching (RIE) approach at the Technical University of Denmark (DTU). This dataset was then further expanded as a collaboration was built with the US wafer producer, 1366 Technologies, who were able to provide a variety of textures fabricated using parameter sweeps on industrial-scale RIE and metal catalysed chemical etching (MCCE) setups. In total, over 60 different textured silicon samples were sourced. All samples were optically characterised in terms of reflectance and transmittance over the full wavelength range of interest, and surface topography was determined using scanning electron microscopy (SEM) and atomic force microscopy (AFM). Example SEM images of two representative textured samples are shown in Figure 6.30.1, highlighting the substantial differences in feature shapes and sizes achievable with industrial "black silicon" fabrication approaches.

As expected, the majority of black silicon textures investigated consisted of feature sizes similar to the wavelengths of visible light. In some cases, samples showed multiple scales of feature size, with both nanoscale and microscale texture. Such textures present a significant challenge for rapid optical modelling as the texture straddles multiple optical regimes, with geometric optics typically being an appropriate approach at short incident wavelengths and wave optics approaches being appropriate at longer wavelengths. This mixture of regimes was confirmed through use of the AFM data to determine optical validity regions for a representative group of textures, in accordance with the methodology detailed in Tang et al. As the validity plot of Figure 6.30.2 shows, the samples studied here typically cross multiple regions of validity, in contrast to typical random pyramid texturing used for monocrystalline solar cells which lies firmly in the geometric optics regime.

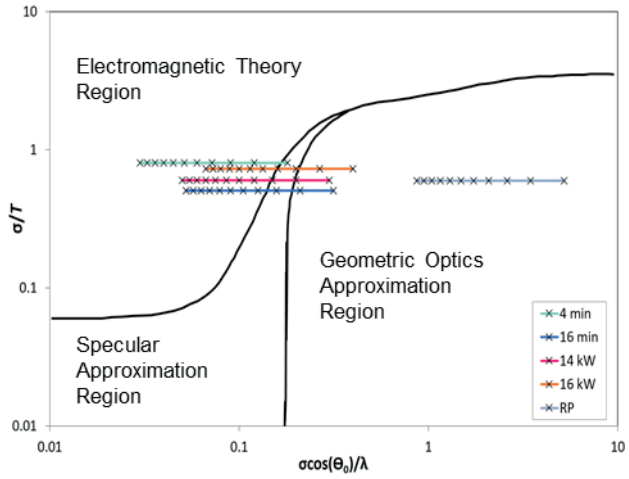

Figure 6.30.2: Plot of regions of validity based on approach by Tang et al. Validity regions of several textures from this project fabricated using various RIE process times and coil powers are shown along with random pyramid texture.

Textures such as these can be optically modelled through direct calculation of Maxwell's equations using finite element techniques, however this requires large computational resources and extensive simulation time. Alternatively, textures that lie completely in the geometric optics regime can be modelled using ray-tracing approaches, and certain textures that fall fully into the wave optics regime can be approximated in ray optics using effective medium approaches. For the case of the majority of black silicon textured samples studied within this project, testing of ray-tracing approaches using PV Lighthouse's *SunSolve* tool found that neither geometric ray-tracing or effective medium theory could accurately reproduce the optical

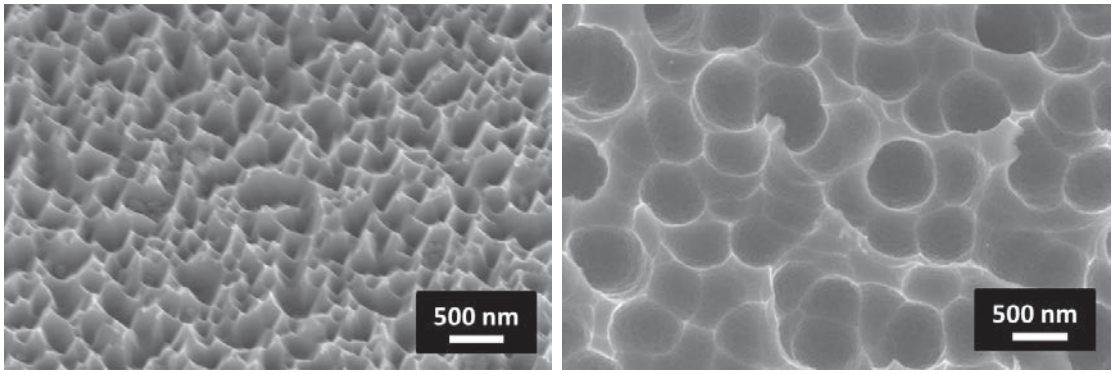

Figure 6.30.1: Example SEM images showing typical black silicon texture achieved using reactive ion etching process (left) and metal catalysed chemical etching process (right).

characteristics. This finding was presented at the 34th European Photovoltaic Solar Energy Conference along with suggested approaches for overcoming these limitations while maintaining high simulation speeds. As this work progressed, it was found that through a combination of these ray-tracing-based modelling approaches, a good fit between measured and simulated reflectance could be achieved, as illustrated in Figure 6.30.3.

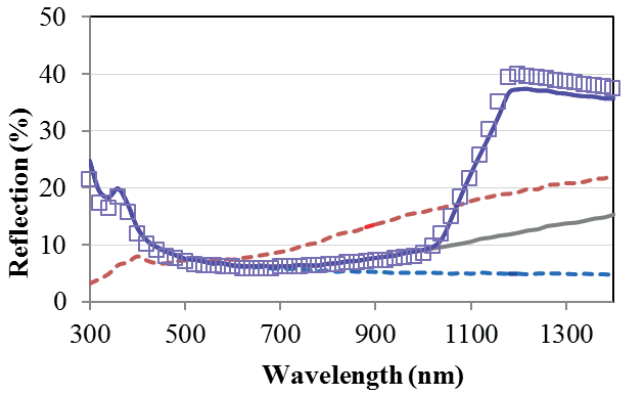

Figure 6.30.3: Example curve fit to the measured reflectance (squares) of an RIE textured wafer. The combined simulation including escape light (purple line) and without escape light (grey line) is comprised of modelling results from geometric optics (blue dashed) and effective medium (red dashed) approaches.

A key challenge when using this mixing of approaches is the determination of the wavelength-dependent mixing ratios. It was found that measured wavelength-dependent reflectance haze characteristics can provide one route towards defining these ratios, with high haze values being indicative of the need for a larger portion of the geometric optics approach and low haze suggesting a higher portion of the effective medium approach. The evident usefulness of the haze characteristic also led to the incorporation of haze modelling into the PV Lighthouse *SunSolve* ray tracer used throughout this work. In this case, knowledge of the RMS roughness of the textured surface is required and scalar scattering theory is then used to determine the approximate wavelength-dependent haze. Comparison with reflectance haze measurements reveals reasonably good agreement for a broad range of textures (see Figure 6.30.4).

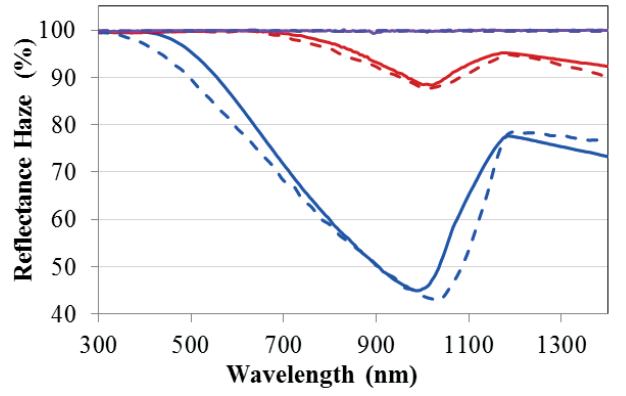

Figure 6.30.4: Measured (circles) and simulated (dashes) reflectance haze characteristics for samples with deep (purple), medium (red) and shallow (blue) texture.

Highlights

- A broad range of industrially produced black silicon textures have been extensively characterised, with most variants found to straddle both the geometric optics and wave optics regimes.
- Progress towards rapid optical modelling of these complex structures has shown that a combined approach of geometric ray-tracing and effective medium theory can be successfully applied.
- Implementation of modelling of reflectance haze based on scalar scattering theory has now been added to the PV Lighthouse *SunSolve* ray-tracer tool.

Future Work

- Further validation of the modelling technique is ongoing, this includes optimisation of the methodology for converting surface topography data to a multilayered effective medium as well as fine-tuning of the approach to combine geometric optics and effective medium based results.
- This project laid the groundwork for a larger grant application with the Australian Renewable Energy Agency (ARENA) on the topic of integrating industrial black silicon with high efficiency multicrystalline solar cells. That three-year project was successfully awarded in December 2017 and will build upon the current rapid modelling work while also investigating and optimising the compatibility of industrially produced black silicon textures with subsequent state-of-the-art and next generation photovoltaic fabrication processes.

References

Payne, D., Abbott, M., Claville Lopez, A., Zeng, Y., Fung, T., McIntosh, K., Cruz-Campa, J., Davidson, R., Plakhotnyuk M. and Bagnall, D., 2017, “Rapid Optical Modelling of Plasma Textured Silicon”, 34th European Photovoltaic Solar Energy Conference.

Tang, K., Dimenna, R.A. and Buckius, R.O., 1997, “Regions of validity of the geometric optics approximation for angular scattering from very rough surfaces”, Int. J. Heat Mass Transf., 40, 49–59.

6.31 Optical Characterisation of Passivated Contacts for Silicon Solar Cells

Lead Partner
ANU

ANU Team
Prof Andrew Blakers, Dr Kean Fong

Academic Partner
University of Central Florida, Dr Soe Zin Ngwe

Industry Partner
PV Lighthouse, Dr. Keith McIntosh

Funding Support
ARENA, ACAP, ANU

Aim

Passivated contacts on silicon solar cells provide electrical contact interfaces with low surface recombination, but at a higher contact resistance to typical diffused Si-metal contacts. The higher contact resistance necessitates large contact areas, often full rear surface contacts, thus increasing the significance of its optical characteristics to the overall device performance.

This project aims to investigate the optical characteristics of typical passivated contacts, and to provide insight into improvements to the optics of solar cells implementing passivated contacts.

Progress

Based on ray-tracing, we were able to perform a preliminary investigation on the potential optical performance of solar cells implementing passivated contacts on the rear surface of the device. The ray-tracing assumes single anti-reflection coating on the front textured surface, and a planar rear surface with a range of passivated contacts, assuming a 2 nm thick dielectric followed by a thick Al coating. The results presented in Figure 6.31.1 show that there is negligible difference between the choices of thin dielectric, all of which perform significantly poorer than an optically optimised rear configuration of a thick dielectric between the Si and Al, as would be the case for typical PERC, PERL or PERT cell designs. As an example, a 200 µm thick solar cell with 150 nm oxide between the rear surface Si and Al would have approximately 0.6 mAcm^{-2} higher ph

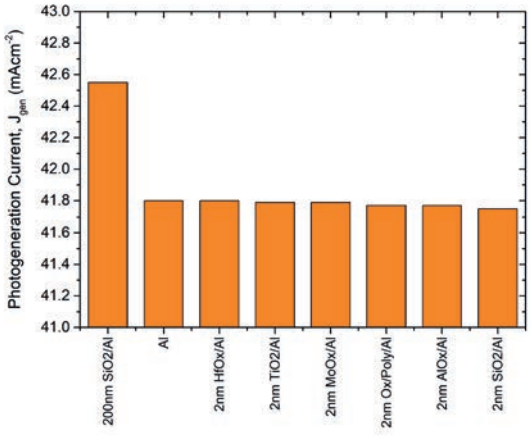

Fig. 6.31.1: Ray-tracing results comparing photogeneration current in the Si wafer for the case of an optimised rear reflector versus passivated contacts with 2 nm tunnel oxide layer.

The tunnel oxide layer is necessarily very thin in passivated contacts for its electrical properties, and is therefore impossible to optimise optically. However, the deposited rear metal of choice makes a significant difference, as is demonstrated in the figure below, once again assuming a varied range of rear metals. The simulations assume a 200 µm thick solar cell with rear surface consisting of 2 nm tunnel SiO_2 followed by a thick metal layer. By comparing a wide range of metal types, it appears that Ag, Cu and Al are among the best performing optically. From the perspective of a laboratory cell, evaporated Al is the simplest to integrate into a cell design due to proven electrical and adhesion properties to oxides.

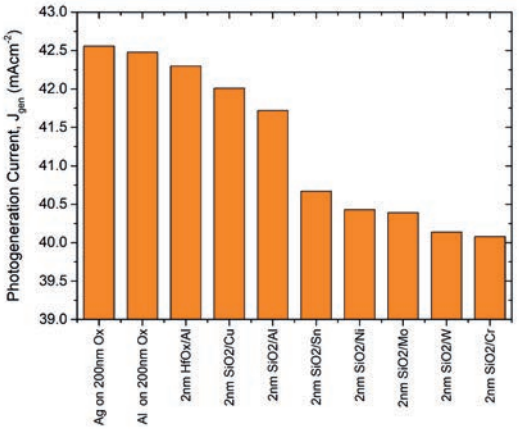

Fig. 6.31.2: Ray-tracing results comparing photogeneration current in the Si wafer for a range of metals deposited over 2 nm SiO_2.

To take advantage of the benefits of Al, and the optical advantages of Ag and Cu, we plan to explore the implementation of stacked metal layers to improve the rear optics of passivated contacts, where a layer of very thin Al (e.g. 1–2 nm) is first evaporated on the tunnel oxide, or Poly-Ox contacts, followed by the evaporation of a thick Ag or Cu for its better optical performance. The figure below shows the generation current, J_{gen} when Al is swept from 0 to 20 nm, and when the rear metal is either Ag or Cu. The figure suggests that to attain any optical benefits, the Al must be thinner than 10 nm. With the Al at 1 nm, the gains from Ag and Cu are approximately 0.45 mAcm^{-2} and 0.25 mAcm^{-2}. Similar optical gains are observed for simulations with a rear poly-ox passivated contact stack of 1 nm SiO_2 / 20 nm polysilicon. As such, the proposed metal stack method is likely applicable for a wide range of passivated contacts.

Experimental verification of these observations will be carried out in the coming months.

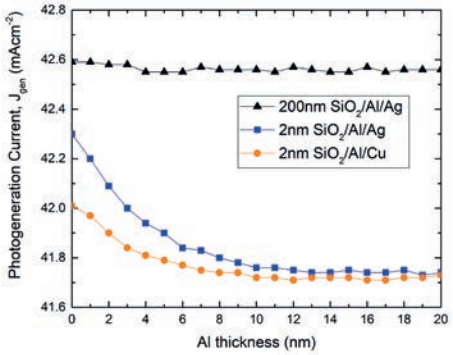

Fig. 6.31.3: Ray-tracing results investigating the potential benefit of using a stack of metal type for improved optical performance.

Highlights

- Completed ray-tracing of the effect of rear metal type on optical performance of passivated contacts.
- Proposed investigation of novel implementation of a stack of metal layer for improved optical performance.

Future Work

- Experimental verification of ray-tracing results, and development of rear metal stack for improved optical performance.
- Experimental verification for optical performance of various choices for rear metal.
- Experimental verification for optical performance of rear metal stacks with thin Al.

6.32 High Efficiency Heterojunction Solar Cells Based on Low-Cost Solar-Grade Silicon Wafers

Lead Partner
ANU

ANU Team
Prof Daniel Macdonald, Dr Chang Sun, Mr Rabin Basnet

Academic Partner
A/Prof Zachary Holman, Arizona State University (ASU)

Funding Support
ARENA, ANU, ASU

Aim

Solar-grade silicon wafers are attractive due to their low cost, however they are often adversely affected by high temperature steps (around 900°C) during solar cell fabrication, especially during the boron diffusions required for high efficiency n-type devices. In this project we will apply a low temperature heterojunction cell fabrication process (below 250°C) at Arizona State University (ASU), based on doped thin amorphous silicon films, to solar-grade wafers prepared at the Australian National University (ANU). The project will aim for cell efficiencies above 22%, which would represent a world record for solar-grade silicon, and demonstrate an attractive pathway to realising high efficiency, low-cost solar-grade silicon cells.

Progress

This two-year project commenced in February 2017. To date, four batches of solar-grade silicon wafers have been prepared at ANU and sent to ASU for processing, initially for surface passivation tests, and more recently for full solar cell fabrication.

An important early outcome of the project has been the development of optimised processes at ANU to maximise the wafer quality prior to shipping to ASU. The use of a "Tabula Rasa" pre-annealing step at 1000°C has been found to eliminate ring defects associated with oxygen precipitation during the subsequent phosphorus gettering step. Phosphorus gettering then removes dissolved metallic impurities in the solar-grade wafers. Combined, these pre-treatments have resulted in carrier lifetimes in excess of 5 ms, and implied open circuit voltages of over 720 mV. A journal manuscript describing these results is currently in preparation.

After initial trials to optimise surface preparation at ANU and ASU, the first complete batch of heterojunction solar cells on solar-grade wafers was completed in October 2017. This resulted in a champion cell efficiency of 21.2%, measured in-house at ASU. This, if independently confirmed, is already a record efficiency for a solar-grade silicon wafer, eclipsing the 21.1% achieved by the team at ANU using a PERL process in late 2016. Further improvements in device fabrication, especially in relation to fill factor losses during metallisation, should enable efficiencies of around 22% in the coming months. These cell results will be submitted to the IEEE PVSC conference to be held in Hawaii in June 2018.

An interesting aspect of the latest batch of solar cells is an ongoing exploration of the impact of pre-hydrogenation of the wafers. Such pre-hydrogenation was achieved by coating the wafers with silicon nitride films after the Tabula Rasa and phosphorus gettering, and then firing the wafers at 600˚C for 5 seconds, to drive hydrogen into the wafers. The wafers were then etched and sent to ASU for heterojunction cell fabrication.

This work is being conducted in collaboration with Dr Brett Hallam's team at UNSW, who are working on a related ACAP collaboration project on hydrogenation with ASU. The hydrogen in the wafers may then allow the subsequent deactivation of the well-known boron-oxygen defect, which normally degrades the performance of solar cells made on the dopant-compensated solar-grade wafers used in this work. By subjecting the completed heterojunction cells to illuminated annealing steps at UNSW, we aim to show that the defect can be completely and permanently deactivated in this n-type material, which would be another world-first achievement. This work is currently underway.

Highlights

- First batches of complete heterojunction solar cells fabricated at ASU on solar-grade silicon wafers pre-treated at ANU, resulting in an efficiency of 21.2%, the highest reported to date for solar-grade wafers.
- Demonstration of the benefits of a Tabula Rasa pre-treatment of solar-grade silicon wafers to avoid ring defects associated with oxygen precipitation.
- Achieving effective lifetimes in excess of 5 ms and implied open circuit voltages of over 720 mV in solar-grade wafers after Tabula Rasa and phosphorus gettering steps applied at ANU.
- Development of a pre-hydrogenation treatment for heterojunction solar cells, which should enable the permanent deactivation of the well-known boron-oxygen defect during subsequent illuminated annealing, in collaboration with colleagues at UNSW.

Future Work

- The next 12 months of the project will see several more batches of heterojunction solar cells fabricated at ASU.
- After optimising the metallisation of these cells, we aim to achieve cell efficiencies of 22% on solar-grade silicon wafers pre-treated at ANU.
- We also intend to demonstrate the complete and permanent deactivation of the boron-oxygen defect in these devices, via illuminated annealing at UNSW on heterojunction cells made at ASU which were pre-hydrogenated at ANU.
- If successful, these outcomes would have a large impact on the silicon PV research community. They will also help to establish a strong collaboration between ANU, ASU and UNSW which we expect will endure beyond the end of this project.

6.33 Discovering and Developing Lead-Free Perovskites for Photovoltaic Application

Lead Partner
ANU

ANU Team
Dr Hemant Kumar Mulmudi, A/Prof Klaus Weber

ANU Student
Nandi Wu

USA Partners
Team

Dr Ghanshyam Pilania (LANL), Los Alamos National Laboratory (New Mexico)

A/Prof Rohan Mishra (Wash U), Washington University in St Louis

Aim

The aim of this project was to identify and develop new materials resembling the properties of lead-based perovskite materials. The lead halide perovskite materials have unique optical and electrical properties due to the hybridisation of the orbitals leading to highly dispersed band structure with low effective mass of charge particles. This has been found to be one of the underlying factors for the relatively high performing solution-processed photovoltaics. Using density functional theory (DFT) based on first principle calculations and data analytics, lead-free perovskites were to be screened to determine the composition of promising materials. Such materials can then be synthesised and characterised and, if suitable, photovoltaic devices fabricated.

Progress

Calculations have been performed to identify potentially suitable materials. Screening of double perovskite compounds with the composition A'A''B'BiX_6, (where A', A'' and B' are different cations and X is an anion) was carried out by considering thermodynamic stability. Thirty-six compounds were found to conform to the defined stability limit after accounting for octahedral distortions to the ideal double perovskite structure. However, most of these compounds exhibit wide and indirect bandgaps. A family of compounds with a general formula of *A'A"*$TeBiO_6$, where *A'* belongs to alkali metals (Na, K, Rb and Cs) and *A"* belongs to alkaline earth metals (Mg, Ca, Sr and Ba), were found to be thermodynamically stable. Calculations indicate that $KBaTeBiO_6$ and $RbBaTeBiO_6$ have indirect bandgaps of 1.94 eV and 1.99 eV but otherwise suitable properties. The issue of indirect bandgaps has to be addressed to make further progress in search of novel Bi-double perovskite oxides. Further cation substitution strategies, such as varying ratio of Bi and Te may be able to allow tuning of the bandgaps within the *A'A"*$TeBiO_6$ family of compounds.

As part of this project, Dr Mulmudi (ANU) initiated this collaborative research effort between Dr Pilania (LANL) and A/Prof Mishra (Wash U) through several conference calls and emails. A visit to ANU for Dr Pilania was also organised to give a seminar and to discuss the progress of the project at the end of 2017. The next step is to look at the possible ways of synthesising the most promising materials identified to date ($KBaTeBiO_6$) by solution-processed methods. It is also envisioned that the materials screened from these methodologies can have other interesting optoelectronic applications such as electro/photo-catalysis.

It has not been possible to date to carry out device processing or material characterisation.

Highlights

- Through a systematic theoretical approach based on structural, thermodynamic and electronic constraints, potentially promising bismuth-based double perovskites were identified.
- Work is in progress to synthesise these novel materials, which not only have photovoltaic applications but also other interesting optoelectronic applications.

References

Huang, X., Huang, S., Biswas, P. and Mishra, R., 2016, "Band Gap Insensitivity to Large Chemical Pressures in Ternary Bismuth Iodides for Photovoltaic Applications", J. Phys. Chem. C, 120 (51), 28924–28932.

Ghosh, B., Wu, B., Mulmudi, H.K., Guet, C., Weber, K., Sum, T.C., Mhaisalkar, S.G. and Mathews, N, 2018, "Limitations of $Cs_3Bi_2I_9$ as lead-free photovoltaic absorber materials", ACS Applied Materials & Interfaces, DOI: 10.1021/acsami.7b14735.

Mulmudi, H.K. et al., "$KBaTeBiO_6$: a lead-free, inorganic double perovskite semiconductor for photovoltaic applications", (Manuscript in preparation).

6.34 In-situ X-ray Characterisation of Printed Organic Solar Cell Films

UoM Team
Dr David Jones, Dr Jegadesan Subbiah

CSIRO
Dr Gerry Wilson, Dr Doojin Vak, Dr Mei Gao

NIST (USA)
Dr Lee Richter, Dr Sebastian Engmann

University of Bayreuth (Germany)
Prof Anna Köhler, Mr Daniel Kroh (student)

Funding Support
AUSIAPV, UoM, CSIRO, NIST, University of Bayreuth (UoM-Bayreuth Polymer/Colloid Network)

Aims

- Non-fullerene acceptors purchased or synthesised and evaluated with ACAP molecular donors.
- Lab scale devices optimised.
- Processing knowledge translated back to the ACAP printing program, two-print trial on 10 cm web printer completed.
- Results published in leading peer-reviewed journals (two papers) and at two international conferences.
- Staff and student exchange visits (four) completed on time and within budget to examine new non-fullerene acceptors in binary and ternary blends.

Progress

A research assistant was employed to complete a large-scale synthesis of the key benzodithiophene-quaterthiophene-rhodanine (BQR) donor material to be used in this program. The synthesis of BQR was completed at a 20 g scale to provide sufficient material for all the required device optimisation and later translation to larger scale printing of the optimised devices. This material has now been distributed to the key partners at NIST, CSIRO and the University of Bayreuth.

Figure 6.34.1: Doojin Vak, Jegadesan Subbiah, Mei Gao, David Jones,and Daniel Kroh (L to R) at CSIRO with a range of printed solar cells.

Figure 6.34.2: David Jones (left) and Lee Richter (right) after a planning meeting at NIST.

We have been able to access a number of commercially available non-fullerene acceptors for use in this project, IDTBR, ITIC and *m*-ITIC. Also, we have a number of in-house non-fullerene acceptors which will be made available once characterised. In addition, BQR has been sent to Northwestern University (USA), University of Calgary (Canada) and KAUST (Saudia Arabia) for testing in devices with non-fullerene acceptors which are not commercially available, and new collaborations have been initiated with these groups.

Researchers at NIST have initiated a detailed characterisation program on BQR and BQR / acceptor blends to better understand its materials properties. Device optimisation of BQR-containing blends, deposited using blade-coating is underway. These studies include in situ X-ray analysis of BQR-containing films, however X-ray contrast is low for non-fullerene acceptor containing blends and alternative techniques are being examined.

We have been able to complement the printing program through a new collaboration through the University of Melbourne-Bayreuth Polymer/Colloid Network with funding to allow a masters student, Mr Daniel Kroh from Prof Anna Köhler's (Bayreuth) group, to complete his Thesis project at CSIRO on printed organic solar cells. We are currently optimising basic slot-die deposited BQR-containing devices. After we have optimised the device deposition and treatment we will translate the printing program to the 10 cm R2R printer.

In the previous year Dr Jones visited NIST to plan the research program, Dr Jegadesan visited NIST to discuss device optimisation and Mr Kroh arrived from Germany to start his research project.

A number of international research groups have shown an interest in the fundamental properties of BQR as a high performance p-type organic semiconductor and the large-scale synthesis of BQR has allowed us to initiate new collaborations with Imperial College London, the University of St Andrews, University of Princeton and Karlsruhe Institute of Technology. The new understanding of fundamental materials properties will allow us to better evaluate BQR as a component in printed organic solar cells.

Highlights

- The key organic p-type donor BQR has been synthesised at scale for the acceptor screening program and translation to large-scale R2R printing trials.
- We have accessed a number of high performing non-fullerene acceptors for the program.

Future Work

- We will complete device optimisation on BQR-containing devices with non-fullerene acceptors.
- The optimised conditions for device assembly for slot-die and doctor-blade deposited films will be translated to R2R printed organic solar cells.
- The key results will be prepared for publication.
- We are planning to have Dr Lee Richter visit Australia in 2018 as part of the program, and UoM team member, David Jones will visit USA partners in the next few months to finalise planning of this work.